



ΠΑΝΕΠΙΣΤΗΜΙΟ ΠΕΙΡΑΙΩΣ

ΤΜΗΜΑ ΨΗΦΙΑΚΩΝ ΣΥΣΤΗΜΑΤΩΝ

Επίδοση μεθόδων επικοινωνίας με πολλαπλούς
αναμεταδότες σε γενικευμένους διαύλους
ασύρματων επικοινωνιών

Διδακτορική Διατριβή

Νικόλαος Μπίσιας

Πειραιάς, Δεκέμβριος 2012

ΕΠΙΔΟΣΗ ΜΕΘΟΔΩΝ ΕΠΙΚΟΙΝΩΝΙΑΣ
ΜΕ ΠΟΛΛΑΠΛΟΥΣ ΑΝΑΜΕΤΑΔΟΤΕΣ
ΣΕ ΓΕΝΙΚΕΥΜΕΝΟΥΣ ΔΙΑΥΛΟΥΣ ΑΣΥΡΜΑΤΩΝ ΕΠΙΚΟΙΝΩΝΙΩΝ

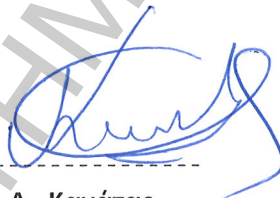
ΔΙΔΑΚΤΟΡΙΚΗ ΔΙΑΤΡΙΒΗ
ΤΟΥ
ΝΙΚΟΛΑΟΥ Σ. ΜΠΙΣΙΑ

Συμβουλευτική Επιτροπή: Γεώργιος Ευθύμογλου
Αθανάσιος Κανάτας
Παναγιώτης Δεμέστιχας

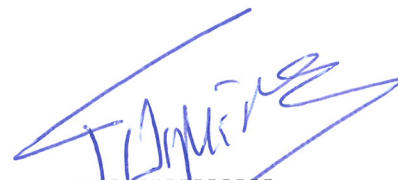
Εγκρίθηκε από την επταμελή εξεταστική επιτροπή την 8^η Μαρτίου 2013.



Γ. Ευθύμογλου
Αναπλ. Καθηγητής
Παν/μίου Πειραιώς



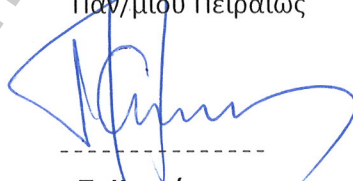
Α. Κανάτας
Καθηγητής
Παν/μίου Πειραιώς



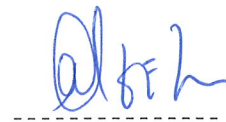
Π. Δεμέστιχας
Καθηγητής
Παν/μίου Πειραιώς



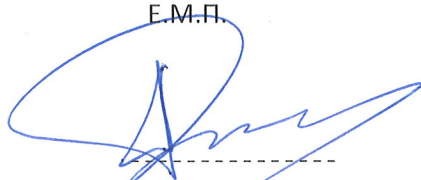
Φ. Κωνσταντίνου
Καθηγητής
Ε.Μ.Π.



Π. Κωττής
Καθηγητής
Ε.Μ.Π.



Α. Αλεξίου
Επικ. Καθηγήτρια
Παν/μίου Πειραιώς



Α. Ρούσκας
Επικ. Καθηγητής
Παν/μίου Πειραιώς

ΠΑΝΕΠΙΣΤΗΜΙΟ ΠΕΙΡΑΙΩΣ

Στη μητέρα μου

ΠΕΡΙΛΗΨΗ

Το τελευταίο χρονικό διάστημα υπάρχει μεγάλο ενδιαφέρον για τη χρήση αναμεταδοτών (relays) για τη μετάδοση σημάτων με σκοπό την βελτίωση της επίδοσης των συστημάτων ασύρματων επικοινωνιών και την επίτευξη διαφορικής λήψης μέσω συνεργασίας (cooperative diversity), η οποία μπορεί να καταπολεμήσει προβλήματα όπως οι διαλείψεις στα ασύρματα συστήματα επικοινωνιών. Επίσης, η τεχνολογία των πολλαπλών αναμεταδοτών (multi-hop relaying) έχει αποδειχθεί ως ένα αποτελεσματικό εργαλείο για την αύξηση της φασματικής απόδοσης αλλά και της επέκτασης της κάλυψης σε κυβελωτά και ad hoc ασύρματα δίκτυα. Ειδικότερα, το multi-hop relaying έχει τη δυνατότητα να επιτρέπει στον πομπό και στο δέκτη να επικοινωνήσουν μέσα από μια σειρά συνεργαζόμενων κόμβων αναμετάδοσης, με στόχο την επέκταση της ραδιοκάλυψης και τη βελτίωση της επίδοσης του δικτύου. Για παράδειγμα, οι αδρανείς σταθμοί μεταξύ της πηγής και του προορισμού μπορούν να χρησιμοποιηθούν ως κόμβοι αναμετάδοσης για την παροχή επιπλέον συνδέσμων στο δίκτυο για την δημιουργία εναλλακτικών μονοπατιών ραδιο-μετάδοσης.

Στην παρούσα διδακτορική διατριβή, αποδεικνύουμε αναλυτικές εκφράσεις για διάφορα κριτήρια επίδοσης των συστημάτων πολλαπλών αναμεταδοτών σε περιβάλλοντα διάδοσης που χαρακτηρίζονται από σύνθετα μοντέλα διάλειψης. Στο Κεφάλαιο 1 κάνουμε μία επισκόπηση των μοντέλων διάλειψης μικρής και μεγάλης κλίμακας για το ασύρματο κανάλι. Σε αυτή τη διατριβή χρησιμοποιούμε τη Γενικευμένη-K κατανομή για να μοντελοποιήσουμε τη διάλειψη στο κανάλι επικοινωνίας, διότι η συγκεκριμένη κατανομή συνδυάζει την επίδραση μικρής και μεγάλης κλίμακας διάλειψης στο σήμα λήψης. Στο Κεφάλαιο 2 δίνουμε μία επισκόπηση των κυριότερων συστημάτων αναμεταδοτών που έχουν προταθεί για τα ασύρματα συστήματα με βάση την ενίσχυση που χρησιμοποιείται και τον τρόπο συνδεσμολογίας αλλά και επιλογής των αναμεταδοτών. Στο Κεφάλαιο 3, αποδεικνύουμε νέες και εύκολα υπολογίσιμες μαθηματικές εκφράσεις για την πιθανότητα σφάλματος σε συστήματα που υποστηρίζουν πολλαπλούς αναμεταδότες σε παράλληλη συνδεσμολογία και απευθείας διαδρομή με maximal ratio combining στο δέκτη. Επειδή είναι αρκετά δύσκολο να βρεθεί μια έκφραση κλειστής μορφής για τη moment generating function (MGF) του συνολικού (end-to-end) σηματοθυροβικού λόγου (ΣΘΛ) στον τελικό προορισμό, χρησιμοποιούμε δύο διαφορετικές

προσεγγίσεις για το άνω φράγμα του συνολικού ΣΘΛ, εκ των οποίων η πρώτη υλοποιείται με βάση το ελάχιστο ΣΘΛ των δύο ζεύξεων για κάθε αναμεταδότη και η δεύτερη βασίζεται στο γεωμετρικό μέσο όρο των ΣΘΛ των δύο ζεύξεων. Στη συνέχεια αποδεικνύουμε τα αντίστοιχα κατώτερα όρια για την πιθανότητα σφάλματος συμβόλου και bit για διάφορες ψηφιακές διαμορφώσεις χρησιμοποιώντας την MGF προσέγγιση. Οι τελικές εκφράσεις είναι χρήσιμες για την αξιολόγηση των επιδόσεων της τεχνικής αναμετάδοσης ενίσχυση-και-προώθηση (ΕΠ) σε ένα σύνθετο περιβάλλον διάδοσης.

Στο Κεφάλαιο 4, παρουσιάζουμε νέες μαθηματικές σχέσεις για την αξιολόγηση της επίδοσης ενός δικτύου με αναμετάδοση δύο ζεύξεων και επιλογή του καλύτερου αναμεταδότη σε περιβάλλον με ανεξάρτητα κανάλια διάλειασης. Δεδομένου ότι είναι δύσκολο να βρεθεί μια κλειστή μορφής έκφραση για τη συνάρτηση πυκνότητας πιθανότητας για το συνολικό ΣΘΛ στον κόμβο προορισμού ακόμη και για την περίπτωση ενός ΕΠ αναμεταδότη, χρησιμοποιούμε ένα άνω όριο για το ΣΘΛ. Χρησιμοποιώντας την προσεγγιστική σχέση για το συνολικό ΣΘΛ, βρίσκουμε εκφράσεις για τη στατιστική του ΣΘΛ, για τη μέση πιθανότητα σφάλματος συμβόλου και bit, καθώς και για την εργοδική χωρητικότητα ενός συστήματος με ένα ΕΠ αναμεταδότη σε κανάλι με Γενικευμένη-Κ διάλειαση. Στη συνέχεια, για ανεξάρτητες αλλά μη-ταυτόσημες συνθήκες διάλειασης, βρίσκουμε την επίδοση για ένα σύστημα με πολλαπλούς αναμεταδότες δύο ζεύξεων που χρησιμοποιεί επιλογή του καλύτερου αναμεταδότη. Οι τελικές εκφράσεις είναι χρήσιμες για την αξιολόγηση των επιδόσεων των ΕΠ συστημάτων με επιλογή αναμεταδότη σε ένα σύνθετο περιβάλλον διάδοσης. Επίσης, δίνουμε αποτελέσματα Monte Carlo προσομοίωσης για την επαλήθευση των αναλυτικών αποτελεσμάτων.

Στο Κεφάλαιο 5, αποδεικνύουμε νέες μαθηματικές σχέσεις μέτρων επίδοσης για συστήματα πολλαπλών αναμεταδοτών (multi-hop relays) που λειτουργούν σε ένα σύνθετο περιβάλλον διαλείψεων, το οποίο μοντελοποιείται με τη Γενικευμένη-Κ κατανομή. Χρησιμοποιώντας την προσέγγιση του συνολικού ΣΘΛ για το σύστημα πολλαπλών αναμεταδοτών το οποίο δίνεται από το ελάχιστο ΣΘΛ όλων των ζεύξεων, παρέχεται ένας εύκολος τρόπος υπολογισμού για την πιθανότητα διακοπής και της μέσης πιθανότητας σφάλματος συμβόλου και bit για διάφορες ψηφιακές διαμορφώσεις. Τα αποτελέσματα από τον υπολογισμό των αναλυτικών εκφράσεων για τα κάτω όρια επίδοσης συγκρίνονται με εκείνα της προσομοίωσης της ακριβής

επίδοσης των συστημάτων πολλαπλών αναμεταδοτών, από όπου φαίνεται η ακρίβεια της προσέγγισης.

Στο Κεφάλαιο 6, αποδεικνύουμε κατώτερα όρια κλειστής μορφής για την επίδοση των συστημάτων πολλαπλών αναμεταδοτών που λειτουργούν σε ένα Nakagami-m κανάλι διαλείψεων. Το συνολικό ΣΘΛ στον προορισμό προσεγγίζεται από το γεωμετρικό μέσο όρο όλων των ζεύξεων. Με αυτή την προσέγγιση, βρίσκουμε μαθηματικές εκφράσεις κλειστής μορφής για τις στατιστικές του συνολικού ΣΘΛ. Αυτές, με τη σειρά τους, χρησιμοποιούνται για να υπολογίσουμε την πιθανότητα διακοπής, τη μέση πιθανότητα σφάλματος συμβόλου και ένα ανώτερο όριο για τη μέση εργοδική χωρητικότητα του συστήματος πολλαπλών αναμεταδοτών.

Τέλος, στο Κεφάλαιο 7 εξετάζουμε την επίδραση ομοδιαυλικής παρεμβολής στην πιθανότητα διακοπής ενός ασύρματου συστήματος με ένα ΕΠ αναμεταδότη σε περιβάλλον με Rayleigh διάσπριση. Χρησιμοποιούμε ένα μοντέλο με τέσσερις παραμέτρους, στο οποίο δύο παράμετροι προσδιορίζουν τον τύπο της ενίσχυσης στον αναμεταδότη και οι άλλες δύο την ύπαρξη θορύβου και παρεμβολών στο δέκτη προορισμού. Για το παραμετροποιημένο αυτό μοντέλο αποδεικνύουμε μαθηματικές εκφράσεις της πιθανότητας διακοπής συναρτήσει του ολοκληρώματος Weber, το οποίο μπορεί να υπολογιστεί αριθμητικά εύκολα και με ακρίβεια.

Abstract

There is growing interest in the use of relay-assisted transmission schemes to provide system performance improvement in terms of system reliability and cooperative diversity. Cooperative diversity can combat channel impairments due to fading in wireless communication systems. The cooperative diversity through multihop relaying technology has emerged as an effective tool to enhance the spectral efficiency and extend the coverage of cellular and ad hoc wireless networks. In particular, multihop relaying can enable source and destination nodes to communicate through a set of cooperating relay nodes in which the transmitted signals propagate through cascaded relay nodes, with the aim of extending coverage and improving the performance of the network. In addition, idle mobile stations between the source and destination may be employed as relay nodes to provide extra diversity links.

In this dissertation, we investigate the performances of multihop relaying systems in composite fading environments. A review of small and large-scale fading for the wireless channel is given in Chapter 1, where the statistical characterization of various channel models is presented. In this work, we consider the generalized- K fading channel, which is a composite fading model that considers the effects of both small- and large-scale fading on the received signal. Then, in Chapter 2 we review various relay systems that have been proposed for wireless communications according to the relay gain employed and the selection of the relays utilized. In Chapter 3, we present novel and easy-to-evaluate expressions for the error rate performance of cooperative dual-hop relaying with maximal ratio combining operating over independent generalized- K fading channels. As it is hard to obtain a closed-form expression for the moment generating function (MGF) of the end-to-end signal-to-noise ratio (SNR) at the destination, even for the case of a single dual-hop relay link, we employ two different upper bound approximations for the output SNR, of which one is based on the minimum SNR of the two hops for each dual-hop relay link and the other is based on the geometric mean of the SNRs of the two hops. Lower bounds for the symbol and bit error rates for a variety of digital modulations can

then be evaluated using the MGF based approach. The final expressions are useful in the performance evaluation of amplify-and-forward (AF) relaying in a generalized composite radio environment.

In Chapter 4, we present novel and easy-to-evaluate expressions for the performance of dual-hop relaying with best relay selection operating over generalized- K fading channels. Since it is hard to find a closed-form expression for the probability density function (PDF) of the exact SNR at the destination node even for the single dual-hop system with amplify-and-forward relaying, we use a tight upper bound value instead. Using the approximate value for the end-to-end SNR, closed-form expressions for the statistics of the SNR, the average bit and symbol error probabilities, and the ergodic capacity for the single dual-hop AF relay system, are derived. Moreover, assuming independent nonidentical fading conditions across multiple dual-hop relay links, we derive lower performance bounds for the single relay selection scheme with AF relaying. The final expressions are useful in the performance evaluation of AF opportunistic relaying in a generalized composite radio environment. Simulation results are also given to verify the analytical results.

In Chapter 5, we evaluate performance measures of multihop relaying systems operating in a composite fading environment modeled by the generalized- K distribution. By approximating the end-to-end signal-to-noise ratio of the multihop relay system by the minimum SNR of all the links, we provide easy to compute analytical expressions for the outage probability and the average bit and symbol error rates for a variety of digital modulation schemes. The derived expressions are validated by computer simulation and provide tight lower bounds to the exact performance of multihop relaying transmissions in a generalized fading environment.

In Chapter 6 we derive closed-form lower bounds on the performance of multihop communication systems with non-regenerative relays operating in a Nakagami- m fading channel. The relay gains are assumed to be chosen to maximize the end-to-end SNR, which is bounded by the geometric mean of the positive random variables. Closed-form expressions are then derived for the statistics of the geometric mean of the optimum

end-to-end SNR. These, in turn, are used to derive tight bounds for the outage as well as average error performances of the system. An upper bound is also derived for the mean ergodic capacity of the end-to-end SNR.

Finally, in Chapter 7 we study the effect of co-channel interference on the outage probability of dual-hop wireless communication systems with amplify-and-forward relaying operating in a Rayleigh fading channel. A four-parameter model for the dual-hop AF relay system is introduced, in which two of the parameters specify the type of gain adopted at the relay node while the other two parameters account for the presence of channel noise and co-channel interference at the destination node. We then derive the exact outage probability in terms of the well-known incomplete Weber integral, which can be easily and accurately evaluated numerically.

Contents

| | |
|---|-------------|
| Abstract | vi |
| Contents | ix |
| List of Figures | xiii |
| 1 Fading Channels Characterization and Stochastic Modeling | 1 |
| 1.1 Large Scale Fading-Shadowing | 2 |
| 1.2 Small Scale Fading-Multipath | 3 |
| 1.2.1 Factors Influencing Small-Scale Fading | 5 |
| 1.2.2 Envelope and Phase Fluctuations | 7 |
| 1.2.3 Slow and Fast Fading | 7 |
| 1.2.4 Frequency-Flat and Frequency-Selective Fading..... | 8 |
| 1.3 Stochastic Modeling of Flat-Fading Channels | 8 |
| 1.3.1 Small Scale Fading Stochastic Modeling | 9 |
| 1.3.2 Large Scale Fading Stochastic Modeling | 14 |
| 1.3.3 Composite multipath/shadowing fading environments | 15 |
| 2 Introduction to Relay Systems | 17 |
| 2.1 Dual-hop AF relaying system | 18 |
| 2.1.1 Blind Relays | 20 |
| 2.1.2 Semi-Blind Relays | 21 |
| 2.2 Multi-hop AF relaying system..... | 21 |

| | | |
|----------|--|-----------|
| 2.3 | Multi-hop DF relay system..... | 23 |
| 3 | On the Error Rate Analysis of Dual-Hop Amplify-and-Forward Relaying in Generalized-K Fading Channels | 24 |
| 3.1 | Introduction..... | 24 |
| 3.2 | Statistics of the Generalized- K Distribution..... | 26 |
| 3.3 | End-to-End Error Rate Analysis..... | 27 |
| 3.3.1 | Performance using the minimum SNR approximation..... | 28 |
| 3.3.2 | Performance Using The Geometric Mean Approximation..... | 30 |
| 3.4 | Numerical Results..... | 32 |
| 3.5 | Conclusion..... | 34 |
| 4 | Performance Analysis of Dual-Hop Relay Systems with Single Relay Selection in Composite Fading Channels | 36 |
| 4.1 | Introduction..... | 37 |
| 4.2 | The Generalized- K Fading Model..... | 39 |
| 4.3 | Performance Analysis of Single Dual-Hop Relay System..... | 40 |
| 4.3.1 | Statistics of the end-to-end SNR..... | 41 |
| 4.3.2 | Amount of Fading..... | 43 |
| 4.3.3 | Outage Probability..... | 43 |
| 4.3.4 | Average BER..... | 44 |
| 4.3.5 | Average SER..... | 46 |
| 4.3.6 | Ergodic Capacity..... | 46 |
| 4.4 | Extension to the best relay selection scheme..... | 46 |
| 4.5 | Numerical Results..... | 47 |
| 4.6 | Conclusions..... | 51 |
| 5 | Performance of Multihop Relaying Systems over Composite Fading Channels | 53 |
| 5.1 | Introduction..... | 53 |

| | | |
|----------|--|-----------|
| 5.2 | Statistics of Generalized- K Distribution | 55 |
| 5.3 | Multihop Relaying System | 57 |
| 5.3.1 | Outage Probability | 59 |
| 5.3.2 | Average Bit Error Rate | 59 |
| 5.3.3 | Average Symbol Error Rate | 61 |
| 5.4 | Numerical Results | 62 |
| 5.5 | Conclusion | 64 |
| 6 | On the Performance of Multihop Relay Systems in Nakagami Fading Channel | 69 |
| 6.1 | Introduction | 69 |
| 6.2 | End-To-End SNR | 70 |
| 6.3 | Performance in Nakagami Fading Channel | 72 |
| 6.3.1 | PDF of End-to-End SNR Bound | 72 |
| 6.3.2 | Outage Probability | 73 |
| 6.3.3 | Moments of End-to-End SNR Bound | 73 |
| 6.3.4 | Average Symbol Error Probability | 74 |
| 6.3.5 | Average Bit Error Probability | 75 |
| 6.3.6 | Ergodic Capacity | 76 |
| 6.4 | Numerical Results | 76 |
| 6.5 | Conclusions | 78 |
| 7 | Exact Outage Probability of Dual-Hop Relay Systems in a Rayleigh Fading Channel with Multiple Interferers | 79 |
| 7.1 | Introduction | 79 |
| 7.2 | System Model | 81 |
| 7.3 | Outage Probability | 84 |
| 7.3.1 | Distinct interferers | 85 |
| 7.3.2 | Identical interferers | 88 |

| | |
|-----------------------------|-----------|
| 7.4 Numerical Results | 89 |
| 7.5 Conclusion | 91 |
| Bibliography | 92 |

ΠΑΝΕΠΙΣΤΗΜΙΟ ΠΕΙΡΑΙΩΣ

List of Figures

| | | |
|-----|---|----|
| 1.1 | Path loss, shadowing and multipath fading versus log-distance | 2 |
| 1.2 | Small-scale and large-scale fading | 4 |
| 1.3 | Power (in dB) of small-scale fading | 6 |
| 2.1 | Example of dual-hop relaying system | 19 |
| 2.2 | Relay Categories | 21 |
| 2.3 | Multi-hop relay system with the presence of interference and noise | 22 |
| 3.1 | Cooperative dual-hop relay transmission scheme with MRC at the destination | 29 |
| 3.2 | Average SER for 4-PSK vs average SNR per hop for $N = 1$ and $N = 2$ dual-hop links with MRC | 33 |
| 3.3 | Average SER for 16-QAM vs average SNR per hop for $N = 1$ and $N = 2$ dual-hop links with MRC | 35 |
| 4.1 | Dual-hop relay transmission scheme with best relay selection. | 41 |
| 4.2 | Outage Probability vs SNR per hop for best relay selection scheme with $N = 1, 2, 3$ and $(m_i = 1, k_i = 1.5)$, $i = 1, 2, 3$ | 48 |
| 4.3 | Average BER of BPSK vs SNR per hop for best relay selection scheme with $N = 1, 2, 3$ and $(m_i = 1, k_i = 1.5)$, $i = 1, 2, 3$ | 49 |
| 4.4 | Average BER of 16-QAM vs SNR per hop for best relay selection scheme with $N = 1, 2, 3$ and $(m_i = 1, k_i = 1.5)$, $i = 1, 2, 3$ | 50 |

| | | |
|-----|---|----|
| 4.5 | Average BER of BPSK vs SNR per hop for best relay selection scheme with $N = 3$ and various fading conditions. | 51 |
| 4.6 | Average BER of 16-QAM vs SNR per hop for best relay selection scheme with $N = 3$ and various fading conditions. | 52 |
| 5.1 | Multihop relay system. | 58 |
| 5.2 | Outage probability vs average SNR of the first hop for $\gamma_{th} = 3$ dB with $N=2,3,4$ balanced hops with different fading conditions. | 63 |
| 5.3 | Average BER vs average SNR per bit of the first hop for BPSK and 16-QAM with $N=2,3,4$ balanced hops with different fading conditions. | 65 |
| 5.4 | Average BER vs average SNR per bit of the first hop for BPSK and 16-QAM with $N=2,3,4$ unbalanced hops with different fading conditions. ... | 66 |
| 5.5 | Average SER vs average SNR of first hop for QPSK with $N=2,3,4$ in different fading conditions. | 67 |
| 5.6 | Average SER vs average SNR of first hop for 16-QAM with $N=2,3,4$ in different fading conditions. | 68 |
| 6.1 | The PDF of γ_α for identical fading conditions and $N = 2, 3$ | 74 |
| 6.2 | Outage Probability versus the average input SNR for several values of m and $N=3$ | 77 |
| 6.3 | Average BER for BDPSK vs $\bar{\gamma}$ for $N = 2, 3$ and several values of m_i | 78 |
| 7.1 | Outage probability for a dual-hop relay system with optimum CSI gain in the presence of distinct-power interferers. | 90 |
| 7.2 | Outage probability for different categories of dual-hop AF relay systems with $M = 0$ (no interferer) and $M = 5$ equal-power interferers. | 91 |

Chapter 1

Fading Channels Characterization and Stochastic Modeling

THE WIRELESS radio channel is considered to be a very important part of the high-speed communication systems. However, Radiowave propagation through wireless channels is a complicated phenomenon characterized by various effects, including multipath fading, shadowing, and path loss. Path loss is caused by dissipation of the power radiated by the transmitter as well as effects of the propagation channel. Path loss models generally assume that path loss is the same at a given transmit-receive distance. Shadowing is caused by obstacles between the transmitter and receiver that attenuate signal power through absorption, reflection, scattering, and diffraction. When the attenuation is very strong, the signal is blocked. Variation due to path loss occurs over very large distances (100-1000 meters), whereas variation due to shadowing occurs over distances proportional to the length of the obstructing object (10-100 meters in outdoor environments and less in indoor environments). Variation due to multipath occurs over very short distances, on the order of the signal wavelength, so these variations are sometimes referred to as small-scale propagation effects. In Fig. 1.1, the ratio of the received-to-transmit power in dB versus log-distance for the combined effects of path loss, shadowing, and multipath is depicted.

The primary purpose of this chapter is to briefly review the principal characteristics and models for multipath fading and/or shadowing channels. A precise mathematical

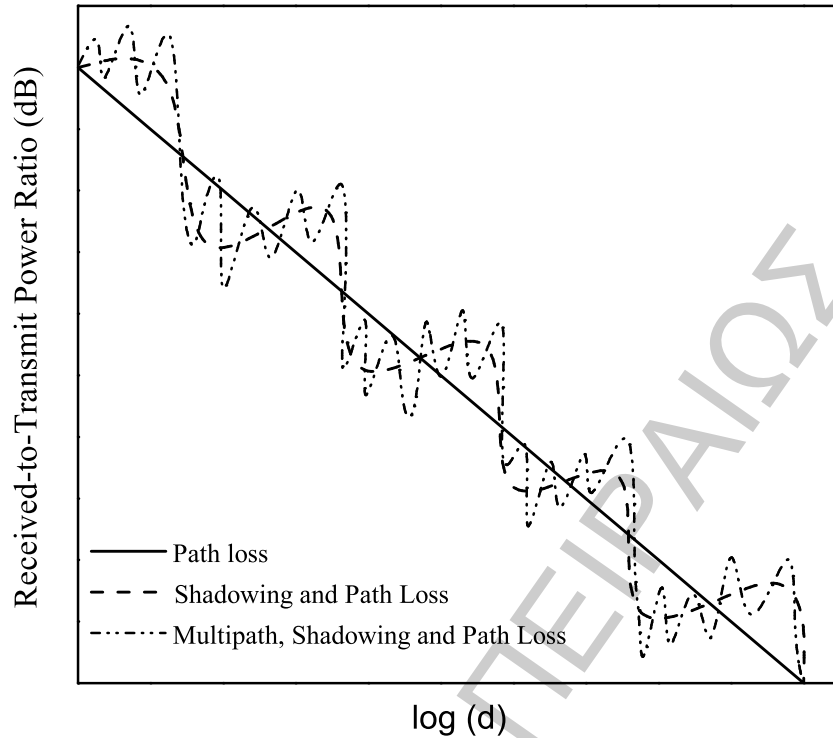


Figure 1.1: Path loss, shadowing and multipath fading versus log-distance

description of these phenomena is either unknown or too complex for tractable communication systems analyses. However, considerable efforts have been devoted to the statistical modeling and characterization of these different effects. The result is a range of relatively simple and accurate statistical models for fading channels that depend on the particular propagation environment and the underlying communication scenario. The primary purpose of this chapter is to briefly review the principal characteristics and models for fading channels and provide their statistical metrics.

1.1 Large Scale Fading-Shadowing

A signal transmitted through a wireless channel will typically experience random variation due to blockage from objects in the signal path, giving rise to random variations of the received power at a given distance. Such variations are also caused by changes in reflecting surfaces and scattering objects. Thus, a model for the random attenuation due to these effects is also needed. Since the location, size, and dielectric properties of the

blocking objects as well as the changes in reflecting surfaces and scattering objects that cause the random attenuation are generally unknown, statistical models must be used to characterize this attenuation. The most common model for this additional attenuation is log-normal shadowing. This model has been confirmed empirically to accurately model the variation in received power in both outdoor and indoor radio propagation environments (see e.g. [1], [2].)

In the log-normal shadowing model the ratio of transmit-to-receive power $\psi = P_t/P_r$ is assumed random with a log-normal distribution given by

$$p(\psi) = \frac{\xi}{\sqrt{2\pi}\sigma_{\psi_{\text{dB}}}\psi} \exp\left[-\frac{(10\log(\psi) - \mu_{\psi_{\text{dB}}})^2}{2\sigma_{\psi_{\text{dB}}}^2}\right], \quad \psi \geq 0 \quad (1.1)$$

where $\xi = 10/\ln 10$, $\mu_{\psi_{\text{dB}}}$ is the mean of $\psi_{\text{dB}} = 10\log_{10}\psi$ in dB and $\sigma_{\psi_{\text{dB}}}$ is the standard deviation of ψ_{dB} , also in dB. The mean can be based on an analytical model or empirical measurements. For empirical measurements $\mu_{\psi_{\text{dB}}}$ equals the empirical path loss, since average attenuation from shadowing is already incorporated into the measurements. For analytical models, $\mu_{\psi_{\text{dB}}}$ must incorporate both the path loss (e.g. from free-space or a ray tracing model) as well as average attenuation from blockage. Note that if the ψ is log-normal, then the received power and receiver signal-to-noise ratio (SNR) will also be log-normal since these are just constant multiples of ψ . For received SNR the mean and standard deviation of this log-normal random variable are also in dB. In Fig. 1.2 the small-scale fading and the slower large-scale variations for an indoor radio communication system are illustrated. It is noted in this figure that the signal fades rapidly as the receiver moves, but the signal fades more slowly with distance.

1.2 Small Scale Fading-Multipath

Small scale fading or multipath fading is used to describe the rapid fluctuation of the amplitude of a radio signal over a short period of time or travel distance, so that larger-scale path loss effects may be ignored. Fading is caused by interference between two or

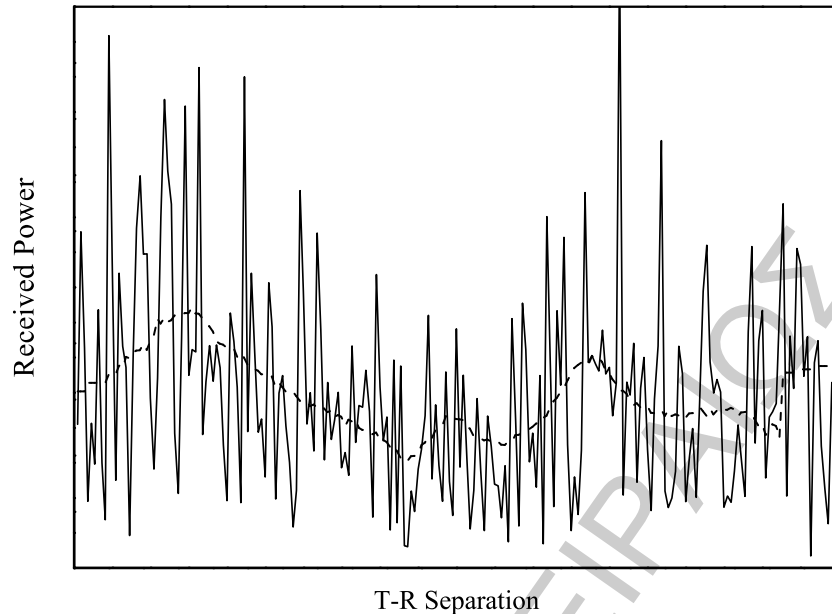


Figure 1.2: Small-scale and large-scale fading

more versions of the transmitted signal which arrive at the receiver at slightly different times. These waves, called multipath waves, combine at the receiver antenna to give a resultant signal which can vary widely in amplitude and phase, depending on the distribution of the intensity and relative propagation time of the waves and the bandwidth of the transmitted signal. Multipath in the radio channel creates small-scale fading effects. The three most important effects are:

- Rapid changes in signal strength over a small travel distance or time interval.
- Random frequency modulation due to varying Doppler shifts on different multipath signals.
- Time dispersion (echoes) caused by multipath propagation delays.

In built-up urban areas, fading occurs because the height of the mobile antennas are well below the height of surrounding structures, so there is no single line-of-sight (LoS) path to the base station. Even when a LoS exists, multipath still occurs due to reflections from the ground and surrounding structures. The incoming radio waves arrive from different directions with different propagation delays. The signal received by the mobile at

any point in space may consist of a large number of plane waves having randomly distributed amplitudes, phases and angles of arrival. These multipath components combine vectorially at the receiver antenna, and can cause the signal received by the mobile to distort or fade. Even when a mobile receiver is stationary, the received signal may fade due to movement of surrounding objects in the radio channel.

If objects in the radio channel are static and motion is considered to be only due to that of the mobile, then fading is purely a spatial phenomenon. The spatial variations of the resulting signal are seen as temporal variations by the receiver as it moves through the multipath field. Due to the **constructive** and **destructive** effects of multipath waves summing at various points in space, a receiver moving at high speed can pass through several fades in a small period of time. In a more serious case a receiver may stop at a particular location at which the received signal is in a deep fade. Maintaining good communications can then become very difficult, although passing vehicles or people walking in the vicinity of the mobile can often disturb the field pattern, thereby diminishing the likelihood of the received signal remaining in a deep null for a long period of time. Due to the relative motion between the mobile and the base station, each multipath wave experiences an apparent shift in frequency. The shift in received signal frequency due to motion is called Doppler shift, and is directly proportional to the velocity and direction of motion of the mobile with respect to the direction of arrival of the received multipath wave. In Fig. 1.3, the rapid variations of the small scale fading power are plotted as a function of the distance.

1.2.1 Factors Influencing Small-Scale Fading

Many physical factors in the radio propagation channel influence small-scale fading. These include the following:

- **Multipath Propagation:** The presence of reflecting objects and scatterers in the channel creates a constantly changing environment that dissipates the signal energy in amplitude, phase and time. These effects result in multiple versions of

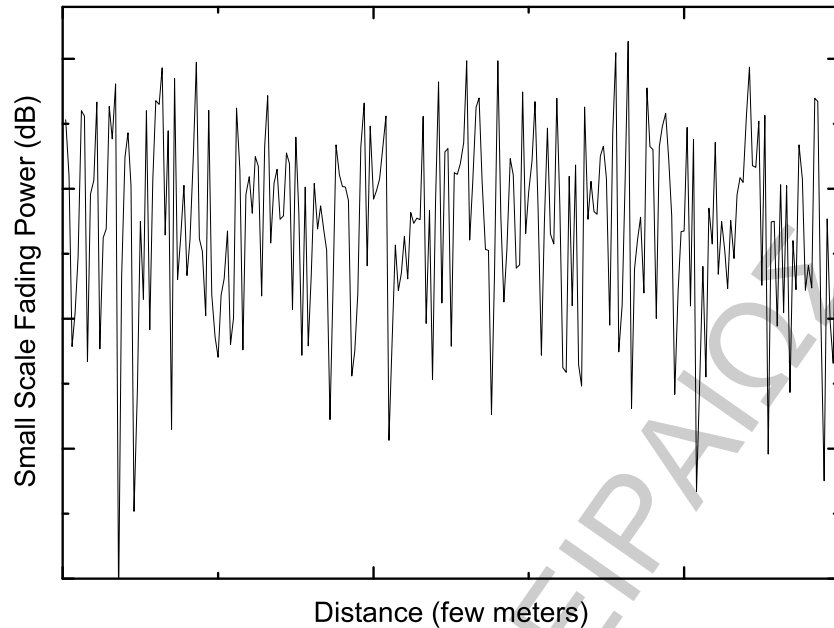


Figure 1.3: Power (in dB) of small-scale fading

the transmitted signal that arrive at the receiving antenna, displaced with respect to one another in time and spatial orientation. The random phase and amplitudes of the different multipath components cause fluctuations in signal strength thereby inducing small-scale fading, signal distortion or both.

- **Speed of the mobile:** The relative motion between the base station and the mobile results in random frequency modulation due to different Doppler shifts on each of the multipath components. Doppler shift will be positive or negative depending on whether the mobile receiver is moving toward or away from the base station.
- **Speed of surrounding objects:** If objects in the radio channel are in motion, they induce a time varying Doppler shift on multipath components. If the surrounding objects move at a greater rate than the mobile, then this effect dominates the small-scale fading. Otherwise motion of surrounding objects may be ignored and only the speed of the mobile need to be considered.
- **The transmission bandwidth of the signal:** If the transmitted radio signal bandwidth is greater than the "bandwidth" of the multipath channel, the received

signal will be distorted, but the received signal strength will not fade much over a local area, i.e., the small-scale fading will not be significant. If the transmitted signal has a narrow bandwidth as compared to the channel, the amplitude of the signal will change rapidly, but the signal will not be distorted. Thus the statistics of small-scale signal strength and the likelihood of signal smearing appearing over small-scale distances are very much related to the specific amplitudes and delays of the multipath channel, as well as the bandwidth of the transmitted signal.

1.2.2 Envelope and Phase Fluctuations

When a received signal experiences fading during transmission, both its envelope and phase fluctuate over time. For coherent modulations, the fading effects on the phase can severely degrade performance unless measures are taken to compensate for them at the receiver. Most often, analyses of systems employing such modulations assume that the phase effects due to fading are perfectly corrected at the receiver resulting in what is referred to as "ideal" coherent demodulation. For noncoherent modulations, phase information is not needed at the receiver and therefore the phase variation due to fading does not affect the performance. Hence, performance analyses for both ideal coherent and noncoherent modulations over fading channels requires knowledge of only the fading envelope statistics and will be the case most often considered in this text.

1.2.3 Slow and Fast Fading

The distinction between slow and fast fading is important for the mathematical modeling of fading channels and for the performance evaluation of communication systems operating over these channels. This notion is related to the coherence time T_c of the channel, which measures the period of time over which the fading process is correlated (or equivalently, the period of time after which the correlation function of two samples of the channel response taken at the same frequency but different time instants drops below a certain predetermined threshold). The coherence time is also related to the channel

Doppler spread f_d by $T_c \simeq 1/f_d$. The fading is said to be slow if the symbol time duration T_s is smaller than the channel's coherence time T_c ; otherwise it is considered to be fast. In slow fading a particular fade level will affect many successive symbols, which leads to burst errors, whereas in fast fading the fading decorrelates from symbol to symbol. In this latter case and when the communication receiver decisions are based on an observation of the received signal over two or more symbol times (such as differentially coherent or coded communications), it becomes necessary to consider the variation of the fading channel from one symbol interval to the next.

1.2.4 Frequency-Flat and Frequency-Selective Fading

Frequency selectivity is also an important characteristic of fading channels. If all the spectral components of the transmitted signal are affected in a similar manner, the fading is said to be frequency-nonsselective or equivalently frequency-flat. This is the case for narrowband systems, in which the transmitted signal bandwidth is much smaller than the channel's coherence bandwidth f_c . This bandwidth measures the frequency range over which the fading process is correlated and is defined as the frequency bandwidth over which the correlation function of two samples of the channel response taken at the same time but different frequencies falls below a suitable value. In addition the coherence bandwidth is related to the maximum delay spread τ_{\max} by $f_c \simeq 1/\tau_{\max}$. On the other hand, if the spectral components of the transmitted signal are affected by different amplitude gains and phase shifts, the fading is said to be frequency selective. This applies to wideband systems in which the transmitted bandwidth is bigger than the channel's coherence bandwidth.

1.3 Stochastic Modeling of Flat-Fading Channels

When fading affects narrowband systems, the received carrier amplitude is modulated by the fading amplitude X , where X is a RV with mean-square value $\Omega = E \langle X^2 \rangle$ and probability density function (PDF) $f_X(x)$, which is dependent on the nature of the

radio propagation environment. After passing through the fading channel, the signal is perturbed at the receiver by additive white Gaussian noise (AWGN), which is typically assumed to be statistically independent of the fading amplitude X , and which is characterized by a one-sided power spectral density N_0 Watts/Hertz. Equivalently, the received instantaneous signal power is modulated by X^2 . Thus, we define the instantaneous SNR per symbol by $\gamma = X^2 E_s / N_0$ and the average SNR per symbol by $\bar{\gamma} = \Omega E_s / N_0$, where E_s is the energy per symbol.

1.3.1 Small Scale Fading Stochastic Modeling

Multipath fading is due to the constructive and destructive combination of randomly delayed, reflected, scattered, and diffracted signal components. This type of fading is relatively fast and is therefore responsible for the short-term signal variations. Depending on the nature of the radio propagation environment, there are different models describing the statistical behavior of the multipath fading envelope.

1.3.1.1 Rayleigh

The Rayleigh distribution is frequently used to model multipath fading with no direct LOS path. In this case, the channel fading amplitude X is distributed according to

$$f_x(x) = \frac{2x}{\Omega} \exp\left(-\frac{x^2}{\Omega}\right), \quad x \geq 0 \quad (1.2)$$

where Ω is distribution scaling parameter. The instantaneous SNR per symbol of the channel γ is distributed according to

$$f_\gamma(\gamma) = \frac{1}{\bar{\gamma}} \exp\left(-\frac{\gamma}{\bar{\gamma}}\right), \quad \gamma \geq 0 \quad (1.3)$$

with cumulative distribution function (CDF) given by

$$\mathcal{F}_\gamma(\gamma) = 1 - \exp\left(-\frac{\gamma}{\bar{\gamma}}\right), \quad \gamma \geq 0. \quad (1.4)$$

The moments generating function (MGF) for this fading model is given by¹

$$\mathcal{M}_\gamma(s) = \frac{1}{1 + s\bar{\gamma}} \quad (1.5)$$

while the moments are given by

$$\mu_\gamma(n) = \Gamma(1 + n)\bar{\gamma}^n \quad (1.6)$$

where $\Gamma(\cdot)$ is Gamma function [4, eq. (8.310.1)]. The Rayleigh fading model therefore has an AF equal to 1, and typically agrees very well with experimental data for mobile systems where no LOS path exists between the transmitter and receiver antennas [3]. It also applies to the propagation of reflected and refracted paths through the troposphere [5] and ionosphere [6], and to ship-to-ship [7] radio links.

1.3.1.2 Nakagami- m

The Nakagami- m PDF is in essence a central chi-square distribution given by [8, eq. (11)]

$$f_R(x) = \frac{2m^m x^{2m-1}}{\Omega^m \Gamma(m)} \exp\left(-\frac{mx^2}{\Omega}\right), \quad x \geq 0 \quad (1.7)$$

where m is the Nakagami- m fading shaping parameter, $0.5 \leq m < \infty$ [8]. The PDF of γ can be obtained as

$$f_\gamma(\gamma) = \frac{m^m \gamma^{m-1}}{\bar{\gamma}^m \Gamma(m)} \exp\left(-\frac{m\gamma}{\bar{\gamma}}\right), \quad \gamma \geq 0 \quad (1.8)$$

with the corresponding CDF given by

$$\mathcal{F}_\gamma(\gamma) = 1 - \frac{\Gamma(m, m\gamma/\bar{\gamma})}{\Gamma(m)} \quad (1.9)$$

where $\Gamma(\cdot, \cdot)$ is the upper incomplete Gamma function [4, eq. (8.350/2)]. The MGF is given by

$$\mathcal{M}_\gamma(s) = \left(1 + \frac{s\bar{\gamma}}{m}\right)^{-m} \quad (1.10)$$

¹It is noted that the definition of all the MGF expressions presented in this theses is $\mathcal{M}_\gamma(s) \triangleq \mathbb{E} \langle \exp(-s\gamma) \rangle$, [3, eq. (5.62)].

and the moments are equal to

$$\mu_{\gamma}(n) = \frac{\Gamma(m+n)}{\Gamma(m)m^n} \bar{\gamma}^n. \quad (1.11)$$

Nakagami- m distribution includes as special cases the Gaussian distribution for $m = 0.5$ and Rayleigh for $m = 1$. As a limiting case, for $m \rightarrow \infty$, Nakagami- m converge to AWGN channel. Finally, the Nakagami- m distribution often gives the best fit to land•mobile and indoor•mobile [9] multipath propagation, as well as scintillating ionospheric radio links [10].

1.3.1.3 Weibull

The Weibull distribution [11] is yet another mathematical description of a probability model for characterizing amplitude fading in a multipath environment, particularly that associated with mobile radio systems operating in the 800/900 MHz frequency range [12, 13]. The PDF of the Weibull distribution is given by

$$f_R(x) = \beta \left[\frac{\Gamma(1+2/\beta)}{\Omega} \right]^{\beta/2} x^{\beta-1} \exp \left[- \left(\frac{x^2}{\Omega} \Gamma \left(1 + \frac{2}{\beta} \right) \right)^{\beta/2} \right], \quad x \geq 0 \quad (1.12)$$

where β is a parameter that is chosen to yield a best fit to measurement results and as such affords the shape flexibility of the Nakagami distributions. Furthermore, for $\beta = 2$ (1.12) becomes equal to the Rayleigh PDF. The PDF of γ is given by

$$f_{\gamma}(\gamma) = \frac{\beta}{2} \left[\frac{\Gamma(1+2/\beta)}{\bar{\gamma}} \right]^{\beta/2} \gamma^{\beta/2-1} \exp \left[- \left(\frac{\gamma}{\bar{\gamma}} \Gamma \left(1 + \frac{2}{\beta} \right) \right)^{\beta/2} \right], \quad \gamma \geq 0 \quad (1.13)$$

and the CDF is

$$\mathcal{F}_{\gamma}(\gamma) = 1 - \exp \left[- \left(\frac{\gamma}{\bar{\gamma}} \Gamma \left(1 + \frac{2}{\beta} \right) \right)^{\beta/2} \right], \quad \gamma \geq 0. \quad (1.14)$$

The MGF is given by [14]

$$\mathcal{M}_\gamma(s) = \left[\frac{\Gamma(1 + 2/\beta)}{\bar{\gamma}s} \right]^{\beta/2} \frac{\beta \lambda^{\beta/2} \sqrt{\kappa/\lambda}}{2 (\sqrt{2\pi})^{\kappa+\lambda-2}} G_{\lambda,\kappa}^{\kappa,\lambda} \left[\left(\frac{\Gamma(1 + 2/\beta)}{\bar{\gamma}} \right)^{\kappa\beta/2} \frac{\lambda^\lambda}{s^\lambda \kappa^\kappa} \middle| \begin{array}{l} \Delta(1, 1-\beta/2) \\ \Delta(\kappa, 0) \end{array} \right] \quad (1.15)$$

where $G[\cdot]$ is the Meijer-G function [4, eq.(9.301)] and $\Delta(x, y)$ is given by $\Delta(x, y) = y/x, (y+1)/x, \dots, (y+x-1)/x$. Furthermore, in (1.15) κ, λ are positive integers properly chosen in order to satisfy

$$\frac{\lambda}{\kappa} = \frac{\beta}{2}. \quad (1.16)$$

More specifically, depending upon the specific value of β , a set of minimum values of κ and λ can be properly chosen (e.g., for $\beta = 3.5$, we have to choose $\kappa = 2$ and $\lambda = 7$). Finally the moments of γ following Weibull distribution are given by

$$\mu_\gamma(n) = \left[\frac{\bar{\gamma}}{\Gamma(1 + 2/\beta)} \right]^n \Gamma \left(1 + \frac{2n}{\beta} \right). \quad (1.17)$$

1.3.1.4 Generalized-Gamma

The generalized-Gamma distribution (G_G), is a very general distribution for modeling small scale fading, which included all the preceding fading channel models. This distribution was introduced by Stacy, back in 1962, as a generalization of the (two-parameter) Gamma distribution [15]. Interestingly enough, despite its ability to characterize so many different fading channel models, only very recently it has been applied in the context of wireless communications [16, 17]. The PDF of the random variable (RV) R following the Γ_G distribution is given by

$$f_R(x) = \frac{\beta m^m x^{m\beta-1}}{\Omega^m \Gamma(m)} \exp \left(-\frac{m}{\Omega} x^\beta \right), \quad x \geq 0 \quad (1.18)$$

while the corresponding expression for the PDF of the SNR is given by

$$f_\gamma(\gamma) = \frac{\beta \gamma^{m\beta/2-1}}{2\Gamma(m) (\tau\bar{\gamma})^{m\beta/2}} \exp \left[-\left(\frac{\gamma}{\tau\bar{\gamma}} \right)^{\beta/2} \right], \quad \gamma \geq 0 \quad (1.19)$$

where $\tau = \Gamma(m)/\Gamma(m + 2/\beta)$. Setting different values to m and β , (1.19) simplifies to several important distributions for fading channel modeling. More specifically, for $\beta = 2$ and $m = 1$, it becomes Rayleigh, for $\beta = 2$, it becomes Nakagami- m and for $m = 1$, it becomes the Weibull. Moreover, as $b \rightarrow 0$ and $m \rightarrow \infty$, (1.19) approaches the well-known lognormal PDF. The CDF of (1.19) is given by

$$\mathcal{F}_\gamma(\gamma) = 1 - \frac{1}{\Gamma(m)} \Gamma \left[m, \left(\frac{\gamma}{\tau\bar{\gamma}} \right)^{\beta/2} \right], \gamma \geq 0. \quad (1.20)$$

The MGF of γ is given by [18, eq. (3)]

$$\mathcal{M}_\gamma(s) = \frac{\beta}{2\Gamma(m)} \frac{1}{(s\tau\bar{\gamma})^{m\beta/2}} \frac{\lambda^{m\beta/2} \sqrt{\kappa/\lambda}}{(\sqrt{2\pi})^{\kappa+\lambda-2}} G_{\lambda,\kappa}^{\kappa,\lambda} \left[\frac{\lambda^\lambda/\kappa^\kappa}{(s\tau\bar{\gamma})^{\kappa\beta/2}} \middle| \begin{matrix} \Delta(1,1-m\beta/2) \\ \Delta(\kappa,0) \end{matrix} \right] \quad (1.21)$$

while the moments are

$$\mu_\gamma(n) = (\tau\bar{\gamma})^n \frac{\Gamma(m + 2n/\beta)}{\Gamma(m)}. \quad (1.22)$$

1.3.1.5 $\eta - \mu$

The $\eta - \mu$ distribution is a general fading distribution that can be used to better represent the small scale variation of the fading signal in non-line-of-sight condition. The envelope R of the $\eta - \mu$ fading model can be written in terms of the in-phase and quadrature components of each one of the n clusters of the fading signal as

$$R^2 = \sum_{i=1}^n (X_i^2 + Y_i^2) \quad (1.23)$$

where X_i and Y_i are mutually independent Gaussian processes with zero-mean, $\mathbb{E}(X_i) = \mathbb{E}(Y_i) = 0$, with $\mathbb{E}(\cdot)$ denoting expectation, and non-identical variances so that $\mathbb{E}(X_i^2) = \sigma_X^2$ and $\mathbb{E}(Y_i^2) = \sigma_Y^2$. The envelope PDF is given by [19]

$$f_R(x) = \frac{4\sqrt{\pi}\mu^{\mu+1/2}h^\mu}{\Gamma(\mu)H^{\mu-1/2}\hat{x}} \left(\frac{x}{\hat{x}} \right)^{2\mu} \exp \left[-2\mu h \left(\frac{x}{\hat{x}} \right)^2 \right] I_{\mu-1/2} \left[2\mu H \left(\frac{x}{\hat{x}} \right)^2 \right] \quad (1.24)$$

where $\hat{x} = \sqrt{\Omega} = \sqrt{E(R^2)}$, $\eta = \sigma_X^2/\sigma_Y^2$ ($0 \leq \eta \leq 1$) and

$$\begin{aligned} h &= \frac{2 + \eta^{-1} + \eta}{4} \\ H &= \frac{\eta^{-1} - \eta}{4}. \end{aligned} \quad (1.25)$$

In (1.24), $I_\nu(\cdot)$ is the modified Bessel Function of the first kind and arbitrary order ν [4, eq. (8.406/1)] and $\mu > 0$ is the real extension of $n/2$ so that

$$\mu = \frac{E^2(R^2)}{V(R^2)} \times \frac{1 + \eta^2}{(1 + \eta)^2} \therefore \mu = \frac{\Omega^2}{E(R^2) - \Omega^2} \times \frac{1 + \eta^2}{(1 + \eta)^2} \quad (1.26)$$

with $V(\cdot)$ denoting variance. The PDF of the SNR γ of the $\eta - \mu$ distribution is

$$f_\gamma(\gamma) = \frac{2\sqrt{\pi}\mu^{\mu+1/2}h^\mu\gamma^{\mu-1/2}}{\Gamma(\mu)H^{\mu-1/2}\bar{\gamma}^{\mu+1/2}} \exp\left(-2\mu h\frac{\gamma}{\bar{\gamma}}\right) I_{\mu-1/2}\left(2\mu H\frac{\gamma}{\bar{\gamma}}\right) \quad (1.27)$$

while the CDF can be obtained as

$$\mathcal{F}_\gamma(\gamma, y) = \frac{2^{3/2-\mu}\sqrt{\pi}(1-\gamma^2)^\mu}{\Gamma(\mu)\gamma^{\mu-1/2}} \int_y^\infty \exp(-t^2)t^{2\mu}I_{\mu-1/2}(t^2\gamma)dt. \quad (1.28)$$

Furthermore the MGF of $\eta - \mu$ fading channel is obtained as

$$\mathcal{M}_\gamma(s) = \frac{2\sqrt{pi}}{\Gamma(\mu)h^\mu} \sum_{n=0}^{\infty} \frac{2^{-2n-2\mu}}{n!\Gamma(n + \mu + 1/2)} \left(\frac{H}{h}\right)^{2n}. \quad (1.29)$$

1.3.2 Large Scale Fading Stochastic Modeling

Communication system performance will depend only on shadowing if the radio receiver is able to average out the fast multipath fading or if an efficient "micro" diversity system is used to eliminate the effects of multipath. Empirical measurements reveal a general consensus that shadowing can be modeled by a log-normal distribution for various outdoor and indoor environments [10].

1.3.2.1 Lognormal

The PDF of the log-normal distribution is given by

$$f_{\gamma}(\gamma) = \frac{\xi}{\sqrt{2\pi}\sigma\gamma} \exp\left[-\frac{(10\log\gamma - \mu)^2}{2\sigma^2}\right], \quad \gamma \geq 0 \quad (1.30)$$

where $\xi = 10/\ln 10$ and μ, σ are the mean and the standard deviation, in dB, of $10\log\gamma$, respectively. The MGF of γ is

$$\mathcal{M}_{\gamma}(s) \simeq \frac{1}{\sqrt{\pi}} \sum_{n=1}^{N_p} H_{x_n} \exp\left(10^{(\sqrt{2}\sigma x_n + \mu)/10} s\right) \quad (1.31)$$

where x_n and H_{x_n} are the zeros and weight factors of the N_p th order Hermite polynomial, respectively [20, pp. (924)]. Finally, the moments of γ of the lognormal distribution are

$$\mu_{\gamma}(n) = \exp\left[\frac{n}{\xi}\mu + \frac{1}{2}\left(\frac{n}{\xi}\right)^2\sigma^2\right]. \quad (1.32)$$

1.3.3 Composite multipath/shadowing fading environments

Composite multipath/shadowing fading environments are frequently encountered in wireless communication systems. The generalized- K distribution fading model characterizes the combined effect of fast and slow fading on the received signal by using two shaping parameters m and k , where m is the Nakagami parameter for the short-term fading and k is the parameter of the Gamma distribution for the received average power due to shadowing. Assuming that the fading environment is such that the signal envelope X in a receive antenna is a generalized- K distributed random variable, its pdf is given by [21]

$$f_X(x) = \frac{4m^{(k+m)/2}}{\Gamma(m)\Gamma(k)\Omega^{(k+m)/2}} x^{k+m-1} K_{k-m}\left(2\left(\frac{m}{\Omega}\right)^{1/2} x\right), \quad x \geq 0 \quad (1.33)$$

where k and m are the distribution's shaping parameters, $\Omega = E[X^2]/k$ is the mean power with $E[\cdot]$ denoting expectation, $\Gamma[\cdot]$ is the Gamma function, and $K_{k-m}[\cdot]$ is the $(k-m)$ th order modified Bessel function of the second kind [4]. The instantaneous received SNR per bit of a single branch is $\gamma = X^2 E_b/N_0$, where E_b is the average bit energy and N_0

is the single-sided power spectral density of the additive white Gaussian noise (AWGN). The corresponding average received SNR per bit is given as $\bar{\gamma} = k\Omega \cdot E_b/N_0$. The pdf of γ can be obtained from (1.33) by an appropriate change of variables, as [21]

$$f_\gamma(\gamma) = \frac{2\Xi^{\frac{k+m}{2}}}{\Gamma(m)\Gamma(k)} \gamma^{\frac{k+m}{2}-1} K_{k-m} \left(2\sqrt{\Xi\gamma} \right), \quad \gamma \geq 0 \quad (1.34)$$

with $\Xi = (km)/\bar{\gamma}$. Using [22, eq. (03.04.21.0007.01)], the cdf of γ , defined as $F_\gamma(\gamma) \triangleq \int_0^\gamma f_\gamma(\gamma) d\gamma$, is given by [23]

$$F_\gamma(\gamma) = \frac{\Gamma(k-m)}{\Gamma(k)\Gamma(1+m)} (\Xi\gamma)^m {}_1F_2(m; 1-k+m, 1+m; \Xi\gamma) + \frac{\Gamma(m-k)}{\Gamma(m)\Gamma(1+k)} (\Xi\gamma)^k {}_1F_2(k; 1+k-m, 1+k; \Xi\gamma), \quad \gamma \geq 0 \quad (1.35)$$

where ${}_pF_q(\cdot)$ is the generalized hypergeometric function [4, eq. (9.14.1)] and p, q are integers. The formula in (1.35) can be evaluated for arbitrary values of k and m , provided that $(k-m)$ is not an integer. The MGF of γ is defined as $M_\gamma(s) = \int_0^\infty e^{-s\gamma} f_\gamma(\gamma) d\gamma$. Substituting $f_\gamma(\gamma)$ given by (1.34) in this expression and expressing $K_\nu(\cdot)$ in terms of Meijer's G -function using [22, eq. (03.04.26.0009.01)], we obtain

$$M_\gamma(s) = \frac{\Xi^{\frac{k+m}{2}}}{\Gamma(m)\Gamma(k)} \int_0^\infty e^{-s\gamma} \gamma^{\frac{k+m}{2}-1} G_{0,2}^{2,0} \left(\Xi\gamma \left| \begin{matrix} k-m \\ 2 \end{matrix}, -\frac{k-m}{2} \right. \right) d\gamma \quad (1.36)$$

Using [4, eq. (7.813.1)], the integral in (1.36) can be solved in terms of the G -function. Moreover, using the functional relations [4, eq. (9.31.5)] and [4, eq. (9.31.2)], the final result is given in closed form as

$$M_\gamma(s) = \frac{1}{\Gamma(m)\Gamma(k)} G_{2,1}^{1,2} \left(\begin{matrix} s \\ \Xi \end{matrix} \left| \begin{matrix} 1-k, 1-m \\ 0 \end{matrix} \right. \right) \quad (1.37)$$

Note that using [22, eq. (07.34.03.0391.01)] and [22, eq. (07.34.03.0392.01)] for the G -function the result in (1.37) can also be written in terms of the confluent hypergeometric function ${}_1F_1(a; b; z)$ and the Tricomi confluent hypergeometric function $U(a, b, z)$, respectively.

Chapter 2

Introduction to Relay Systems

HERE IS growing interest in the use of relay-assisted transmission schemes to provide system performance improvement in terms of system reliability and cooperative diversity. Cooperative diversity can combat channel impairments due to fading in wireless communication systems. The cooperative diversity through multihop relaying technology has emerged as an effective tool to enhance the spectral efficiency and extend the coverage of cellular and ad hoc wireless networks [24], [25]. In particular, multihop relaying can enable the source and destination nodes to communicate through a set of cooperating relay nodes in which the transmitted signals propagate through cascaded relay nodes, with the aim of extending coverage and improving the performance of the network. For example, idle mobile stations between the source and destination may be employed as relay nodes to provide extra diversity links [26].

The signal received at the relay is usually processed before it is forwarded to the destination and there are several signal relaying protocols [27]. In the most commonly used signal processing technique at the relay, the information from the previous node is simply amplified and forwarded to the next node; this is known as amplify-and-forward (AF) relaying. AF relaying protocol is very simple to implement as the relaying node essentially acts as an analog repeater. However, in large networks with many geographically distributed nodes, AF relaying may be difficult to scale due to the strict synchronization requirement. Alternatively, the receiving node may first decode the information in the

received signal and then re-encode it before forwarding it to the next node; this relaying format is referred to as decode-and-forward (DF) relaying. DF relaying provides the possibility to vary the communication rate and prevents error propagation, but leads to higher decoder complexity. Other relay processing techniques have also been studied in the literature. For example, the decode-amplify-and-forward (DAF) in which the relay performs soft decoding and forwards the reliability information at the output of the decoder instead of that extracted directly from the raw channel, to the destination. The DAF protocol combines the merit of both AF and DF [28]. Also, the estimate-and-forward relay (EF) transmits a hyperbolic tangent function of the received signal to the destination [27]; the piecewise-and-forward (PF) provides a fine segment approximation of the EF protocol [29], while in several other protocols the relays provide more complicated functions of the received signals to the destination [30].

The performances of multihop AF and DF relaying systems in a thermal noise-limited environment have been studied extensively [31, 32, 33]. In these systems, it is well known that the choice of the relay gain that maximizes the end-to-end signal-to-noise ratio (SNR) is to invert the combined instantaneous received power (i.e., sum of desired signal and noise power) at each relay node.

2.1 Dual-hop AF relaying system

We consider a wireless communication system in which a source sends a message $x_s(t)$ to a destination via a non-regenerative relay. The signal received at the relay is given by

$$y_R(t) = \sqrt{P_s}\alpha_1 x_s(t) + n_1(t) \quad (2.1)$$

where P_s is the transmit power, α_1 is the instantaneous fading amplitude of the channel between the source and the relay, and $n_1(t)$ is the additive white Gaussian noise (AWGN) with average power σ_1^2 at the input of the relay. An amplify-and-forward (AF) relay multiplies the signal $y_R(t)$ by a gain G and then re-transmits it to the destination, where

the received signal is given by

$$y_D(t) = \alpha_2 G y_R(t) + n_2(t) = \alpha_2 G \left\{ \sqrt{P_s} \alpha_1 x_s(t) + n_1(t) \right\} + n_2(t). \quad (2.2)$$

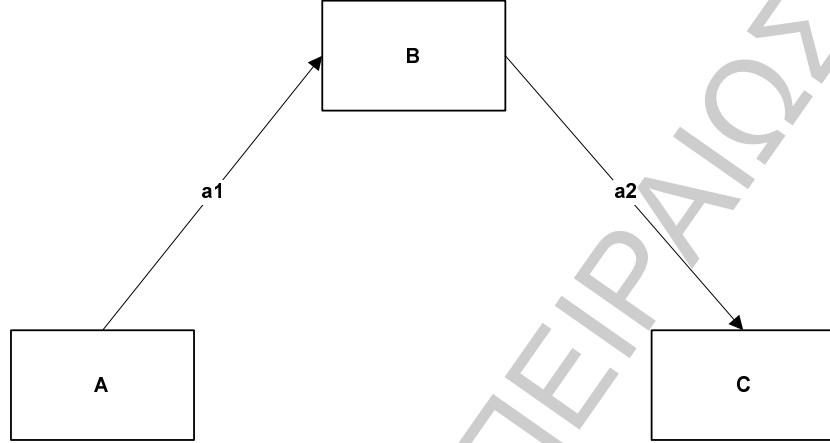


Figure 2.1: Example of Dual-hop relay system

In (2.2), α_2 denotes the fading envelope on the link between the relay and the destination, and σ_2^2 is the noise power at the destination node. In general, the choice of the node gain, G , determines the end-to-end SNR.

The resulting SNR at the destination node may be expressed as

$$\gamma_{eq} = \frac{P_s \alpha_1^2 \alpha_2^2 G^2}{\alpha_2^2 \sigma_1^2 G^2 + \sigma_2^2} = \frac{P_s \alpha_1^2 \alpha_2^2}{\alpha_2^2 \sigma_1^2 + \frac{\sigma_2^2}{G^2}} = \frac{\frac{P_s \alpha_1^2 \alpha_2^2}{\sigma_1^2 \sigma_2^2}}{\frac{\alpha_2^2}{\sigma_2^2} + \frac{1}{G^2 \sigma_1^2}} \quad (2.3)$$

1. The best choice of the relay gain that maximizes the end-to-end SINR requires the knowledge of the channel state information (CSI), which includes the signal fading level as well as the noise power on the source-relay link. In such CSI-based relays, the amplification gain at the relay is chosen to invert the fading state of the preceding link. Following the two-parameter model proposed in [27], the corresponding relay gain is chosen as

$$G^2 = \frac{P_R}{P_s \alpha_1^2 + \sigma_1^2}, \quad (2.4)$$

where P_R is the relay output power.

Substituting (2.4) in (2.3), the end-to-end SNR becomes

$$\gamma_{eq} = \frac{\frac{P_s \alpha_1^2 \alpha_2^2}{\sigma_1^2 \sigma_2^2}}{\frac{\alpha_2^2}{\sigma_2^2} + \frac{P_s \alpha_1^2 + \sigma_1^2}{P_R \sigma_1^2}} = \frac{\frac{P_s \alpha_1^2 P_R \alpha_2^2}{\sigma_1^2 \sigma_2^2}}{\frac{P_R \alpha_2^2}{\sigma_2^2} + \frac{P_s \alpha_1^2 + \sigma_1^2}{\sigma_1^2}} = \frac{\frac{P_s \alpha_1^2 P_R \alpha_2^2}{\sigma_1^2 \sigma_2^2}}{\frac{P_R \alpha_2^2}{\sigma_2^2} + \frac{P_s \alpha_1^2}{\sigma_1^2} + 1} = \frac{\gamma_1 \gamma_2}{\gamma_2 + \gamma_1 + 1} \quad (2.5)$$

where $\gamma_1 = P_s \alpha_1^2 / \sigma_1^2$ is the instantaneous SNR on the source-relay link, $\gamma_2 = P_R \alpha_2^2 / \sigma_2^2$ is the instantaneous SNR on the relay-destination link.

2. A possible option for the gain, is the channel inversion [31]:

$$G^2 = \frac{P_R}{P_s a_1^2} \quad (2.6)$$

The equivalent end-to-end SNR for such a case:

$$\gamma_{eq} = \frac{\gamma_1 \gamma_2}{\gamma_1 + \gamma_2} \quad (2.7)$$

where $\gamma_i = \frac{a_i^2}{N_0}$, $i = 1, 2$ is the instantaneous SNR of the i -th link.

3. There is another category of relays, called Fixed Gain Relays, in which the value of Gain is fixed. Relays belong in this category, due to the fixed gain they do not require complex circuits, and they are efficient enough. Also, for lower values of SNR Fixed Gain Relays perform better than CSI Relays. Fixed Gain Relays are separated into two sub-categories: "Blind" and "Semi-Blind" Relays.

2.1.1 Blind Relays

$$C = \frac{P_R}{G^2 \sigma_1^2} \quad (2.8)$$

The end-to-end SNR at the destination is then given by

$$\gamma_{eq} = \frac{\frac{P_s \alpha_1^2 \alpha_2^2}{\sigma_1^2 \sigma_2^2}}{\frac{\alpha_2^2}{\sigma_2^2} + \frac{1}{G^2 \sigma_1^2}} = \frac{\frac{P_s \alpha_1^2 \alpha_2^2}{\sigma_1^2 \sigma_2^2}}{\frac{\alpha_2^2}{\sigma_2^2} + \frac{C \sigma_1^2}{P_R \sigma_1^2}} = \frac{\frac{P_s \alpha_1^2 P_R \alpha_2^2}{\sigma_1^2 \sigma_2^2}}{\frac{P_R \alpha_2^2}{\sigma_2^2} + C} = \frac{\gamma_1 \gamma_2}{\gamma_2 + C} \quad (2.9)$$

2.1.2 Semi-Blind Relays

The Gain is chosen as:

$$G^2 = E \left[\frac{P_R}{P_s a_1^2 + \sigma_1^2} \right] = \frac{P_R}{P_s E[a_1^2] + \sigma_1^2} \quad (2.10)$$

The end-to-end SNR at the destination is then given by

$$\gamma_{eq} = \frac{\frac{P_s \alpha_1^2 \alpha_2^2}{\sigma_1^2 \sigma_2^2}}{\frac{\alpha_2^2}{\sigma_2^2} + \frac{1}{G^2 \sigma_1^2}} = \frac{\gamma_1 \gamma_2}{\gamma_2 + \bar{\gamma}_1 + 1} \quad (2.11)$$

Fig. 2.2 shows the different categories of relay systems.

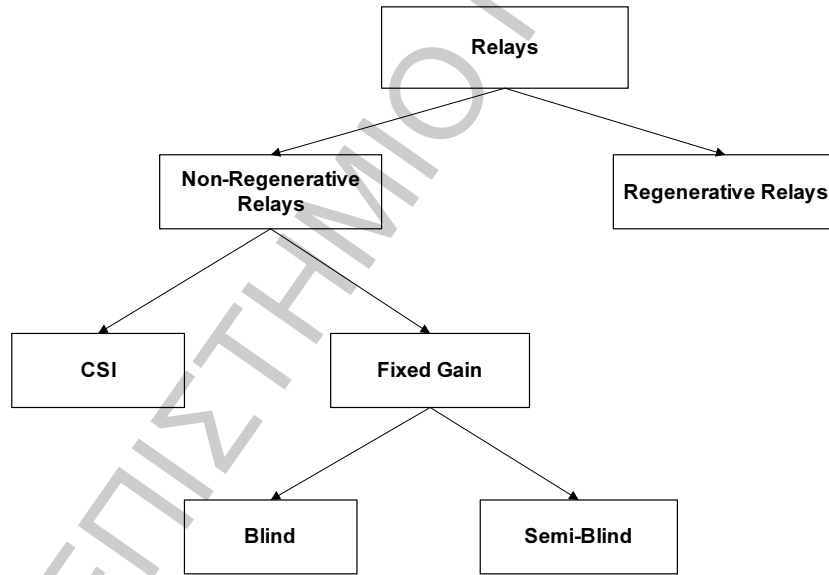


Figure 2.2: Relay Categories

2.2 Multi-hop AF relaying system

In Fig. 2.3, the signal power and the noise power components at the destination hop D are given by

$$S = (\alpha_1^2 \alpha_2^2 \dots \alpha_M^2) (G_1^2 G_2^2 \dots G_{M-1}^2) \quad (2.12)$$

$$\begin{aligned}
 N &= N_{0,1} (G_1^2 G_2^2 \dots G_{M-1}^2) (\alpha_2^2 \alpha_3^2 \dots \alpha_M^2) + N_{0,2} (G_2^2 G_3^2 \dots G_{M-1}^2) (\alpha_3^2 \alpha_4^2 \dots \alpha_M^2) \\
 &+ N_{0,3} (G_3^2 G_4^2 \dots G_{M-1}^2) (\alpha_4^2 \alpha_5^2 \dots \alpha_M^2) + \dots + N_{0,M}
 \end{aligned} \tag{2.13}$$

Consequently, the end-to-end SNR is given by

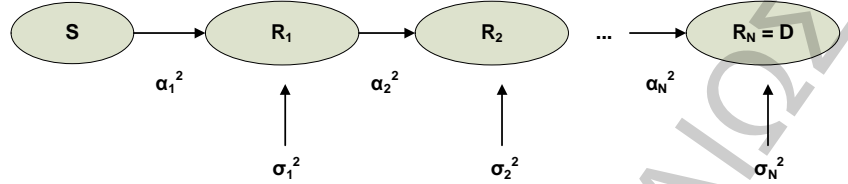


Figure 2.3: Multi-hop relay system with the presence of interference and noise

$$\gamma_{eq} = \frac{\prod_{n=1}^M \alpha_n^2 \prod_{n=1}^{M-1} G_n^2}{\sum_{n=1}^M N_{0,n} \prod_{s=n+1}^M \alpha_s^2 \prod_{s=n}^{M-1} G_s^2} \tag{2.14}$$

Next divide both nominator and denominator in (2.14) by $\prod_{n=1}^M N_{0,n} \prod_{n=1}^{M-1} G_n^2$. The nominator is then given by

$$\text{Nominator} = \prod_{n=1}^M \frac{\alpha_n^2}{N_{0,n}} \tag{2.15}$$

The denominator is given by

$$\text{Denominator} = \sum_{n=1}^M \frac{\prod_{s=n+1}^M \frac{\alpha_s^2}{N_{0,s}}}{\prod_{s=1}^{n-1} G_s^2 \prod_{s=1}^{n-1} N_{0,s}} \tag{2.16}$$

If we select as the AF gain at the j^{th} relay to be

$$G_j^2 = \frac{1}{\alpha_j^2 + N_{0,j}} \tag{2.17}$$

Substituting (2.17) in (2.16), we have

$$\text{Denominator} = \sum_{n=1}^M \prod_{s=n+1}^M \frac{\alpha_s^2}{N_{0,s}} \prod_{s=1}^{n-1} \left(\frac{\alpha_s^2}{N_{0,s}} + 1 \right) \tag{2.18}$$

Dividing (2.15) by (2.18), the equivalent end-to-end SNR is given by

$$\gamma_{eq} = \frac{\prod_{n=1}^M \frac{\alpha_n^2}{N_{0,n}}}{\sum_{n=1}^M \prod_{s=n+1}^M \frac{\alpha_s^2}{N_{0,s}} \prod_{s=1}^{n-1} \left(\frac{\alpha_s^2}{N_{0,s}} + 1 \right)} = \left[\sum_{n=1}^M \frac{1}{\gamma_n} \prod_{s=1}^{n-1} \left(1 + \frac{1}{\gamma_s} \right) \right]^{-1} \tag{2.19}$$

where now

$$\gamma_j = \frac{\alpha_j^2}{N_{0,j}} \quad (2.20)$$

2.3 Multi-hop DF relay system

Since in DF relaying systems, the end-to-end performance is usually dominated by that of the weakest link, it follows that the end-to-end SNR for DF is given by [32], [34]

$$\gamma_{eq} \leq \gamma_{DF} = \min(\gamma_1, \dots, \gamma_N) \quad (2.21)$$

It is well known that, in this case, the cdf of γ_{DF} is given by

$$\begin{aligned} F_{\gamma_{DF}}(\gamma) &= \Pr[\min(\gamma_1, \dots, \gamma_N) < \gamma] = 1 - \Pr[\gamma_1 > \gamma, \dots, \gamma_N > \gamma] = \\ &= 1 - \prod_{n=1}^N (1 - F_{\gamma_n}(\gamma)) \end{aligned} \quad (2.22)$$

The end-to-end SINR for DF relaying given in (2.21) is known to be an upper bound for the end-to-end SINR of AF relaying. Therefore, it is frequently being used in the performance analysis of AF relaying systems to yield lower bound performance bounds of AF transmission schemes. The performances of AF and DF relaying systems converge for high values of the end-to-end SNR.

Chapter 3

On the Error Rate Analysis of Dual-Hop Amplify-and-Forward Relaying in Generalized- K Fading Channels

IN THIS CHAPTER, we present novel and easy-to-evaluate expressions for the error rate performance of cooperative dual-hop relaying with maximal ratio combining operating over independent generalized- K fading channels. It is hard to obtain a closed-form expression for the moment generating function (MGF) of the end-to-end signal-to-noise ratio (SNR) at the destination, even for the case of a single dual-hop relay link. Therefore, we employ two different upper bound approximations for the output SNR, of which one is based on the minimum SNR of the two hops for each dual-hop relay link and the other is based on the geometric mean of the SNRs of the two hops. Lower bounds for the symbol and bit error rates for a variety of digital modulations can then be evaluated using the MGF based approach. The final expressions are useful in the performance evaluation of amplify-and-forward relaying in a generalized composite radio environment.

3.1 Introduction

Cooperative diversity with relays has been shown to provide high data rate coverage and mitigate channel impairments in next generation wireless systems. Amplify-and-forward

relay techniques have attracted a lot of attention recently as they provide a simple way to implement collaborative/cooperative wireless communication systems. For dual-hop non-regenerative systems, the end-to-end signal-to-noise ratio (SNR) at the receiving node depends on the amplification gain employed at the relays. For relays with channel side information (CSI) of the first link, the end-to-end SNR of a single dual-hop relay link has been obtained in [31]. For this relay transmission scenario, analytical performance results have been obtained by approximating the end-to-end SNR by the harmonic mean of the SNRs of the two hops [35], their geometric mean [36], and the minimum SNR of the two hops [37], [38]. Among the proposed approximations for the end-to-end SNR of dual-hop transmission, the harmonic mean and the minimum SNR bounds have been shown to result in tight performance bounds [35], [37], whereas the geometric mean bound has been shown to give accurate results for low and medium values of the SNR per hop [36], [37]. Using one of the above proposed upper bounds for the total SNR, the performance of dual-hop relaying has been studied in terms of outage probability and average bit error rate (BER) for various symmetrical fading conditions, such as Rayleigh [31], Nakagami- m [35], [37], Weibull [38], and generalized Gamma [39] fading, as well as for asymmetrical links [40], although most analyzes have been restricted to single dual-hop relay links.

The generalized- K fading model [21] has also attracted considerable attention as one of the most general wireless fading models that can characterize the combined effects of fast and slow fading on the received signal. This fading model corresponds to a Nakagami-Gamma composite distribution and is controlled by two shaping parameters m and k , where m is the Nakagami parameter for the short-term fading and k is the parameter of the gamma distribution for the received average power due to shadowing [21]. Note that the K distribution [41] is derived as a special case of the generalized- K distribution by letting $m = 1$ (i.e., Rayleigh short-term fading). A number of results on the performance analysis of communication links in this fading model can be found in the literature [42], [43].

Recently, analytical expressions for the error rate performance of dual-hop relaying

over generalized- K fading channels were given in terms of convergent infinite series in [44], using the minimum SNR upper bound for the end-to-end SNR and averaging the conditional BER over the derived probability density function (pdf) of the total SNR. However, these expressions are restricted to a single dual-hop relay system and result in some truncation error depending on the number of terms employed. Furthermore, the expressions in [44] cannot be evaluated for integer values of the shaping parameter k . In this chapter, using both the minimum SNR and the geometric mean upper bounds for the end-to-end SNR of a single relay link and employing the moment generating function (MGF) based approach, we present novel expressions for the error rate performance of multiple dual-hop relaying with MRC operating over independent generalized- K fading channels with integer values of fading parameter m and arbitrary values of fading parameter k . Note that using the geometric mean approximation of the total SNR, independent non-identical fading in the two hops of each relay, i.e., source-to-relay and relay-to-destination, can be considered, whereas the minimum SNR performance bound is restricted to independent and identically distributed (i.i.d.) fading channels.

The rest of the chapter is organized as follows. In Section II we present the statistics of the generalized- K distribution, i.e., the pdf, cumulative density function (cdf), and MGF of the instantaneous received SNR of a single direct link. In Section III, using the MGF based approach, we derive the average symbol error rate (SER) of multiple dual-hop relay links with MRC at the receiver side. Numerical and simulation results are given in Section IV, while concluding remarks are given in Section V.

3.2 Statistics of the Generalized- K Distribution

We assume that the fading environment is such that the signal envelope X in a receive antenna is a generalized- K distributed random variable with pdf given by [21]

$$f_X(x) = \frac{4m^{(k+m)/2}}{\Gamma(m)\Gamma(k)\Omega^{(k+m)/2}} x^{k+m-1} K_{k-m} \left(2 \left(\frac{m}{\Omega} \right)^{1/2} x \right), \quad x \geq 0 \quad (3.1)$$

where k and m are the distribution's shaping parameters, $\Omega = E[X^2]/k$ is the mean power with $E[\cdot]$ denoting expectation, $\Gamma(\cdot)$ is the Gamma function, and $K_{k-m}(\cdot)$ is the $(k-m)$ th order modified Bessel function of the second kind [4].

The instantaneous received SNR per symbol of a single receive branch is $\gamma = X^2 E_s / N_0$, where E_s is the average symbol energy and N_0 is the single-sided power spectral density of the additive white Gaussian noise (AWGN). The corresponding average received SNR per symbol is given as $\bar{\gamma} = k\Omega E_s / N_0$. The PDF of γ is given by

$$f_\gamma(\gamma) = \frac{2\Xi^{\frac{k+m}{2}}}{\Gamma(m)\Gamma(k)} \gamma^{\frac{k+m}{2}-1} K_{k-m}\left(2\sqrt{\Xi\gamma}\right), \gamma \geq 0 \quad (3.2)$$

with $\Xi = (km)/\bar{\gamma}$. The CDF of γ , defined as $F_\gamma(\gamma) = \int_0^\gamma f_\gamma(x)dx$, has been obtained in [45] for integer values of m and arbitrary values of k , as

$$F_\gamma(\gamma) = 1 - \frac{2(\Xi\gamma)^{\frac{k}{2}}}{\Gamma(k)} \sum_{q=0}^{m-1} \frac{1}{q!} (\Xi\gamma)^{\frac{q}{2}} K_{k-q}\left(2\sqrt{\Xi\gamma}\right), \quad (3.3)$$

Moreover the MGF of γ defined as $M_\gamma(-s) = \int_0^\infty e^{-s\gamma} f_\gamma(\gamma)d\gamma$, is given by [45]

$$M_\gamma(-s) = \frac{1}{\Gamma(m)\Gamma(k)} G_{2,1}^{1,2} \left[\frac{s}{\Xi} \middle| \begin{matrix} 1-k, 1-m \\ 0 \end{matrix} \right] \quad (3.4)$$

where $G[\cdot]$ is the Meijer's G-function [4, eq. (9.301)].

3.3 End-to-End Error Rate Analysis

We consider a dual-hop relay system with N relays as well as a direct link between the source and the destination, as shown in Fig. 3.1. The output SNR, assuming MRC at the destination receiving end, can be written as

$$\gamma_{\text{out}} = \gamma_0 + \sum_{\ell=1}^N \gamma_{\text{end}}(\ell), \quad (3.5)$$

where γ_0 is the SNR of the direct link and $\gamma_{\text{end}}(\ell)$ is the end-to-end SNR of the ℓ -th relay. For amplify-and-forward relays with CSI at the relays, $\gamma_{\text{end}}(\ell)$ is known to be given by the harmonic mean of the three positive random variables $(\gamma_{\ell 1}, \gamma_{\ell 2}, \gamma_{\ell 1}\gamma_{\ell 2})$, i.e.,

$\gamma_{\text{end}}(\ell) = \frac{\gamma_{\ell 1} \gamma_{\ell 2}}{\gamma_{\ell 1} + \gamma_{\ell 2} + 1}$ [31]. Assuming independent fading in all relay links, the MGF of the output SNR is then given by

$$\mathcal{M}_{\gamma_{\text{out}}}(-s) = \mathcal{M}_{\gamma_0}(-s) \prod_{\ell=1}^N \mathcal{M}_{\gamma_{\text{end}}(\ell)}(-s) \quad (3.6)$$

For the generalized- K fading environment, $M_{\gamma_0}(-s)$ is given by (3.4). In order to obtain mathematically tractable results for the MGF of $\gamma_{\text{end}}(\ell)$, the end-to-end SNR for the relay channel has been approximated by different upper bounds [35],[36], [37]. In this chapter, for the generalized- K fading environment, we consider the approximations of minimum SNR [37] and geometric mean [36].

It follows that the average SER and BER performances for a variety of digital modulations can be evaluated using the MGF based approach. For example, the average SER for M -ary phase-shift keying (M -PSK) is given by

$$P_{e,\text{MPSK}} = \frac{1}{\pi} \int_0^{(M-1)\pi/M} \mathcal{M}_{\gamma_{\text{out}}}\left(-\frac{g_M}{\sin^2\theta}\right) d\theta, \quad (3.7)$$

where $g_M = \sin^2(\pi/M)$, whereas for M -ary quadrature amplitude modulation (M -QAM) the average SER is given by

$$P_{e,\text{MQAM}} = \frac{4q}{\pi} \int_0^{\pi/2} \mathcal{M}_{\gamma_{\text{out}}}\left(-\frac{g_Q}{\sin^2\theta}\right) d\theta - \frac{4q^2}{\pi} \int_0^{\pi/4} \mathcal{M}_{\gamma_{\text{out}}}\left(-\frac{g_Q}{\sin^2\theta}\right) d\theta, \quad (3.8)$$

where $q = 1 - 1/\sqrt{M}$ and $g_Q = 3/(2(M-1))$.

3.3.1 Performance using the minimum SNR approximation

The end-to-end SNR of a dual-hop relay system with multiple relays and a direct link between the source and the destination can be approximated by its upper bound γ_a as follows [37]

$$\gamma_{\text{out}} \leq \gamma_a = \gamma_0 + \sum_{\ell=1}^N \gamma_{\text{min}}(\ell), \quad (3.9)$$

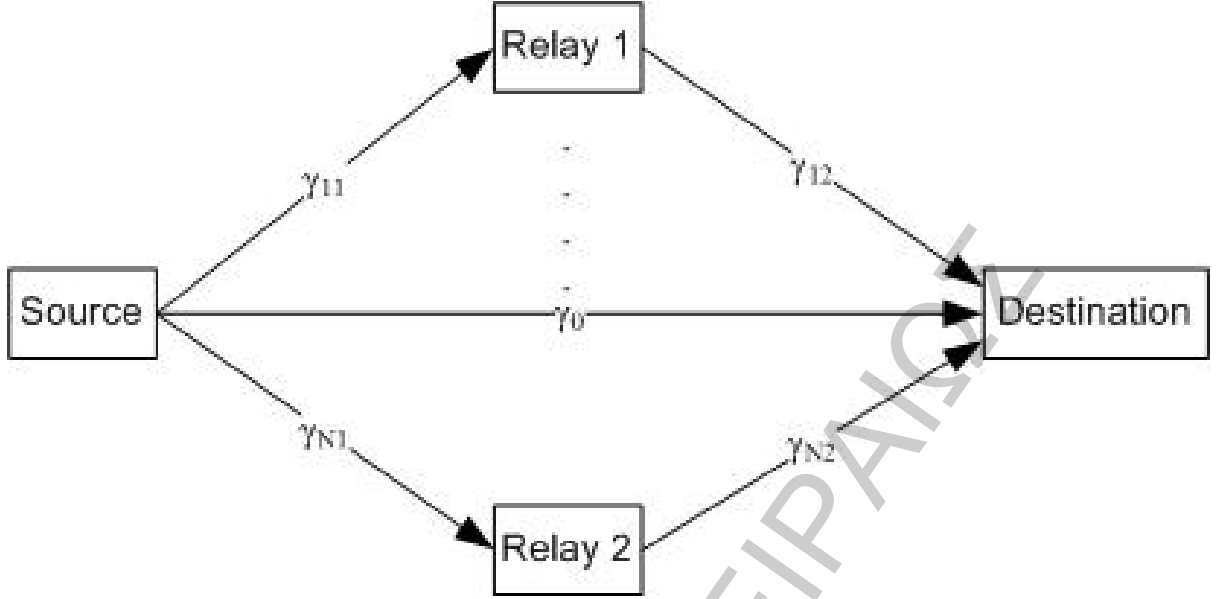


Figure 3.1: Cooperative dual-hop relay transmission scheme with MRC at the destination.

where $\gamma_{\min}(\ell) = \min(\gamma_{\ell 1}, \gamma_{\ell 2})$, $\ell = 1, \dots, N$. The pdf of $\gamma_{\min}(\ell)$ is given by [4]

$$f_{\gamma_{\min}(\ell)}(\gamma) = f_{\gamma_{\ell 1}}(\gamma) + f_{\gamma_{\ell 2}}(\gamma) - [f_{\gamma_{\ell 1}}(\gamma)F_{\gamma_{\ell 2}}(\gamma) + F_{\gamma_{\ell 1}}(\gamma)f_{\gamma_{\ell 2}}(\gamma)] \quad (3.10)$$

Using (3.10), the MGF of $\gamma_{\min}(\ell)$ is given by

$$\begin{aligned} \mathcal{M}_{\gamma_{\min}(\ell)}(-s) &= \int_0^{\infty} e^{-s\gamma} f_{\gamma_{\min}(\ell)}(\gamma) d\gamma \\ &= \mathcal{M}_{\gamma_{\ell 1}}(-s) + \mathcal{M}_{\gamma_{\ell 2}}(-s) - [\mathcal{M}_{\gamma_{\ell 12}}(-s) + \mathcal{M}_{\gamma_{\ell 21}}(-s)] \end{aligned} \quad (3.11)$$

where

$$\mathcal{M}_{\gamma_{\ell ij}}(-s) = \int_0^{\infty} e^{-s\gamma} f_{\gamma_{\ell i}}(\gamma) F_{\gamma_{\ell j}}(\gamma) d\gamma \quad (3.12)$$

for $i, j \in \{1, 2\}$. In order to derive closed form analytical results, we consider i.i.d. fading for the source-to-relay and relay-to-destination links. Using (3.3) in (3.12) we obtain

$$\mathcal{M}_{\gamma_{\ell ij}}(-s) = \mathcal{M}_{\gamma_{\ell i}}(-s) - I(-s) \quad (3.13)$$

where

$$I(-s) = \frac{4\Xi^{\frac{2k+m}{2}}}{\Gamma(m)\Gamma^2(k)} \sum_{r=0}^{m-1} \frac{1}{r!} (\Xi)^{\frac{r}{2}} \int_0^{\infty} e^{-s\gamma} \gamma^{k+\frac{m+r}{2}-1} K_{k-m} \left(2\sqrt{\Xi}\gamma \right) K_{k-r} \left(2\sqrt{\Xi}\gamma \right) d\gamma \quad (3.14)$$

Note that in (3.14) we dropped the subscripts on k , m , and Ξ , for simplicity. By expressing the product of two Bessel K -functions in terms of the Meijer G -function using [22, eq. 03.04.26.0016.01] and evaluating the resulting integral using [4, eq. (7.813.1)], followed by the functional relationships [4, eq. (9.31.5)] and [4, eq. (9.31.2)], the final result is given by

$$I(-s) = \frac{\sqrt{\pi}}{2^{2k+m-1}\Gamma(m)\Gamma^2(k)} \cdot \sum_{r=0}^{m-1} \frac{1}{2^r r!} G_{4,3}^{1,4} \left(\frac{s}{4\Xi} \left| \begin{array}{l} 1-2k, 1-k-r, 1-k-m, 1-m-r \\ 0, 1-k-\frac{m+r}{2}, -k-\frac{m+r-1}{2} \end{array} \right. \right) \quad (3.15)$$

Therefore, assuming i.i.d. fading in the two hops of the l -th relay link, for $\ell = 1, \dots, N$, the MGF of $\gamma_{\min}(\ell)$ in (3.11) becomes $\mathcal{M}_{\gamma_{\min}(\ell)}(-s) = 2I(-s)$, i.e.,

$$\mathcal{M}_{\gamma_{\min}(\ell)}(-s) = \frac{\sqrt{\pi}}{2^{2k_\ell+m_\ell-2}\Gamma(m_\ell)\Gamma^2(k_\ell)} \cdot \sum_{r=0}^{m_\ell-1} \frac{1}{2^r r!} G_{4,3}^{1,4} \left(\frac{s}{4\Xi_\ell} \left| \begin{array}{l} 1-2k_\ell, 1-k_\ell-r, 1-k_\ell-m_\ell, 1-m_\ell-r \\ 0, 1-k_\ell-\frac{m_\ell+r}{2}, -k_\ell-\frac{m_\ell+r-1}{2} \end{array} \right. \right). \quad (3.16)$$

Finally, the MGF of the MRC output SNR is approximated by

$$\mathcal{M}_{\gamma_\alpha}(-s) = \mathcal{M}_{\gamma_0}(-s) \prod_{\ell=1}^N \mathcal{M}_{\gamma_{\min}(\ell)}(-s) \quad (3.17)$$

3.3.2 Performance Using The Geometric Mean Approximation

It is well known that the end-to-end SNR of the l -th relay link can be expressed in terms of the harmonic mean of the three positive random variables $(\gamma_{\ell 1}, \gamma_{\ell 2}, \gamma_{\ell 1}\gamma_{\ell 2})$. Following [36], the end-to-end SNR can be upper bounded using the geometric mean of $(\gamma_{\ell 1}, \gamma_{\ell 2}, \gamma_{\ell 1}\gamma_{\ell 2})$,

as

$$\gamma_{\text{out}} \leq \gamma_b = \gamma_0 + \frac{1}{3} \sum_{\ell=1}^N (\gamma_{\ell 1} \gamma_{\ell 2})^{2/3} \quad (3.18)$$

By letting $\gamma_\ell = \frac{1}{3}(\gamma_{\ell 1} \gamma_{\ell 2})^{2/3}$, the MGF of γ_ℓ is given by

$$\mathcal{M}_{\gamma_\ell}(-s) = \int_0^\infty \int_0^\infty e^{-(s/3)(\gamma_1 \gamma_2)^{2/3}} f_{\gamma_{\ell 1}}(\gamma_1) f_{\gamma_{\ell 2}}(\gamma_2) d\gamma_1 d\gamma_2 \quad (3.19)$$

By replacing (3.2) in (3.19) we obtain (note that in the derivations, for simplicity, we drop the subscript l on the fading parameters)

$$\mathcal{M}_{\gamma_\ell}(-s) = \frac{4 \Xi_1^{\frac{k_1+m_1}{2}} \Xi_2^{\frac{k_2+m_2}{2}}}{\Gamma(m_1) \Gamma(m_2) \Gamma(k_1) \Gamma(k_2)}. \quad (3.20)$$

$$\cdot \int_0^\infty \int_0^\infty e^{-(s/3)\gamma_1^{2/3} \gamma_2^{2/3}} \gamma_1^{\frac{k_1+m_1}{2}-1} \gamma_2^{\frac{k_2+m_2}{2}-1} K_{k_1-m_1}(2\sqrt{\Xi_1} \gamma_1) K_{k_2-m_2}(2\sqrt{\Xi_2} \gamma_2) d\gamma_1 d\gamma_2$$

Following a similar procedure to the one in [36], the inner integral is given by

$$I_1(-s) = \int_0^\infty e^{-(s/3)\gamma_1^{2/3} \gamma_2^{2/3}} \gamma_1^{\frac{k_1+m_1}{2}-1} K_{k_1-m_1}(2\sqrt{\Xi_1} \gamma_1) d\gamma_1 \quad (3.21)$$

By substituting $K_\nu(2\sqrt{x}) = \frac{1}{2} G_{0,2}^{2,0} \left(x \left| \begin{matrix} - \\ \frac{\nu}{2}, -\frac{\nu}{2} \end{matrix} \right. \right)$ and $e^{-x} = G_{0,1}^{1,0} \left(x \left| \begin{matrix} - \\ 0 \end{matrix} \right. \right)$ in (3.21) and using [22, eq. (07.34.21.0013.01)], we obtain the closed-form result

$$I_1(-s) = \frac{\sqrt{3} 2^{k_1+m_1}}{2^4 \pi^2 \Xi_1^{\frac{k_1+m_1}{2}}} G_{4,3}^{3,4} \left(\frac{2^4 s^3 \gamma_2^2}{3^6 \Xi_1^2} \left| \begin{matrix} \Delta(2, k_1), \Delta(2, m_1) \\ 0, \frac{1}{3}, \frac{2}{3} \end{matrix} \right. \right) \quad (3.22)$$

where $\Delta(\cdot, \cdot)$ is defined as $\Delta(p, \mu) = \left\{ \frac{1-\mu}{p}, \dots, \frac{p-\mu}{p} \right\}$, with p being positive integer and μ positive real. Using (3.22), the outer integral in (3.20) becomes

$$I_2(-s) = \frac{\sqrt{3} 2^{k_1+m_1}}{2^4 \pi^2 \Xi_1^{\frac{k_1+m_1}{2}}} \cdot \int_0^\infty G_{4,3}^{3,4} \left(\frac{2^4 s^3 \gamma_2^2}{3^6 \Xi_1^2} \middle| \begin{array}{c} \Delta(2, k_1), \Delta(2, m_1) \\ 0, \frac{1}{3}, \frac{2}{3} \end{array} \right) \gamma_2^{\frac{k_2+m_2}{2}-1} K_{k_2-m_2} (2\sqrt{\Xi_2} \gamma_2) d\gamma_2 \quad (3.23)$$

Again, expressing the Bessel K -function in terms of the G -function and using [22, eq. (07.34.21.0013.01)], followed by some straightforward manipulations, we obtain

$$I_2(-s) = \frac{\sqrt{3} 2^{k_1+m_1+k_2+m_2}}{2^7 \pi^3 \Xi_1^{\frac{k_1+m_1}{2}} \Xi_2^{\frac{k_2+m_2}{2}}} G_{8,3}^{3,8} \left(\frac{2^8 s^3}{3^6 \Xi_1^2 \Xi_2^2} \middle| \begin{array}{c} \Delta(2, k_1), \Delta(2, m_1), \Delta(2, k_2), \Delta(2, m_2) \\ 0, \frac{1}{3}, \frac{2}{3} \end{array} \right) \quad (3.24)$$

Using the above result for $I_2(-s)$, the MGF of γ_ℓ is given by

$$\mathcal{M}_{\gamma_\ell}(-s) = \frac{\sqrt{3} 2^{k_{\ell 1}+m_{\ell 1}+k_{\ell 2}+m_{\ell 2}}}{2^5 \pi^3 \Gamma(m_{\ell 1}) \Gamma(m_{\ell 2}) \Gamma(k_{\ell 1}) \Gamma(k_{\ell 2})} \cdot G_{8,3}^{3,8} \left(\frac{2^8 s^3}{3^6 \Xi_{\ell 1}^2 \Xi_{\ell 2}^2} \middle| \begin{array}{c} \Delta(2, k_{\ell 1}), \Delta(2, m_{\ell 1}), \Delta(2, k_{\ell 2}), \Delta(2, m_{\ell 2}) \\ 0, \frac{1}{3}, \frac{2}{3} \end{array} \right). \quad (3.25)$$

Finally, owing to the independency of γ_ℓ , $\ell = 1, \dots, N$, the MGF of the MRC output SNR is approximated by the product of the MGFs, as

$$\mathcal{M}_{\gamma_b}(-s) = \mathcal{M}_{\gamma_0}(-s) \prod_{\ell=1}^N \mathcal{M}_{\gamma_\ell}(-s) \quad (3.26)$$

3.4 Numerical Results

In this section we present some numerical and simulation results on the error rate performance of the cooperative dual-hop relay transmission scheme with MRC operating over independent generalized- K fading channels. This fading model corresponds to a Nakagami-Gamma composite distribution and is controlled by two shaping parameters

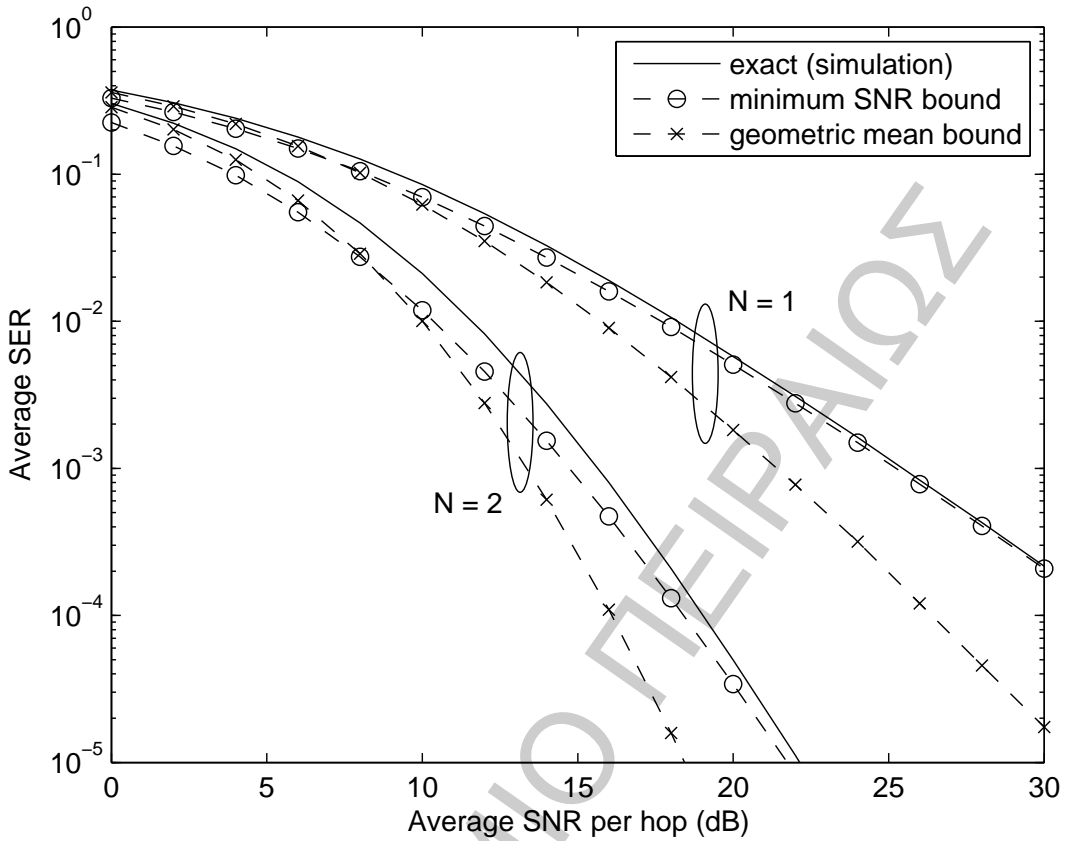


Figure 3.2: Average SER for 4-PSK vs average SNR per hop for $N = 1$ and $N = 2$ dual-hop links with MRC assuming $m_0 = 1$, $k_0 = 0.5$ for the direct link, $m_1 = 1$, $k_1 = 1.5$ for the first relay link, and $m_2 = 2$, $k_2 = 3$ for the second relay link.

m and k , where the parameter $m \geq 1/2$ inversely reflects the multipath fading severity and the positive parameter k inversely reflects the shadowing severity [21]. For demonstration purposes, we assume different fading conditions for each relay link, i.e., $m_0 = 1$, $k_0 = 0.5$ for the direct link, $m_1 = 1$, $k_1 = 1.5$ for the first relay link, and $m_2 = 2$, $k_2 = 3$ for the second relay link. Using the MGF based approach for performance evaluation over fading channels and the two approximations for the end-to-end SNR of a single dual-hop relay link, Fig. 3.2 and 3.3 plot, respectively, the average SER for 4-PSK and 16-QAM versus the average SNR per hop of a single relay system (i.e., $N = 1$) and a multiple relay system with $N = 2$. Moreover, we plot the exact numerical results from simulation using the end-to-end SNR given by (3.5) for the MRC receiver.

A number of observations on the accuracy of each analytical lower bound of the error

performance can be drawn from these graphs. We observe that for values of the average SNR per hop less than 10dB the geometric mean performance bound gives numerical results that are a little closer to the exact simulation results than the minimum SNR bound. However for SNRs per hop equal to or greater than 10dB, the minimum SNR approximation is more accurate than the geometric mean and its accuracy improves as the average SNR per hop increases. Furthermore, the minimum SNR performance bound is shown to be tight for both values of N , although it loses some of its tightness for $N = 2$ compared to $N = 1$. However, for both values of N , increased values of the average SNR per hop result in the minimum SNR bound to converge to the exact values, whereas the geometric mean bound loses its tightness. Finally, the graphs show the effects of diversity order N and fading parameters k and m on the average SER, i.e. the worst performance is obtained for single dual-hop relay and fading conditions with high amount of fading due to shadowing (e.g., $k = 1.5$) and multipath (e.g., $m = 1$), whereas the SER improves as N increases and fading conditions become less severe (e.g., $k = 3$ and $m = 2$ for the second relay channel).

3.5 Conclusion

In this chapter, we provided closed-form expressions for the MGF of the minimum SNR and geometric mean upper bounds for the end-to-end SNR of a single dual-hop relay system operating over a generalized- K fading environment. Then, for independently faded relay links and MRC diversity receiver, the average SER and BER can be easily evaluated for various modulation schemes using the MGF based approach. Simulation results of the exact SER were used to verify the analytical results and evaluate the tightness of the two lower performance bounds.

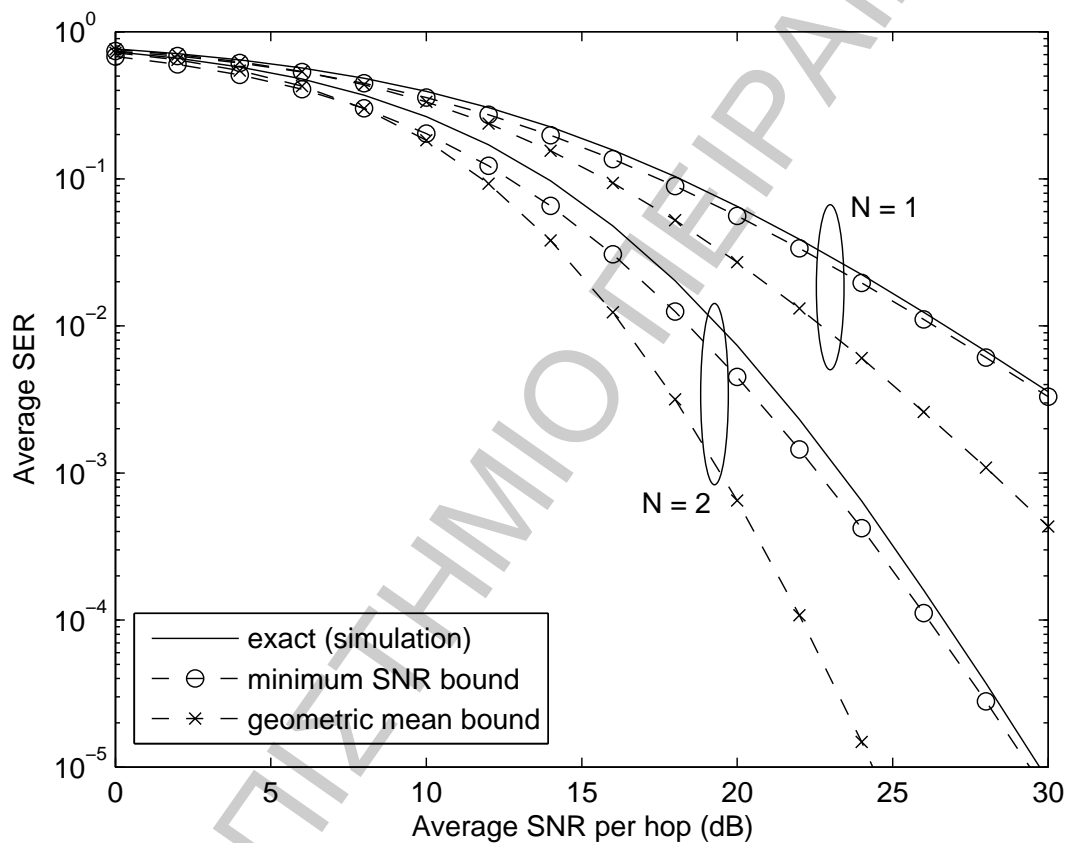


Figure 3.3: Average SER for 16-QAM vs average SNR per hop for $N = 1$ and $N = 2$ dual-hop links with MRC assuming $m_0 = 1$, $k_0 = 0.5$ for the direct link, $m_1 = 1$, $k_1 = 1.5$ for the first relay link, and $m_2 = 2$, $k_2 = 3$ for the second relay link.

Chapter 4

Performance Analysis of Dual-Hop Relay Systems with Single Relay Selection in Composite Fading Channels

IN THIS CHAPTER, we present novel and easy-to-evaluate expressions for the performance of dual-hop relaying with best relay selection operating over generalized- K fading channels. Since it is hard to find a closed-form expression for the probability density function (PDF) of the exact end-to-end signal-to-noise ratio (SNR) at the destination node even for the single dual-hop system with amplify-and-forward (AF) relaying, we use a tight upper bound value instead. Using the approximate value for the end-to-end SNR, closed-form expressions for the statistics of the SNR, the average bit and symbol error probabilities, and the ergodic capacity for the single dual-hop AF relay system, are derived. Moreover, assuming independent nonidentical fading conditions across multiple dual-hop relay links, we derive lower performance bounds for the single relay selection scheme with AF relaying. The final expressions are useful in the performance evaluation of AF opportunistic relaying in a generalized composite radio environment. Simulation results are also given to verify the analytical results.

4.1 Introduction

It is well known that the cooperative diversity realized through relays can provide an increase in link quality and reliability, high data rate coverage, and mitigate channel impairments in next generation wireless systems. An overview of cooperative diversity protocols is presented in [27]. In general, there are two types of processing that can be performed at the relays. In a decode-and-forward (DF) scheme, the relay station decodes the received signal, re-encodes and then retransmits the restored signal to the destination. On the other hand, amplify-and-forward (AF) relays simply amplify and forward the signal to the destination and have attracted a lot of attention recently as they provide a simple way to implement collaborative/cooperative wireless communication systems. Furthermore, Bletsas et. al. proposed in [46] a cooperative diversity protocol named opportunistic relaying technique, which selects (using a selection policy) the “best” relay among multiple available relays. It was then shown that the best-relay selection reduces the amount of required resources while improving the performance.

For dual-hop AF relay systems, the end-to-end SNR at the receiving end depends on the amplification gain employed at the relays. For relays with channel state information (CSI) of the first link, the end-to-end SNR has been obtained in [31]. For this relay transmission scheme, analytical performance results have been obtained by approximating the end-to-end SNR by the harmonic mean of the SNRs of the two hops [35], their geometric mean [36], and the minimum SNR of the two hops [37], [39]. In particular, using the minimum SNR approximation for the end-to-end SNR, the performance of dual-hop relaying has been studied in terms of outage probability and average bit error rate (BER) in various fading conditions, such as Rayleigh [31], Nakagami- m [37], Weibull [47] and generalized Gamma [39] fading channels.

The minimum SNR of the two hops has also been used as a selection policy as well as a bound in the performance evaluation of the best relay selection scheme based on AF [46], [48], [49] and DF [50], [51] relaying protocols. For example, in [49], the authors presented an asymptotic analysis (at high SNR values) of the average symbol error rate

(SER) of an AF best relay selection scheme, and compared it with the regular cooperative systems. Furthermore, in [50], the authors derived closed-form expressions for the outage probability and the average BER of opportunistic relaying with DF relays. However, in the existing literature, almost all performance results of this transmission scheme have been restricted to the case of Rayleigh fading channel.

Recently, the generalized- K fading model [21] has attracted considerable attention as one of the most general wireless fading models that can characterize the combined effects of small and large-scale fading on the received signal. This model corresponds to a Nakagami-Gamma composite distribution and is controlled by two shaping parameters m and k , where m is the Nakagami parameter for the small-scale fading and k is the parameter of the Gamma distribution for the received average power due to shadowing [21]. Note that the K distribution [41] is derived as a special case of the generalized- K distribution by letting $m = 1$ (i.e., Rayleigh multipath fading). The performance analysis of single link communication systems in this fading model was given in [42], whereas for relay systems, results that have recently appeared in the literature, are restricted to the performance of dual-hop single relay systems with CSI-assisted [44] and fixed gain [52] transmission schemes. However, the analytical expressions in [44] are too complicated to be used in the performance analysis of the best relay selection scheme.

In this chapter, we focus on AF dual-hop cooperative diversity networks to study their end-to-end performance over independent nonidentical generalized- K fading channels when the best relay selection scheme is employed. The main contribution of this paper includes the derivation of novel closed-form expressions for the PDF, CDF, and moment generating function (MGF) of a tight upper bound on the total SNR at the destination of the single dual-hop relayed signal. Then, using the derived CDF expression, we present performance metrics such as the outage probability and the average BER for the multiple dual-hop relay system with best relay selection operating in a generalized- K fading model with integer values for fading parameter m and arbitrary values for fading parameter k .

The rest of the chapter is organized as follows. In Section 2 we present the channel model statistics. In Section 3, we derive the statistics of an upper bound approximation to the end-to-end SNR of a single dual-hop AF relay system and closed-form expressions for various performance metrics. Then, in Section 4, for the case of independent nonidentical fading across multiple relay links, we derive analytical lower performance bounds for dual-hop relay systems with single relay selection. Numerical and simulation results are given in Section 5, followed by concluding remarks in Section 6.

4.2 The Generalized- K Fading Model

In many fading environments, the received signal envelope can usually be characterized by the Nakagami- m distribution. In a shadowed environment, the average power of the received signal is also random. In this work, we assume that the fading environment is such that the signal envelope X in a receive antenna is a generalized- K distributed random variable with pdf given by [21],

$$f_X(x) = \frac{4(m/\Omega)^{\frac{k+m}{2}}}{\Gamma(m)\Gamma(k)} x^{k+m-1} K_{k-m} \left(2 \left(\frac{m}{\Omega} \right)^{1/2} x \right), x \geq 0 \quad (4.1)$$

where k and m are the distribution's shaping parameters, $\Omega = E[X^2]/k$ is the mean power with $E[\cdot]$ denoting expectation, $\Gamma(\cdot)$ is the Gamma function, and $K_{k-m}(\cdot)$ is the $(k-m)$ th order modified Bessel function of the second kind [4]. The generalized- K fading model can describe different fading conditions by the appropriate choice of fading parameters m and k . Low values of m and k can be used to describe fading conditions with severe multipath fading and shadowing, respectively, whereas fading conditions improve as the values of the fading parameters increase.

The instantaneous received SNR per symbol of a single receive branch is $\gamma = X^2 E_s / N_0$, where E_s is the average symbol energy and N_0 is the single-sided power spectral density of the additive white Gaussian noise (AWGN). The corresponding average received SNR

per symbol is given as $\bar{\gamma} = k\Omega E_s/N_0$. The PDF of γ is given by

$$f_\gamma(\gamma) = \frac{2\Xi^{\frac{k+m}{2}}}{\Gamma(m)\Gamma(k)} \gamma^{\frac{k+m}{2}-1} K_{k-m} \left(2\sqrt{\Xi\gamma} \right), \gamma \geq 0 \quad (4.2)$$

with $\Xi = (km)/\bar{\gamma}$. The CDF of γ is defined as $F_\gamma(\gamma) = \int_0^\gamma f_\gamma(x)dx$. For integer values of m and arbitrary values of k , the CDF of γ is given by [45]

$$F_\gamma(\gamma) = 1 - \frac{2(\Xi\gamma)^{\frac{k}{2}}}{\Gamma(k)} \sum_{q=0}^{m-1} \frac{1}{q!} (\Xi\gamma)^{\frac{q}{2}} K_{k-q} \left(2\sqrt{\Xi\gamma} \right), \quad (4.3)$$

which agrees with [41] for the special case of K -fading (i.e., $m = 1$). Moreover the MGF of γ defined as $M_\gamma(-s) = \int_0^\infty e^{-s\gamma} f_\gamma(\gamma) d\gamma$, is given by [45]

$$M_\gamma(-s) = \frac{1}{\Gamma(m)\Gamma(k)} G_{2,1}^{1,2} \left[\frac{s}{\Xi} \middle| \begin{matrix} 1-k, 1-m \\ 0 \end{matrix} \right] \quad (4.4)$$

where $G_{p,q}^{m,n} (x | \frac{\alpha_p}{b_q})$ is the Meijer's G-function [4, chap. 9.3].

4.3 Performance Analysis of Single Dual-Hop Relay System

In this section we study the performance of a single dual-hop AF relay system operating in the generalized- K fading channel. Assuming CSI-based amplification gain at the ℓ -th relay (see Fig. 4.1), the exact end-to-end SNR of the ℓ -th dual-hop link is given by [31], [35]

$$\gamma_{\text{end}}(\ell) = \frac{\gamma_{\ell_1} \gamma_{\ell_2}}{\gamma_{\ell_1} + \gamma_{\ell_2} + 1}. \quad (4.5)$$

In the literature, this relay transmission scheme is usually considered as a benchmark for cooperative performance. Since it is hard to find a closed-form expression for the PDF of the exact end-to-end SNR of the relayed signal at the destination node, we use an approximate value instead, given by the upper bound [37]

$$\gamma_{\text{end}}(\ell) \leq \gamma_{\min}(\ell) \quad (4.6)$$

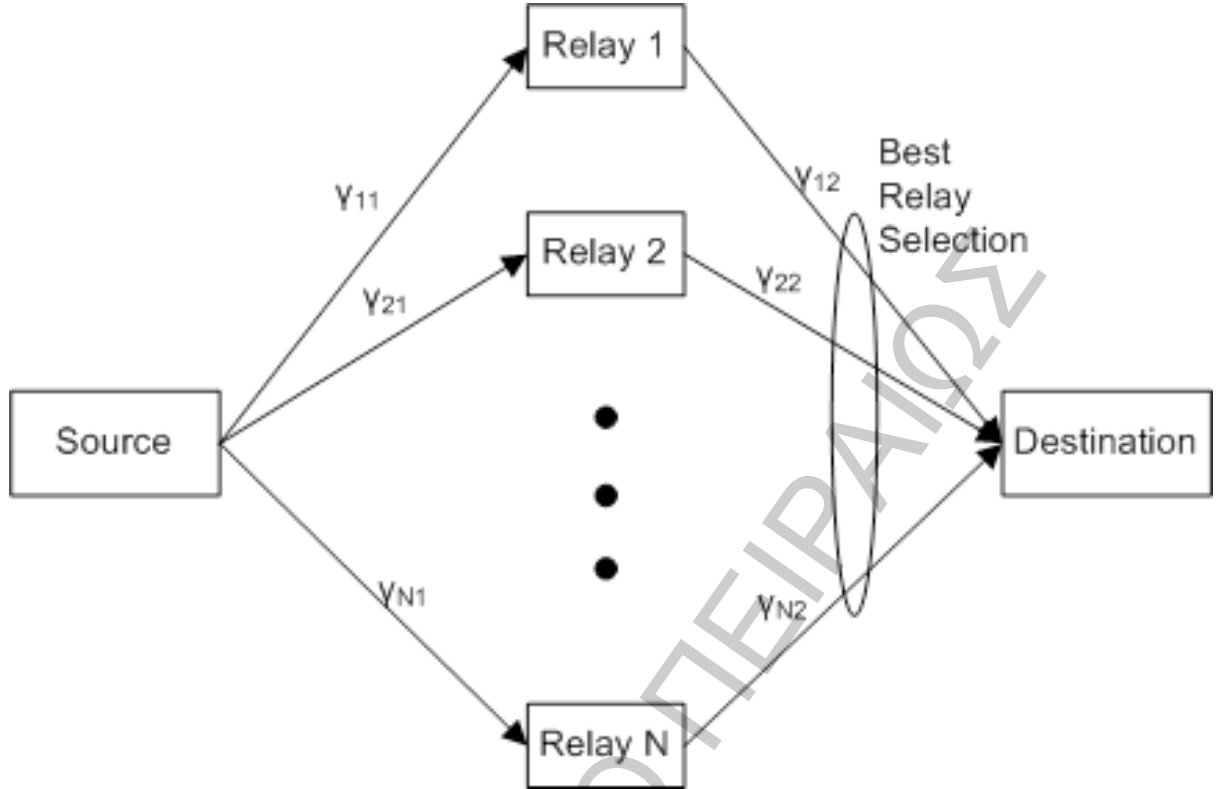


Figure 4.1: Dual-hop relay transmission scheme with best relay selection.

where $\gamma_{\min}(\ell) = \min(\gamma_{\ell_1}, \gamma_{\ell_2})$. This approximation is also adopted in many recent papers (e.g., [37], [47]) and it is shown to be accurate enough, especially at medium and high SNR values as will be discussed in Section 5.

4.3.1 Statistics of the end-to-end SNR

Using the bound in (4.6), a closed-form expression for the PDF of the total SNR at the destination can be derived. The PDF of $\gamma_{\min}(\ell)$ is given by

$$f_{\gamma_{\min}(\ell)}(\gamma) = f_{\gamma_{\ell_1}}(\gamma) + f_{\gamma_{\ell_2}}(\gamma) - \left[f_{\gamma_{\ell_1}}(\gamma)F_{\gamma_{\ell_2}}(\gamma) + F_{\gamma_{\ell_1}}(\gamma)f_{\gamma_{\ell_2}}(\gamma) \right] \quad (4.7)$$

where $f_{\gamma_{\ell_i}}(\gamma)$ and $F_{\gamma_{\ell_i}}(\gamma)$, $i = 1, 2$, are, respectively, the PDF and the CDF of the generalized- K distributed SNR of the i -th link of the ℓ -th relay.

For the case of symmetrical links, i.e., independent identically distributed (i.i.d.) fading and equal average SNRs for the user-to-relay and relay-to-destination links, dropping subscripts 1 and 2 in (4.7), and substituting (4.2) and (4.3) in (4.7), the PDF of

$\gamma_{\min}(\ell), \ell = 1, \dots, N$ is given by

$$f_{\gamma_{\min}(\ell)}(\gamma) = 2 \frac{4 (\Xi_{\ell} \gamma)^{k_{\ell} + \frac{m_{\ell}}{2}} \gamma^{-1}}{\Gamma(m_{\ell}) \Gamma^2(k_{\ell})} \sum_{q=0}^{m_{\ell}-1} \frac{(\Xi_{\ell} \gamma)^{\frac{q}{2}}}{q!} K_{k_{\ell}-m_{\ell}} \left(2\sqrt{\Xi_{\ell} \gamma} \right) K_{k_{\ell}-q} \left(2\sqrt{\Xi_{\ell} \gamma} \right). \quad (4.8)$$

Using [22, eq. (03.04.26.0016.01)], i.e.,

$$K_{\mu}(\sqrt{z}) K_{\nu}(\sqrt{z}) = \frac{\sqrt{\pi}}{2} G_{2,4}^{4,0} \left[z \left| \begin{matrix} 0, \frac{1}{2} \\ \frac{\mu+\nu}{2}, \frac{\mu-\nu}{2}, \frac{\nu-\mu}{2}, -\frac{\mu+\nu}{2} \end{matrix} \right. \right] \quad (4.9)$$

and the functional identity [4, eq. (9.31.5)], the PDF of $\gamma_{\min}(\ell), \ell = 1, \dots, N$, can also be written in terms of the G -function as

$$f_{\gamma_{\min}(\ell)}(\gamma) = \frac{4^{2-k_{\ell}-\frac{m_{\ell}}{2}} \sqrt{\pi} \Xi_{\ell}}{\Gamma(m_{\ell}) \Gamma^2(k_{\ell})} \sum_{q=0}^{m_{\ell}-1} \frac{4^{-\frac{q}{2}}}{q!} G_{2,4}^{4,0} \left[4\Xi_{\ell} \gamma \left| \begin{matrix} a_1, a_2 \\ b_1, b_2, b_3, b_4 \end{matrix} \right. \right] \quad (4.10)$$

where $a_1 = k_{\ell} + (m_{\ell} + q) / 2 - 1, a_2 = k_{\ell} + (m_{\ell} + q - 1) / 2, b_1 = 2k_{\ell} - 1, b_2 = k_{\ell} + q - 1, b_3 = k_{\ell} + m_{\ell} - 1, b_4 = m_{\ell} + q - 1$. The CDF of $\gamma_{\min}(\ell), \ell = 1, \dots, N$, is then given by

$$F_{\gamma_{\min}(\ell)}(\gamma) = \int_0^{\gamma} f_{\gamma_{\min}(\ell)}(x) dx. \quad (4.11)$$

Substituting (4.10) in (4.11) and using [22, eq. (07.34.21.0003.01)]

$$\int_0^{\gamma} x^{\alpha-1} G_{p,q}^{m,n} \left[\omega x \left| \begin{matrix} (a_p) \\ (b_q) \end{matrix} \right. \right] dx = \gamma^{\alpha} G_{p+1,q+1}^{m,n+1} \left[\omega \gamma \left| \begin{matrix} 1-\alpha, a_1, \dots, a_n, a_{n+1}, \dots, a_p \\ b_1, \dots, b_m, b_{m+1}, \dots, b_q, -\alpha \end{matrix} \right. \right] \quad (4.12)$$

the final expression for the CDF of $\gamma_{\min}(\ell), \ell = 1, \dots, N$, is given also in terms of the G -function as

$$F_{\gamma_{\min}(\ell)}(\gamma) = \frac{4^{1-k_{\ell}+\frac{m_{\ell}}{2}} \sqrt{\pi}}{\Gamma(m_{\ell}) \Gamma^2(k_{\ell})} \sum_{q=0}^{m_{\ell}-1} \frac{4^{-\frac{q}{2}}}{q!} G_{3,5}^{4,1} \left[4\Xi_{\ell} \gamma \left| \begin{matrix} 1, a_1+1, a_2+1 \\ b_1+1, b_2+1, b_3+1, b_4+1, 0 \end{matrix} \right. \right]. \quad (4.13)$$

Moreover, using the PDF in (4.10), the MGF of the end-to-end SNR bound, $M_{\gamma_{\min}(\ell)}(s)$, can be expressed as

$$M_{\gamma_{\min}(\ell)}(s) = \int_0^{\infty} \exp(-s\gamma) f_{\gamma_{\min}(\ell)}(\gamma) d\gamma. \quad (4.14)$$

By substituting (4.8) into (4.14) and using [22, eq. (07.34.21.0088.01)], we can obtain

$$M_{\gamma_{\min}(\ell)}(\gamma) = \frac{4^{1-k_\ell+\frac{m_\ell}{2}} \sqrt{\pi}}{\Gamma(m_\ell)\Gamma^2(k_\ell)} \sum_{q=0}^{m_\ell-1} \frac{4^{-\frac{q}{2}}}{q!} G_{3,4}^{4,1} \left[\frac{4\Xi_\ell}{s} \middle| \begin{matrix} 1, a_1+1, a_2+1 \\ b_1+1, b_2+1, b_3+1, b_4+1 \end{matrix} \right]. \quad (4.15)$$

To the best of our knowledge, closed-form expressions (4.10), (4.13), and (4.15) are novel. Note that the Meijer G -function is available in most of the well-known mathematical software packages such as Maple and Mathematica.

4.3.2 Amount of Fading

With the equivalent PDF as shown in (4.10), the n -th moment of $\gamma_{\min}(\ell)$, $\ell = 1, \dots, N$, can be evaluated by the formula

$$\mu_{\gamma_{\min}(\ell)}(n) = \int_0^\infty \gamma^n f_{\gamma_{\min}(\ell)}(\gamma) d\gamma. \quad (4.16)$$

Substituting (4.10) in (4.16) and using [4, eq.(7.811.4)] the moments of $\gamma_{\min}(\ell)$, $\ell = 1, \dots, N$ can be obtained in closed form as

$$\mu_{\gamma_{\min}(\ell)}(n) = \frac{4^{1-k_\ell-\frac{m_\ell}{2}-n} \sqrt{\pi} \Xi_\ell^{-n}}{\Gamma(m_\ell)\Gamma^2(k_\ell)} \sum_{q=0}^{m_\ell-1} \frac{4^{-\frac{q}{2}}}{q!} \frac{\prod_{j=1}^4 \Gamma[b_j + n + 1]}{\prod_{j=1}^2 \Gamma[a_j + n + 1]}. \quad (4.17)$$

The amount of fading (AoF) used to measure the severity of fading can then be computed by the formula [53]

$$AoF_\ell = \frac{\mu_{\gamma_{\min}(\ell)}(2)}{\mu_{\gamma_{\min}(\ell)}^2(1)} - 1. \quad (4.18)$$

4.3.3 Outage Probability

The outage probability, defined as the probability that the received total SNR falls below a threshold, γ_{th} , can be obtained directly as $P_{\text{out}} = F_\gamma(\gamma_{\text{th}})$.

4.3.4 Average BER

The average BER is obtained by integrating the conditional bit error probability $P_b(e|\gamma)$ over the PDF of the upper bound of the end-to-end SNR, $f_{\gamma_{\min}(\ell)}(\gamma)$. Following the approach used in [54], the average error probability can be written in terms of the CDF $F_{\gamma_{\min}(\ell)}(\gamma)$, i.e.,

$$P_b(e) = - \int_0^\infty \frac{dP_b(e|\gamma)}{d\gamma} F_{\gamma_{\min}(\ell)}(\gamma) d\gamma. \quad (4.19)$$

Next, we present tight lower bounds of the average BER of the CSI-assisted AF dual-hop single relay system in generalized- K fading channels for various modulation schemes according to their conditional BER forms.

1. $P_b(e|\gamma) = \frac{\Gamma(\beta, \alpha\gamma)}{2\Gamma(\beta)}$: where parameters α and β depend on the type of modulation/detection scheme and take the values ($\alpha=1, \beta=1/2$) for coherent binary phase shift keying (BPSK), ($\alpha=1/2, \beta=1/2$) for coherent binary frequency shift keying (BFSK), ($\alpha=1, \beta=1$) for differentially coherent BPSK, and ($\alpha=1/2, \beta=1$) for non-coherent BFSK, while $\Gamma(\alpha, x) = \int_x^\infty t^{\alpha-1} e^{-t} dt$ is the complementary incomplete Gamma function [4, eq.(8.350.2)]. It then follows that the average BER for binary modulation schemes operating over a fading channel can be written in terms of the CDF of the received SNR, as

$$P_b(e) = \frac{\alpha^\beta}{2\Gamma(\beta)} \int_0^\infty \gamma^{\beta-1} e^{-\alpha\gamma} F_{\gamma_{\min}(\ell)}(\gamma) d\gamma. \quad (4.20)$$

Substituting (4.13) in (4.20) and using [4, eq. (7.813.1)] the average BER for binary modulations is derived in closed form as

$$P_b(e) = \frac{4^{1-k_\ell + \frac{m_\ell}{2}} \sqrt{\pi}}{2\Gamma(\beta) \Gamma(m_\ell) \Gamma^2(k_\ell)} \sum_{q=0}^{m_\ell-1} \frac{4^{-\frac{q}{2}}}{q!} G_{4,5}^{4,2} \left[\frac{4\Xi_\ell}{\alpha} \middle| \begin{matrix} 1-\beta, a_1+1, a_2+1 \\ b_1+1, b_2+1, b_3+1, b_4+1, 0 \end{matrix} \right]. \quad (4.21)$$

2. $P_b(e|\gamma) = Q(\sqrt{g\gamma_b})$: The BER of M -ary phase shift keying (M -PSK) and M -ary quadrature amplitude modulation (M -QAM) signal constellations over an AWGN channel can be expressed as a linear summation of the Gaussian $Q(\cdot)$ function,

defined as $Q(x) = \frac{1}{\sqrt{2\pi}} \int_x^\infty \exp(-t^2/2) dt$. Therefore, in order to evaluate the performance of M -ary modulation schemes over a fading channel we need to evaluate integrals of the form $P_b(e, g) = \int_0^\infty Q(\sqrt{g\gamma_b}) f_\gamma(\gamma_b) d\gamma_b$, where γ_b is the instantaneous received SNR per bit and g depends on the modulation type [53]. For instance, using the unified approximation [55], the average BER for M -PSK constellations with Gray coding operating over a fading channel is given by

$$P_{b,\text{MPSK}}(e) \cong \frac{2}{\max(\log_2 M, 2)} \sum_{i=1}^{\max(M/4, 1)} P_b(e, g_{i,\text{MPSK}}) \quad (4.22)$$

where $g_{i,\text{MPSK}} = 2(\log_2 M) \sin^2((2i-1)\pi/M)$. The corresponding average BER of M -QAM constellations with Gray coding, is

$$P_{b,\text{MQAM}}(e) \cong \frac{4}{\log_2 M} \left(1 - \frac{1}{\sqrt{M}}\right) \sum_{i=1}^{\sqrt{M}/2} P_b(e, g_{i,\text{MQAM}}) \quad (4.23)$$

where $g_{i,\text{MQAM}} = 3(2i-1)^2(\log_2 M)/(M-1)$. Using the result in [49], the integral $P(e, g)$ can be expressed in terms of the CDF of the received SNR at the destination, as

$$P(e, g) = \frac{1}{\sqrt{2\pi}} \int_0^\infty e^{-t^2/2} F_{\gamma_{\min}(\ell)}(t^2/g) dt. \quad (4.24)$$

For the generalized- K fading channel, inserting (4.13) in (4.24), making the change of variables $y = t^2$ and using again [4, eq. (7.813.1)], $P(e, g)$ can be obtained in closed form as

$$P(e, g) = \frac{4^{1-k_\ell + \frac{m_\ell}{2}}}{2\Gamma(m_\ell)\Gamma^2(k_\ell)} \sum_{q=0}^{m_\ell-1} \frac{4^{-\frac{q}{2}}}{q!} G_{4,5}^{4,2} \left[\frac{8\Xi_\ell}{g} \middle| \begin{matrix} 1/2, a_1+1, a_2+1 \\ b_1+1, b_2+1, b_3+1, b_4+1, 0 \end{matrix} \right]. \quad (4.25)$$

Then, the average BER of M -PSK and M -QAM can be easily evaluated numerically using widely available mathematical software programs by combining the closed-form result in (4.25) with (4.22) and (4.23), respectively.

4.3.5 Average SER

For non-coherent demodulation schemes with conditional SER given by $P_{e,non}(\gamma) = C \exp(-D\gamma)$, where C and D are constants depending on the modulation scheme, the average SER can be given directly by the MGF of γ_{\min} as $\bar{P}_{e,non} = C M_{\gamma_{\min}(\ell)}(D)$. Furthermore, using the MGF-based approach, the average SER for several M -ary signaling schemes can be evaluated as [56]

$$\bar{P}_s = \sum_{k=1}^K \int_0^{\Theta_k} \alpha_k(\theta) M_{\gamma_{\min}(\ell)} \left(\frac{\phi_k}{\sin^2 \theta} \right) d\theta \quad (4.26)$$

where parameters K , Θ_k , α_k and ϕ_k can be found in [56, Table I].

4.3.6 Ergodic Capacity

The ergodic capacity of the ℓ -th dual-hop system with CSI-assisted AF relay is given by [57]

$$C_{\gamma_{\min}(\ell)} = \frac{B_w}{2} \int_0^{\infty} \log_2(1 + \gamma) f_{\gamma_{\min}(\ell)}(\gamma) d\gamma \quad (4.27)$$

where B_w (in Hz) is the transmitted bandwidth. Expressing $\ln(1 + \gamma) = G_{2,2}^{1,2} \left[\gamma \left| \begin{matrix} 1, 1 \\ 1, 0 \end{matrix} \right. \right]$ (i.e., [22, eq. (07.34.03.0456.01)]) and substituting (4.10) in (4.27) the ergodic capacity of $\gamma_{\min}(\ell)$, $\ell = 1, \dots, N$ normalized to the transmitted bandwidth can be obtained in a closed form using [22, eq. (07.34.21.0011.01)] as

$$\frac{C_{\gamma_{\min}(\ell)}}{B_w} = \frac{4^{1-k_\ell + \frac{m_\ell}{2}} \sqrt{\pi}}{2 \ln(2) \Gamma(m_\ell) \Gamma^2(k_\ell)} \sum_{q=0}^{m_\ell-1} \frac{4^{-\frac{q}{2}}}{q!} G_{4,6}^{6,1} \left[\frac{4\Xi_\ell}{s} \left| \begin{matrix} 0, 1, a_1+1, a_2+1 \\ b_1+1, b_2+1, b_3+1, b_4+1, 0, 0 \end{matrix} \right. \right]. \quad (4.28)$$

4.4 Extension to the best relay selection scheme

We now consider a cooperative diversity system where a source node communicates with a destination node through N relays, as depicted in Fig. 4.1. Assume that the CSI-assisted opportunistic AF relaying protocol is employed. Following the work in [46], in the opportunistic relaying mechanisms, one best relay among the multiple relays is selected

during a predetermined transmission period and only that chosen relay forwards packets to the destination while the other relays are kept idle. Therefore, the best relay is selected as the relay node that can achieve the highest SNR at the destination node. Considering N available relays, the relay selection algorithm selects the best relay (denoted relay c) such that

$$c = \arg \max_{\ell \in \{1, 2, \dots, N\}} \gamma_{\min}(\ell). \quad (4.29)$$

Using the minimum SNR approximation, the total instantaneous SNR of the N relay system with single relay selection, will be given by

$$\gamma_c = \max \{ \gamma_{\min}(1), \dots, \gamma_{\min}(N) \}. \quad (4.30)$$

Assuming independent but not necessarily identical fading for the N relay links, the CDF of the highest end-to-end SNR of the scheduled relay, γ_c , is then given by [53]

$$F_{\gamma_c}(\gamma) = \prod_{\ell=1}^N F_{\gamma_{\min}(\ell)}(\gamma). \quad (4.31)$$

Therefore, using the CDF based approach and the previously obtained analytical result for $F_{\gamma_{\min}(\ell)}(\gamma)$ in (4.13) for the dual-hop relay system, useful performance metrics for the best relay selection scheme can be easily evaluated. The outage probability can be obtained directly as $P_{out} = F_{\gamma_c}(\gamma_{th})$. Moreover, using the methodology described in Section 3.4, the average BER for binary and multilevel modulation schemes can be obtained by replacing $F_{\gamma_{\min}(\ell)}(\cdot)$ with $F_{\gamma_c}(\cdot)$ in (4.20) and (4.24), respectively.

4.5 Numerical Results

In this section we present some numerical and simulation results for the performance of dual-hop relay transmission scheme with best relay selection, in the absence of a direct link, operating over generalized- K fading channels. The generalized- K fading model can describe different fading conditions by the appropriate choice of fading parameters m and k . For demonstration purposes, we assume N parallel dual-hop relay links with i.i.d fading

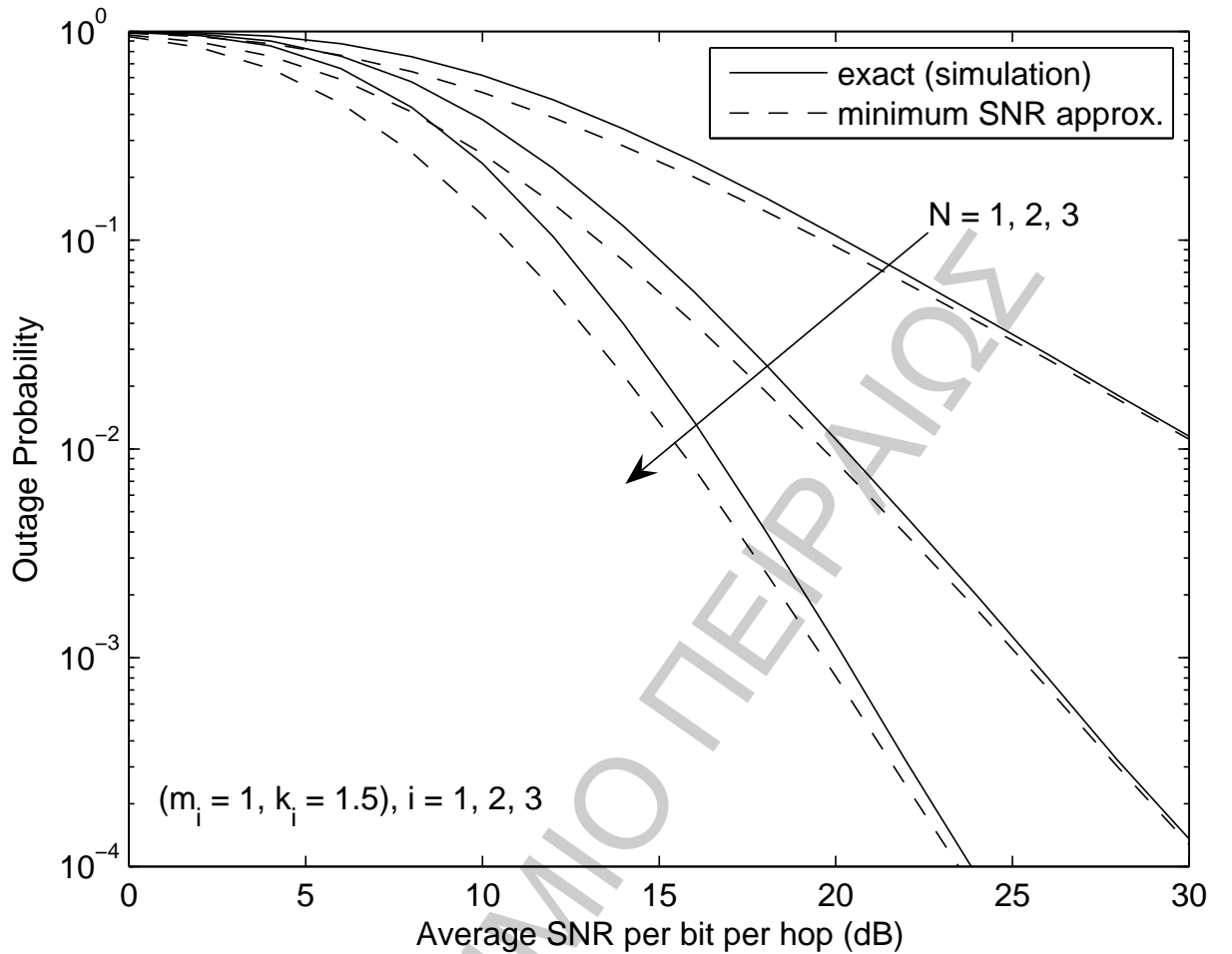


Figure 4.2: Outage Probability vs SNR per hop for best relay selection scheme with $N = 1, 2, 3$ and $(m_i = 1, k_i = 1.5), i = 1, 2, 3$.

conditions given by $\{m_i = 1, k_i = 1.5\}_{i=1}^N$, i.e., Rayleigh fading with medium amount of shadowing. Fig. 4.2 plots the outage probability versus the average SNR per hop for threshold $\gamma_{\text{th}} = 3$ dB and $N = 1, 2, 3$. The figure depicts the diversity gain achieved by the best relay selection scheme as N increases. Furthermore, for CSI-assisted AF relays, it compares the exact performance (using simulation) to the bound given by (4.13). We observe that the performance bound of the minimum SNR approximation loses some of its tightness to the exact performance as N increases but it always converges to the exact values at high values of SNR per hop.

For the same fading conditions across the multiple dual-hop relay links, Figs. 4.3 and 4.4 plot, respectively, the average BER for BPSK and 16-QAM versus the average SNR per hop for $N = 1, 2, 3$. Note that for $N = 1$ (i.e., single relay system) the average BER

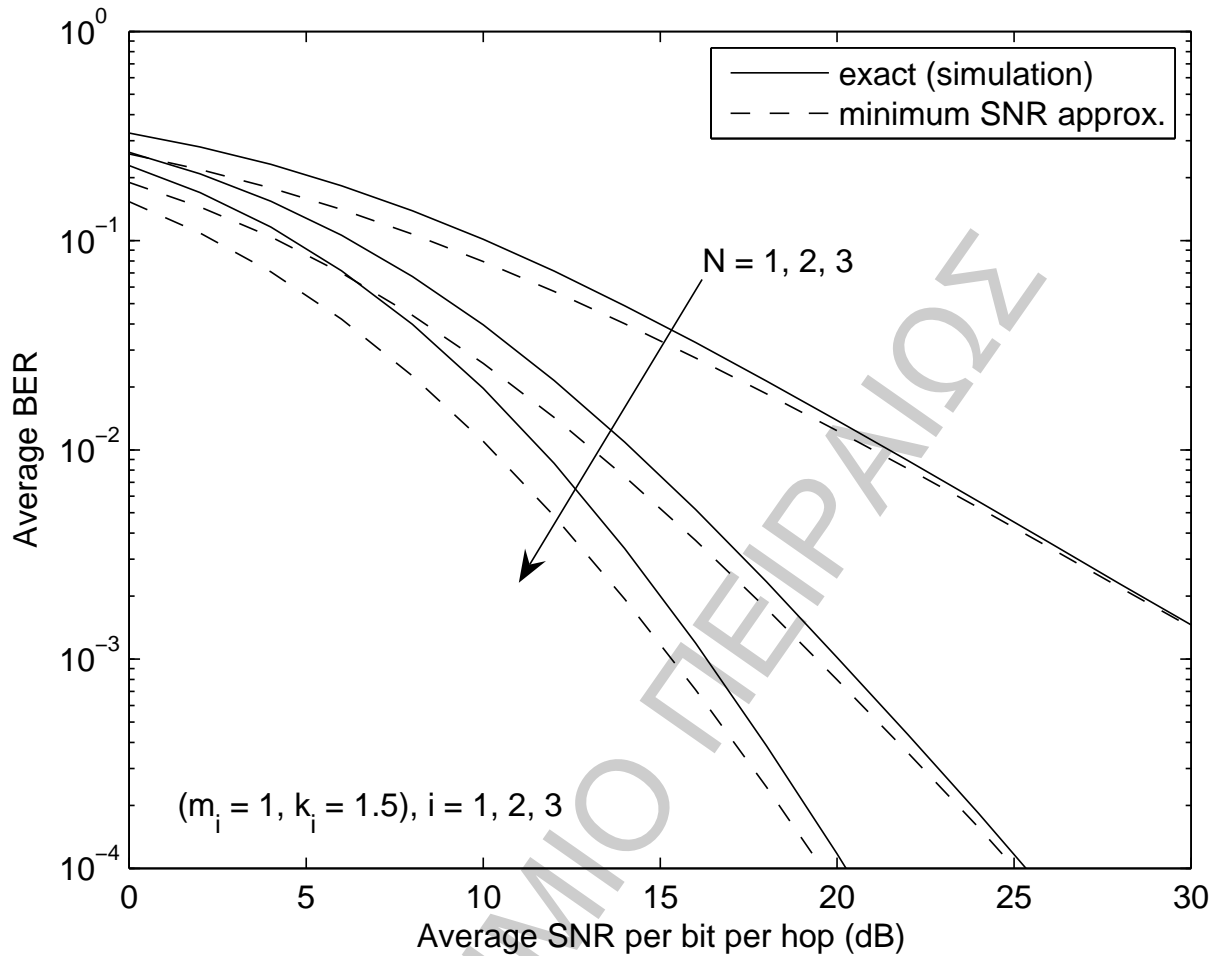


Figure 4.3: Average BER of BPSK vs SNR per hop for best relay selection scheme with $N = 1, 2, 3$ and $(m_i = 1, k_i = 1.5), i = 1, 2, 3$.

for BPSK was computed using (4.21) whereas for 16-QAM it was evaluated after inserting (4.25) in (4.23). Both figures show the performance improvement attained by the best relay selection scheme. Moreover, we observe that the BER performance evaluated by the derived analytical expressions based on the SNR bound loses its tightness at low and medium SNR values with the increase of N , but it converges to the exact performance as the average SNR increases.

Finally, in Figs. 4.5 and 4.6 we plot, respectively, the average BER of BPSK and 16-QAM vs the average SNR per hop for best relay selection with $N = 3$ in various shadowing conditions that include identical and non-identical fading across the parallel dual-hop relay links. In order to show the impact of fading parameter k on the average BER performance, we consider a multipath environment with $m = 2$ and three shadowing

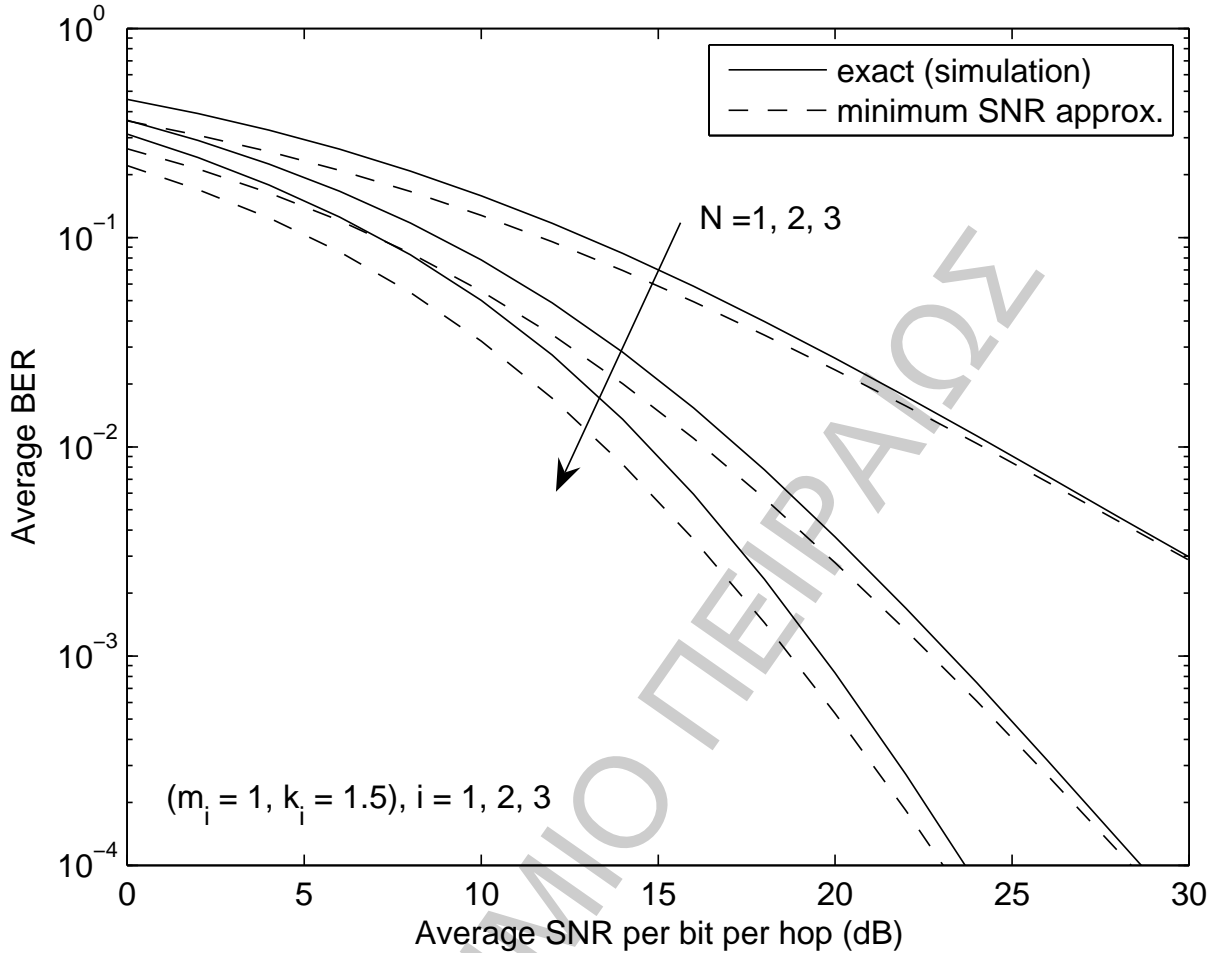


Figure 4.4: Average BER of 16-QAM vs SNR per hop for best relay selection scheme with $N = 1, 2, 3$ and $(m_i = 1, k_i = 1.5), i = 1, 2, 3$.

conditions as follows. We select $\{k_i = 0.5\}_{i=1}^N$ to model heavy shadowing, $\{k_i = 2.5\}_{i=1}^N$ for medium amount of shadowing, whereas we assume $k_1 = 0.5, k_2 = 1$, and $k_3 = 1.5$ for non-identical shadowing conditions. The two graphs depict the effect of fading parameter k on the average BER for both modulation schemes and the accuracy of the analytical results based on the end-to-end SNR bound for the best relay selection scheme. By comparing the tightness of curves (a) and (c) to the corresponding exact performance, we observe that for a fixed value of N the accuracy of the minimum SNR approximation depends on the fading severity of the dual hop links, i.e., the less amount of shadowing exists across the relay links the looser the performance bound becomes at the low and medium SNR values. However the performance bound converges to the exact performance in the high SNR regime.

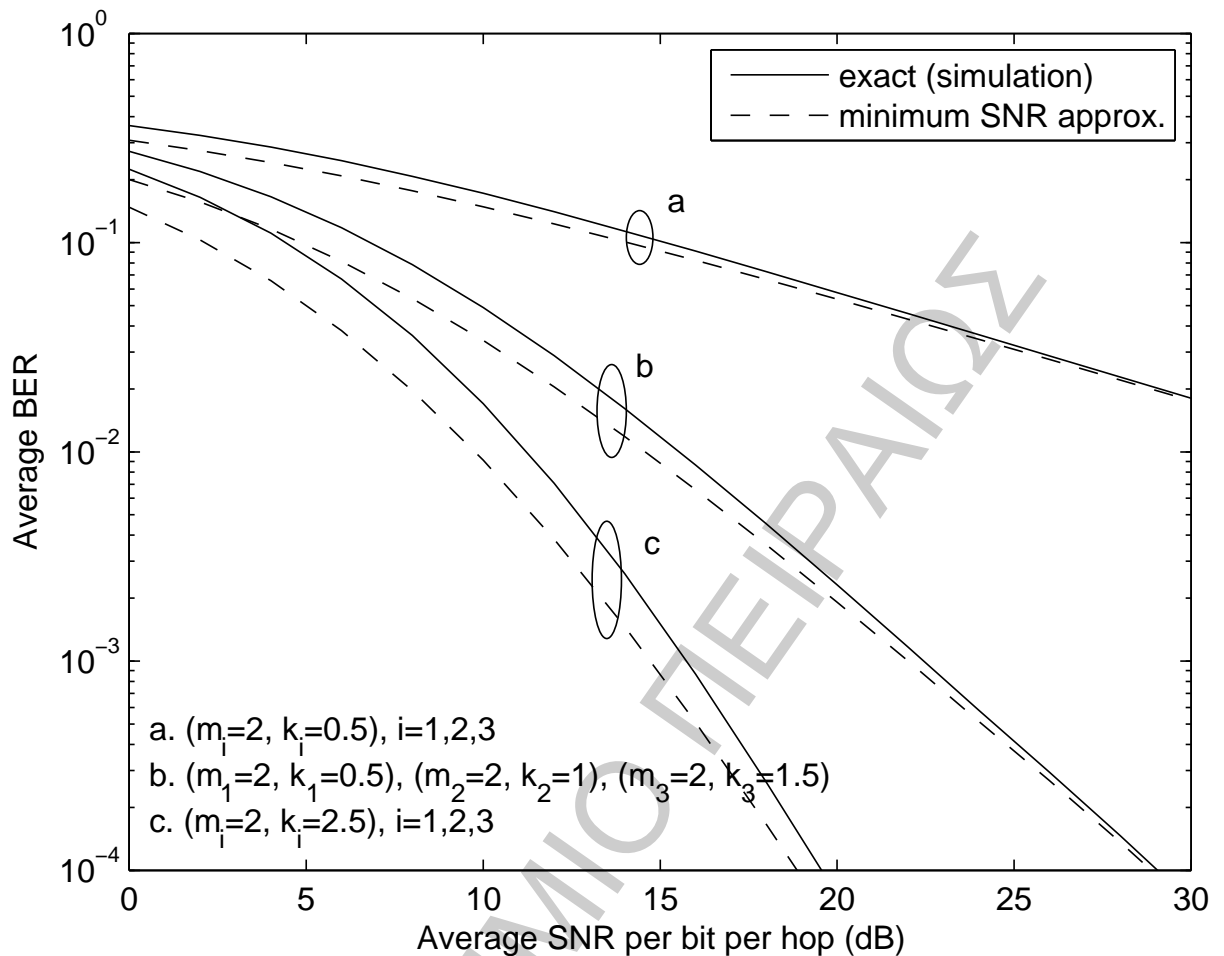


Figure 4.5: Average BER of BPSK vs SNR per hop for best relay selection scheme with $N = 3$ and various fading conditions.

4.6 Conclusions

In this chapter, we used a tight upper bound on the end-to-end SNR of a single dual-hop AF relay system to derive novel closed-form expressions for its SNR statistics, outage probability, bit error probability, and ergodic capacity. Then, using the CDF based approach, we studied the performance of the best-relay selection scheme for cooperative diversity networks operating over independent but not necessarily identical generalized- K fading channels. Computer simulation results verified the accuracy and the correctness of the derived expressions.

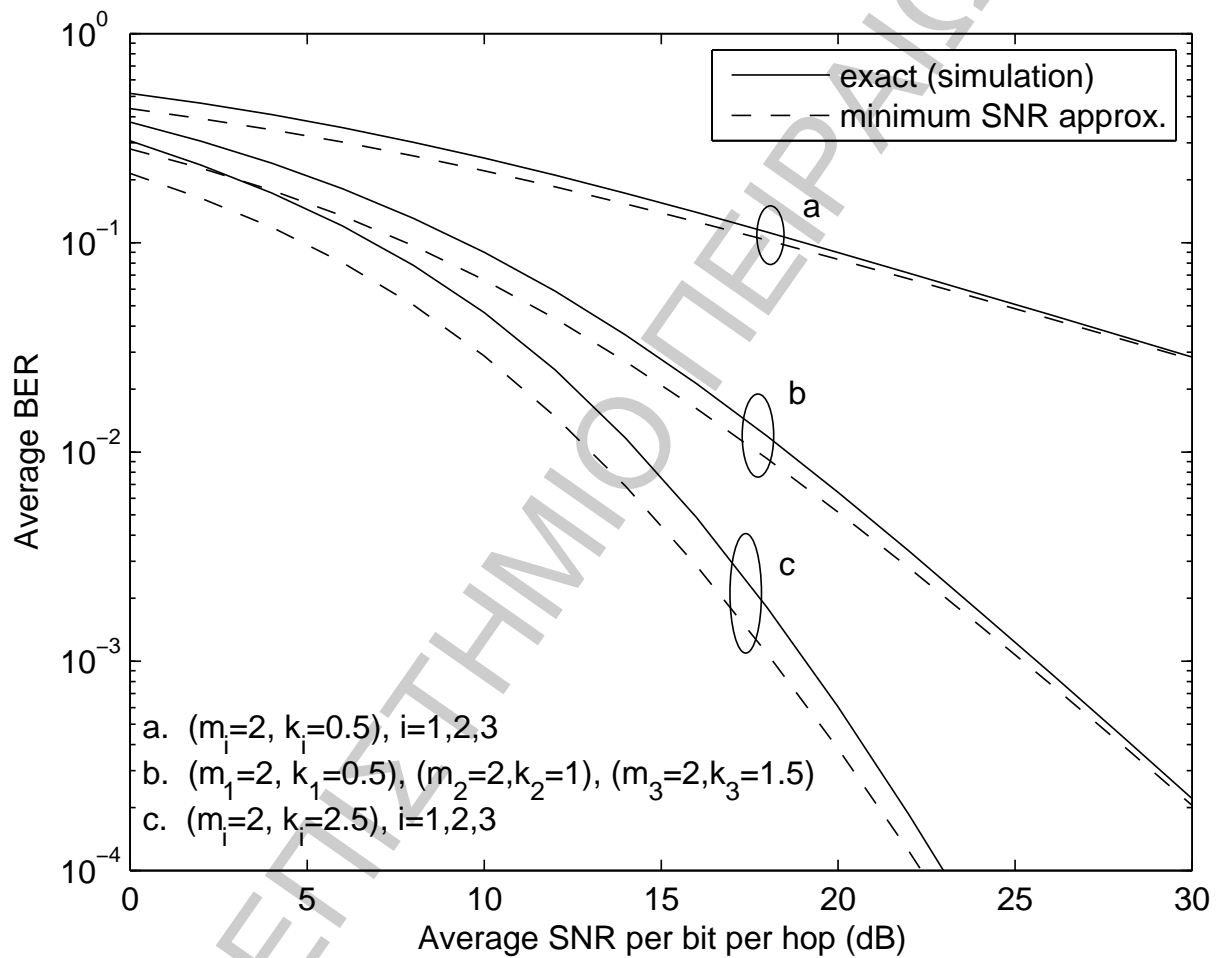


Figure 4.6: Average BER of 16-QAM vs SNR per hop for best relay selection scheme with $N = 3$ and various fading conditions.

Chapter 5

Performance of Multihop Relaying Systems over Composite Fading Channels

IN THIS CHAPTER we evaluate performance measures of multihop relaying systems operating in a composite fading environment modeled by the generalized- K distribution. By approximating the end-to-end signal-to-noise ratio (SNR) of the multihop relay system by the minimum SNR of all the links, we provide easy to compute analytical expressions for the outage probability and the average bit and symbol error rates for a variety of digital modulation schemes. The derived expressions are validated by computer simulation and provide tight lower bounds to the exact performance of multihop relaying transmissions in a generalized fading environment.

5.1 Introduction

Multihop relay systems can extend the coverage and enhance the throughput of wireless communication systems by enabling a source node to communicate with the destination node through intermediate relay stations. It is well known that the cooperative diversity realized through multihop relays can provide an improvement in link quality and reliability, high data rate coverage, and mitigate channel impairments in next generation wireless systems [24], [27]. For non-regenerative relay systems with amplify-and-forward

transmission scheme, the end-to-end signal-to-noise ratio (SNR) at the receiving end depends on the amplification gain employed at the relays. In particular, for dual-hop relay systems with relays that use channel state information (CSI) of the first link, the end-to-end SNR has been obtained in [31]. For this relay transmission scenario, analytical performance results have been obtained by approximating the end-to-end SNR by the harmonic mean of the SNRs of the two hops [35], their geometric mean [36], and the minimum SNR of the two hops [37], [39].

Among the proposed approximations for the end-to-end SNR of dual-hop relaying system, the minimum SNR has been shown to provide a tight upper bound for amplify-and-forward relays with CSI-based and fixed gain policies as well as for decode-and-forward relay systems. Using the minimum SNR upper bound to the end-to-end SNR, the performance of dual-hop relaying has been studied in terms of outage probability and average bit error rate (BER) for various symmetrical links with Nakagami- m [37], Weibull [47], and generalized Gamma [39], [58] fading, as well as for asymmetrical links with Rayleigh-Rician fading [23].

The performance of multihop relay systems in generalized fading models has only recently been investigated in the literature. In [59], the end-to-end SNR of the multihop system with CSI-based relays was obtained and the exact average symbol error rate (SER) was derived for the generalized Gamma fading channel using the moment generating function (MGF) based approach. In [47], the minimum SNR approximation to the end-to-end SNR was employed to derive tight lower bounds of various performance measures for a multihop system operating over Weibull fading channel. Moreover, lower bounds for the performance of multihop systems with fixed gain relays over non-identical Nakagami- m and Rician fading channels were obtained in [60] using the geometric mean approximation for the end-to-end SNR.

Recently, the generalized- K fading model [45] has attracted considerable attention as one of the most general wireless fading models that can characterize the combined effects of fast and slow fading on the received signal. This model corresponds to a Nakagami-

Gamma composite distribution and is controlled by two shaping parameters m and k , where m is the Nakagami parameter for the short-term fading and k is the parameter of the gamma distribution for the received average power due to shadowing [21]. Note that the K distribution [41] is derived as a special case of the generalized- K distribution by letting $m=1$ (i.e., Rayleigh short-term fading). The performance analysis of single link digital communication systems in this fading channel was given in [42], whereas for relay systems, results that have recently appeared in the literature are restricted to the performance of dual-hop systems with CSI-based [44], [61] and fixed gain [52] transmission schemes.

In this chapter, we consider multihop relay systems operating in generalized- K fading channels with integer values for fading parameter m and arbitrary values for fading parameter k . Using the minimum SNR approximation for the output SNR of the multihop relaying system, we derive analytical expressions for the lower bounds of performance metrics such as the outage probability and the average BER and SER of various digital modulations. The rest of the chapter is organized as follows. In Section II we derive a closed-form expression for the cumulative density function (cdf) of the SNR for a single link operating in a generalized- K fading channel. In Section III, we use this result to derive the cdf of the weakest SNR among multiple hops. Section IV presents the performance analysis of the multihop relay system in terms of outage probability and average BER and SER for various modulation schemes. Numerical and simulation results are given in Section V, followed by concluding remarks in Section VI.

5.2 Statistics of Generalized- K Distribution

Wireless communication channels result in random fluctuations of the received signal. In many fading environments, the received signal envelope can usually be characterized by the Nakagami- m distribution. In a shadowed environment, the average power of the received signal is also random. A composite fading model which leads to a closed-form compound distribution assumes that the short-term fading component of the received

signal envelope follows the Nakagami- m distribution while the long-term fading component (shadowing) has a gamma distribution. The result is the generalized- K composite fading model [21]. In this work, we assume that the fading environment is such that the signal envelope X in a receive antenna is a generalized- K distributed random variable with probability density function (pdf) given by [42]

$$f_X(x) = \frac{4m^{(k+m)/2}}{\Gamma(m)\Gamma(k)\Omega^{(k+m)/2}} x^{k+m-1} \times K_{k-m} \left(2 \left(\frac{m}{\Omega} \right)^{1/2} x \right), \quad x \geq 0 \quad (5.1)$$

where k and m are the distribution's shaping parameters, $\Omega = E[X^2]/k$ is the mean power with $E[\cdot]$ denoting expectation, $\Gamma(\cdot)$ is the Gamma function, and $K_\nu(\cdot)$ is the ν th order modified Bessel function of the second kind. The instantaneous received SNR per symbol for a single receiver is $\gamma = X^2 E_s / N_0$, where E_s is the transmitted symbol energy and N_0 is the single-sided power spectral density of the additive white Gaussian noise (AWGN). The corresponding average received SNR per symbol is given as $\bar{\gamma} = k\Omega E_s / N_0$. The pdf of γ is given by

$$f_\gamma(\gamma) = \frac{2\Xi^{\frac{k+m}{2}}}{\Gamma(m)\Gamma(k)} \gamma^{\frac{k+m}{2}-1} K_{k-m} \left(2\sqrt{\Xi\gamma} \right), \quad \gamma \geq 0 \quad (5.2)$$

with $\Xi = (km) / \bar{\gamma}$. The cdf of γ is defined as $F_\gamma(\gamma) \triangleq \int_0^\gamma f_\gamma(x) dx$. Expressing $K_\nu(\cdot)$ as [4, eq. (3.471.9)], the cdf of γ can be written as

$$F_\gamma(\gamma) = \frac{2\Xi^{\frac{k+m}{2}}}{\Gamma(m)\Gamma(k)} \int_0^\gamma x^{\frac{k+m}{2}-1} \frac{1}{2} \left(\frac{\Xi}{x} \right)^{\frac{k-m}{2}} \times \int_0^\infty y^{k-m-1} e^{-\frac{x}{y} - \Xi y} dy dx. \quad (5.3)$$

By changing the order of integration and using [4, eq. (3.381.1)] to solve the inner integral, we obtain

$$F_\gamma(\gamma) = \frac{\Xi^k}{\Gamma(m)\Gamma(k)} \int_0^\infty y^{k-1} e^{-\Xi y} \gamma \left(m, \frac{\gamma}{y} \right) dy \quad (5.4)$$

where $\gamma(\cdot, \cdot)$ denotes the lower incomplete gamma function [4]. Expressing the incomplete gamma function with positive integers n , as [4, eq. (8.352.6)]

$$\gamma(n, z) = \Gamma(n) \left[1 - e^{-z} \sum_{q=0}^{n-1} \frac{z^q}{q!} \right] \quad (5.5)$$

and using [4, eq. (3.351.3)] and [4, eq. (3.471.9)] for the integral in (5.4), the cdf of γ for integer values of fading parameter m and arbitrary values of fading parameter k , is obtained as

$$F_\gamma(\gamma) = 1 - I(\gamma; m, k, \Xi), \quad \gamma > 0 \quad (5.6)$$

where function $I(\cdot)$ is defined as

$$I(x; m, k, \Xi) \triangleq \frac{2(\Xi x)^{\frac{k}{2}}}{\Gamma(k)} \sum_{q=0}^{m-1} \frac{1}{q!} (\Xi x)^{\frac{q}{2}} K_{k-q} \left(2\sqrt{\Xi x} \right). \quad (5.7)$$

Therefore the outage probability for a single link, defined as the probability that the received SNR drops below a specified SNR threshold γ_{th} , can be obtained directly as $P_{\text{out}} = F_\gamma(\gamma_{\text{th}})$. It is observed from (5.6) that this closed-form expression contains only standard mathematical functions and can therefore be easily and efficiently evaluated numerically with software packages such as Matlab and Mathematica.

5.3 Multihop Relaying System

We consider the multihop relaying system depicted in Fig. 5.1, where the communication between the source and the destination is achieved with the help of non-regenerative relays. Each link is characterized by its fading severity and its average SNR, i.e., $(m_\ell, k_\ell, \bar{\gamma}_\ell)$, $\ell = 1, \dots, N$. The links between the source and the destination are assumed to undergo independent fading but can be asymmetric and/or unbalanced, i.e., the N hops may experience different per-hop fading severities and/or average SNRs. This is a realistic assumption in most relay applications, since the relays can be located in different fading environments. Assuming CSI-based amplification gain at each relay, the exact

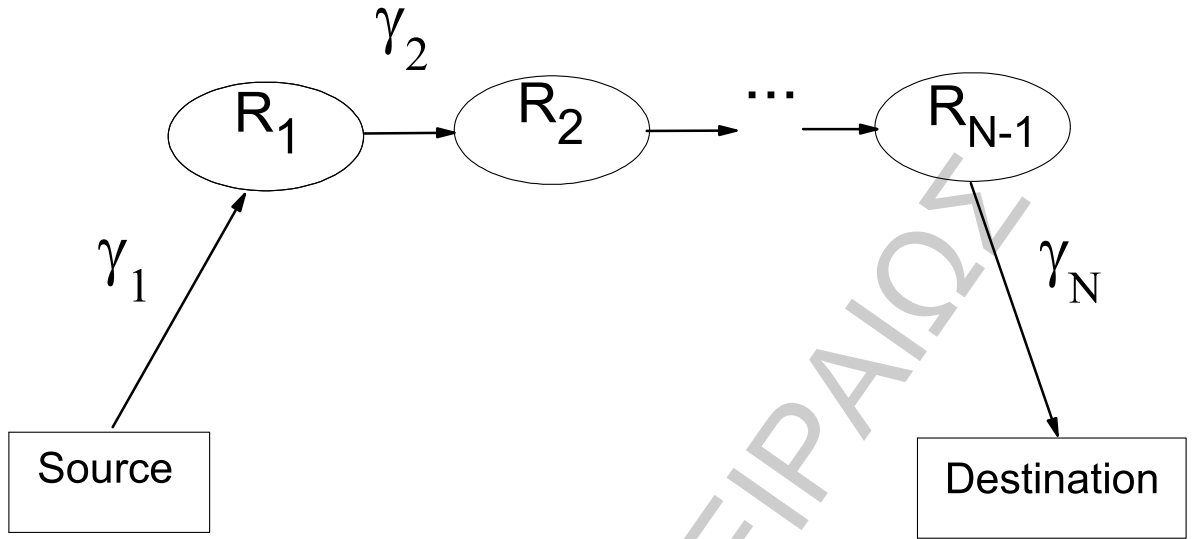


Figure 5.1: Multihop relay system.

end-to-end SNR is given by [31]

$$\gamma_{end} = \frac{1}{\prod_{\ell=1}^N \left(1 + \frac{1}{\gamma_{\ell}}\right) - 1}. \quad (5.8)$$

In the literature, this relay transmission scheme is usually considered as a benchmark for cooperative performance. However, the expression for the end-to-end SNR in (5.8) does not lead to tractable analytical performance results. Therefore, the exact end-to-end SNR is usually approximated by the upper bound given by the minimum SNR of all the links [38], i.e.,

$$\gamma_{end} \leq \gamma_{\min} = \min \{\gamma_1, \dots, \gamma_N\}. \quad (5.9)$$

The cdf of the upper bound to the exact SNR for the multihop relay system, depicted in Fig. 5.1, will then be given by

$$\begin{aligned} F_{\gamma_{\min}}(\gamma) &= 1 - \prod_{\ell=1}^N (1 - F_{\gamma_{\ell}}(\gamma)) \\ &= 1 - \prod_{\ell=1}^N I(\gamma; m_{\ell}, k_{\ell}, \Xi_{\ell}). \end{aligned} \quad (5.10)$$

This closed-form expression can be easily and accurately evaluated numerically since it involves only finite summations of powers and Bessel functions.

5.3.1 Outage Probability

Assuming independent but not necessarily identical fading and arbitrary average received SNRs for the N hops, the outage probability, i.e., the probability that the received end-to-end SNR falls below a predetermined SNR threshold γ_{th} , can be obtained directly as $P_{\text{out}} = F_{\gamma_{\min}}(\gamma_{\text{th}})$.

5.3.2 Average Bit Error Rate

The average BER is obtained by integrating the conditional BER $P_b(e|\gamma)$ over the pdf of the upper bound to the end-to-end SNR, $f_{\gamma_{\min}}(\gamma)$. Following the approach used in [54], the average error probability can be written in terms of the cdf $F_{\gamma_{\min}}(\gamma)$, i.e.,

$$P_b(e) = - \int_0^{\infty} \frac{dP_b(e|\gamma)}{d\gamma} F_{\gamma_{\min}}(\gamma) d\gamma. \quad (5.11)$$

Next, we will present the average BER for various modulation schemes of a multihop system in generalized- K fading channels according to their conditional BER forms.

- (i) $P_b(e|\gamma) = \frac{\Gamma(\beta, \alpha\gamma)}{2\Gamma(\beta)}$. For binary phase shift keying (BPSK) and binary frequency shift keying (BFSK), coherent (i.e., CPSK/CFSK) and differentially coherent/noncoherent (i.e., DPSK/NFSK) detection schemes, the conditional BER in AWGN can be written in a compact form as [62]

$$P_b(e|\gamma) = \frac{\Gamma(\beta, \alpha\gamma)}{2\Gamma(\beta)} \quad (5.12)$$

$$\alpha = \begin{cases} 1, & \text{BPSK} \\ 1/2, & \text{BFSK} \end{cases} \quad \beta = \begin{cases} 1, & \text{DPSK/NFSK} \\ 1/2, & \text{CPSK/CFSK} \end{cases} \quad \text{and } \Gamma(p, x) = \int_x^{\infty} t^{p-1} e^{-t} dt \text{ is the}$$

complementary incomplete gamma function [4]. From (5.11), it follows that the average BER for binary modulation schemes operating over a fading channel can

be written in terms of the cdf of the SNR, as

$$P_b(e) = \frac{\alpha^\beta}{2\Gamma(\beta)} \int_0^\infty \gamma^{\beta-1} e^{-\alpha\gamma} F_\gamma(\gamma) d\gamma. \quad (5.13)$$

Substituting the cdf of the upper bound approximation to the received SNR, $F_{\gamma_{\min}}(\gamma)$, in (5.13), and using [4, eq. (3.351.3)] for the first term, the average BER of binary modulations can be approximated as

$$P_b(e) \cong \frac{1}{2} - \frac{\alpha^\beta}{2\Gamma(\beta)} \int_0^\infty \gamma^{\beta-1} e^{-\alpha\gamma} \times \prod_{\ell=1}^N I(\gamma; m_\ell, k_\ell, \Xi_\ell) d\gamma. \quad (5.14)$$

The final integral can be easily and efficiently evaluated numerically using mathematical software programs such as Matlab and Mathematica.

- (ii) $P_b(e|\gamma) = Q(\sqrt{g\gamma})$. For M -ary phase shift keying (M -PSK) and M -ary quadrature amplitude modulation (M -QAM) signal constellations the conditional BER in an AWGN channel can be expressed as a linear summation of the Gaussian Q -function, defined as $Q(x) = \frac{1}{\sqrt{2\pi}} \int_x^\infty \exp(-t^2/2) dt$. Therefore, in order to evaluate the performance of M -ary modulation schemes over a fading channel we need to evaluate integrals of the form $P_b(e; g) = \int_0^\infty Q(\sqrt{g\gamma}) f_{\gamma_b}(\gamma) d\gamma$ where γ_b is the instantaneous received SNR per bit and g depends on the modulation type [53]. For instance, using the unified approximation in [55], the average BER for M -PSK constellations with Gray coding operating over a fading channel can be expressed as

$$P_{b,\text{MPSK}}(e) \cong \frac{2}{\max(\log_2 M, 2)} \times \sum_{i=1}^{\max(M/4, 1)} P_b(e; g_{i,\text{MPSK}}) \quad (5.15)$$

with $g_{i,\text{MPSK}} = 2(\log_2 M) \sin^2((2i-1)\pi/M)$.

The corresponding average BER for rectangular M -QAM constellations with Gray coding, is

$$P_{b,\text{MQAM}}(e) \cong \frac{4}{\log_2 M} \left(1 - \frac{1}{\sqrt{M}}\right) \times \sum_{i=1}^{\sqrt{M}/2} P_b(e; g_{i,\text{MQAM}}) \quad (5.16)$$

with $g_{i,\text{MQAM}} = 3(2i - 1)^2 (\log_2 M) / (M - 1)$. Furthermore, using the result in [54, eq. (34)], the integral $P_b(e; g)$ can be expressed in terms of the cdf of the upper bound γ_{\min} , as

$$P_b(e; g) = \frac{1}{2} \sqrt{\frac{g}{2\pi}} \int_0^\infty \frac{e^{-g\gamma/2}}{\sqrt{\gamma}} F_{\gamma_{\min}}(\gamma) d\gamma. \quad (5.17)$$

For the generalized- K fading channel, the BER performance of multihop relay networks can be obtained by inserting (5.10) in (5.17) to obtain

$$P_b(e; g) = \frac{1}{2} - \frac{1}{2} \sqrt{\frac{g}{2\pi}} \int_0^\infty \frac{e^{-g\gamma/2}}{\sqrt{\gamma}} \times \prod_{\ell=1}^N I(\gamma; m_\ell, k_\ell, \Xi_\ell) d\gamma. \quad (5.18)$$

Then, by substituting this result in (5.15) and (5.16), the average BER of M -PSK and M -QAM, respectively, can be evaluated numerically using standard mathematical software programs.

5.3.3 Average Symbol Error Rate

For many digital modulation schemes, the conditional SER in AWGN is given by [54]

$$P_s(e; a, b, c|\gamma) = aQ(\sqrt{b\gamma}) - cQ^2(\sqrt{b\gamma}). \quad (5.19)$$

The expression of (5.19) provides either the exact or the high SNR approximation of

the exact SER depending on the modulation format considered. The parameters (a, b, c) can be found in the literature for many digital modulations used in wireless systems. For example, $(a, b, c)=(1, 2, 0)$ for coherent BPSK, $(a, b, c)=(1, 1, 0)$ for coherent BFSK, $(a, b, c)=(2, 2\sin^2(\pi/M), 0)$ for M -PSK with $M > 4$, $(a, b, c)=(2, 1, 1)$ for QPSK, $(a, b, c)=(2, 2, 2)$ for DPSK, and $(a, b, c)=(4(\sqrt{M}-1)/\sqrt{M}, 3/(M-1), 4(\sqrt{M}-1)^2/M)$ for rectangular M -QAM [54], [53]. Based on the cdf based approach, the average SER for the multihop relay system operating in a fading channel can be expressed as [54, eq. (40)]

$$P_s(e; a, b, c) = \sqrt{\frac{b}{2\pi}} \int_0^\infty \frac{e^{-b\gamma/2}}{\sqrt{\gamma}} \left(\frac{a}{2} - cQ(\sqrt{b\gamma}) \right) F_{\gamma_{\min}}(\gamma) d\gamma \quad (5.20)$$

where $F_{\gamma_{\min}}(\gamma)$ is the cdf of the upper bound to the output SNR per symbol. Substituting (5.10) in (5.20), the final result is given by

$$P_s(e; a, b, c) = \frac{a}{2} - \frac{c}{4} - \sqrt{\frac{b}{2\pi}} \int_0^\infty \frac{e^{-b\gamma/2}}{\sqrt{\gamma}} \left(\frac{a}{2} - cQ(\sqrt{b\gamma}) \right) \prod_{\ell=1}^N I(\gamma; m_\ell, k_\ell, \Xi_\ell) d\gamma. \quad (5.21)$$

The expression given in (5.21) can be easily computed numerically using common mathematical software programs. The average SER for a variety of modulation schemes can then be evaluated for the multihop relay system operating in a generalized- K fading channel.

5.4 Numerical Results

In this section we present some numerical and simulation results for the performance of the multihop relay transmission scheme operating over a generalized- K fading channel. The generalized- K fading model can describe different fading conditions by the appropriate choice of fading parameters m and k . Low values of m and k can be used

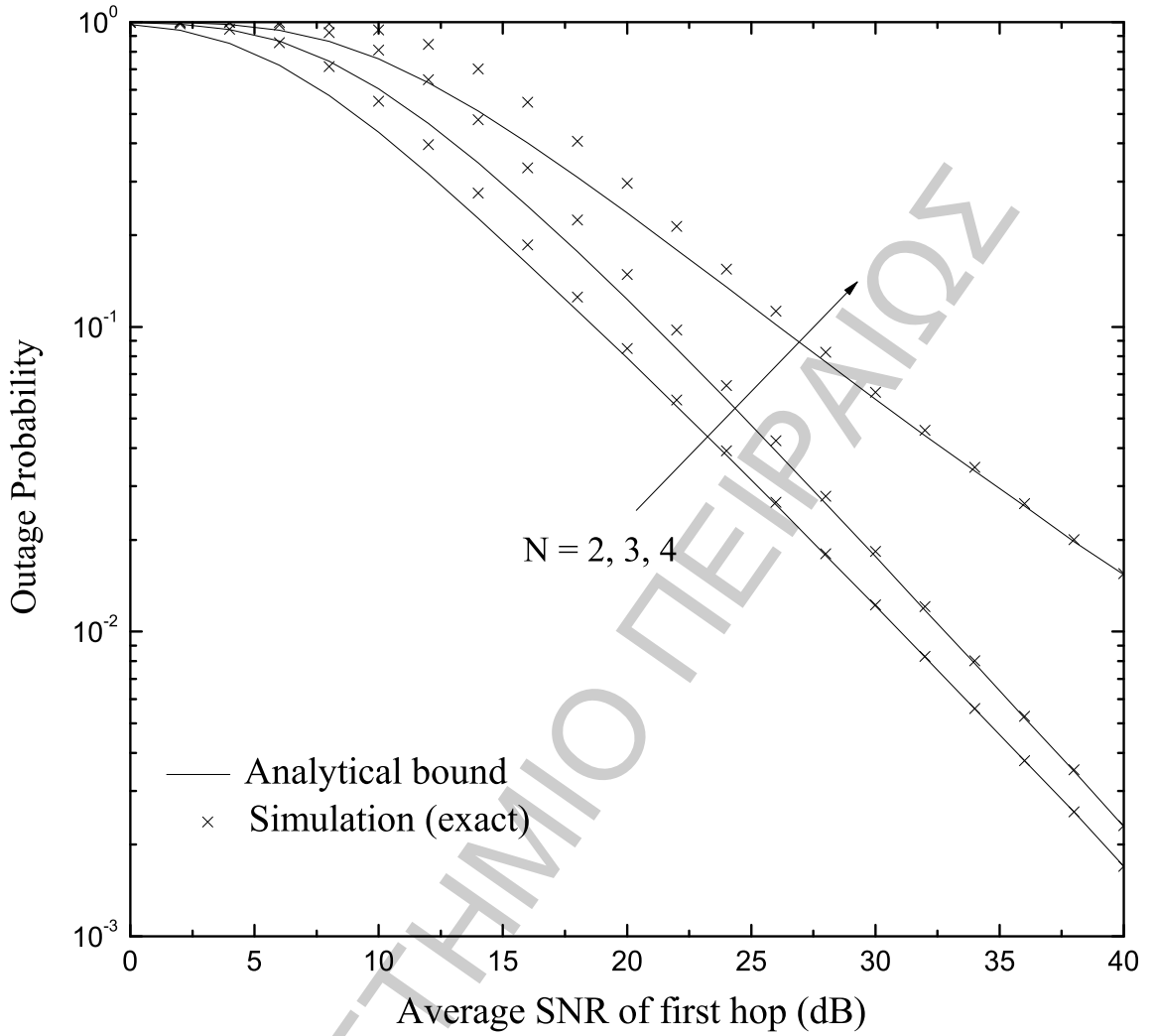


Figure 5.2: Outage probability vs average SNR of the first hop for $\gamma_{\text{th}} = 3$ dB with $N=2,3,4$ balanced hops with different fading conditions.

to describe fading conditions with severe multipath fading and shadowing, respectively, whereas fading conditions improve as the values of the fading parameters increase. For demonstration purposes, we consider non-identical fading conditions per hop with equal and unequal average SNRs, i.e., balanced and unbalanced links, respectively. We select the fading parameters (m, k) per hop as $(m_1 = 1, k_1 = 1)$, $(m_2 = 2, k_2 = 3)$, $(m_3 = 1, k_3 = 1.5)$, and $(m_4 = 3, k_4 = 0.5)$, whereas for the unbalanced case we also select the average SNRs per hop as $\bar{\gamma}_1 = \bar{\gamma}_2/2 = 2\bar{\gamma}_3 = 2\bar{\gamma}_4$. Simulation results of the lower bounds

are found to exactly overlap with the analytical results and therefore they are not shown in the plots.

Using the minimum SNR approximation, Fig. 5.2 plots the outage probability versus the average SNR of the first hop for $\gamma_{\text{th}} = 3$ dB and $N = 2, 3$ and 4. The tightness of the analytical curves is depicted by comparison with the corresponding exact performance curves obtained by simulation. It is evident that the analytical lower bound is tight particularly at medium and high values of the average SNR per hop and its tightness decreases moderately with the increase of the number of hops N . However, it always converges to the exact values at high per-hop average SNRs.

For the same fading conditions, Fig. 5.3 and 5.4 plot the average BER of BPSK and 16-QAM versus the average SNR per bit of the first hop for balanced and unbalanced hops, respectively. Simulation results of the exact BER are also shown in order to demonstrate the tightness of the analytical bound. We observe that for both cases considered, the difference between the analytical bound and the exact performance is larger at the low per-hop average SNR region than at medium and high average SNRs and increases slightly as N increases. Furthermore, we observe that the average BER deteriorates with the increase of the number of hops N , as expected [47]. Finally, Fig. 5.5 and 5.6 plot, respectively, the average SER of QPSK and 16-QAM versus the average SNR of the first hop for both balanced and unbalanced cases. The tightness of the analytical expressions that use the minimum SNR upper bound to the corresponding exact performance is observed, with the approximated SER to converge to the exact values for high values of the average SNR per hop.

5.5 Conclusion

In this paper, we derived a closed-form expression for the cdf of the minimum SNR upper bound to the end-to-end SNR of a multihop relay system operating in a generalized- K fading environment. Using this result, the average BER and SER was then evaluated for a variety of digital modulation schemes using the cdf based approach. The results obtained

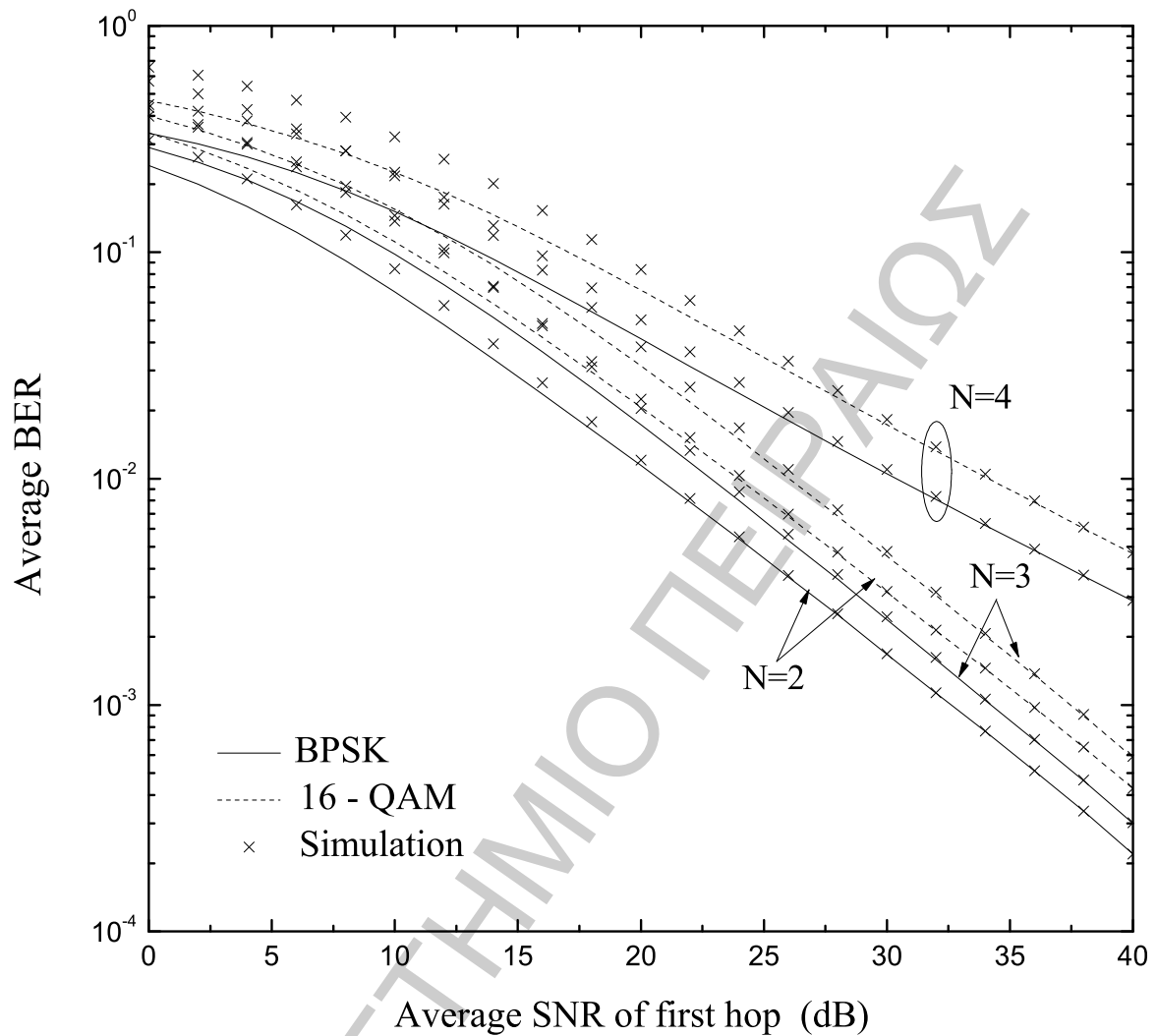


Figure 5.3: Average BER vs average SNR per bit of the first hop for BPSK and 16-QAM with $N=2,3,4$ balanced hops with different fading conditions.

using the derived analytical expressions offer tight lower bounds to the corresponding exact results obtained by simulation.

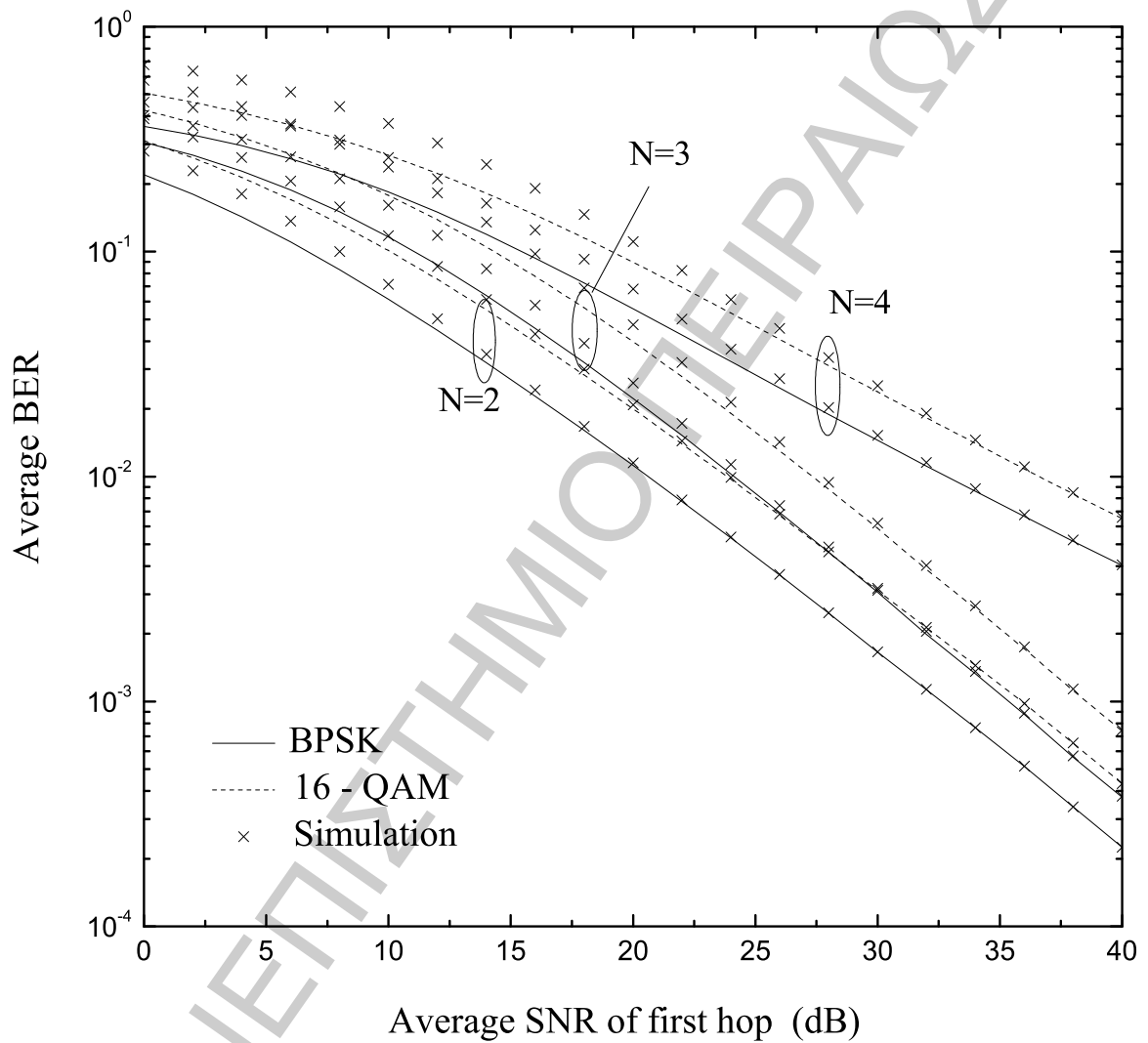


Figure 5.4: Average BER vs average SNR per bit of the first hop for BPSK and 16-QAM with $N=2,3,4$ unbalanced hops with different fading conditions.

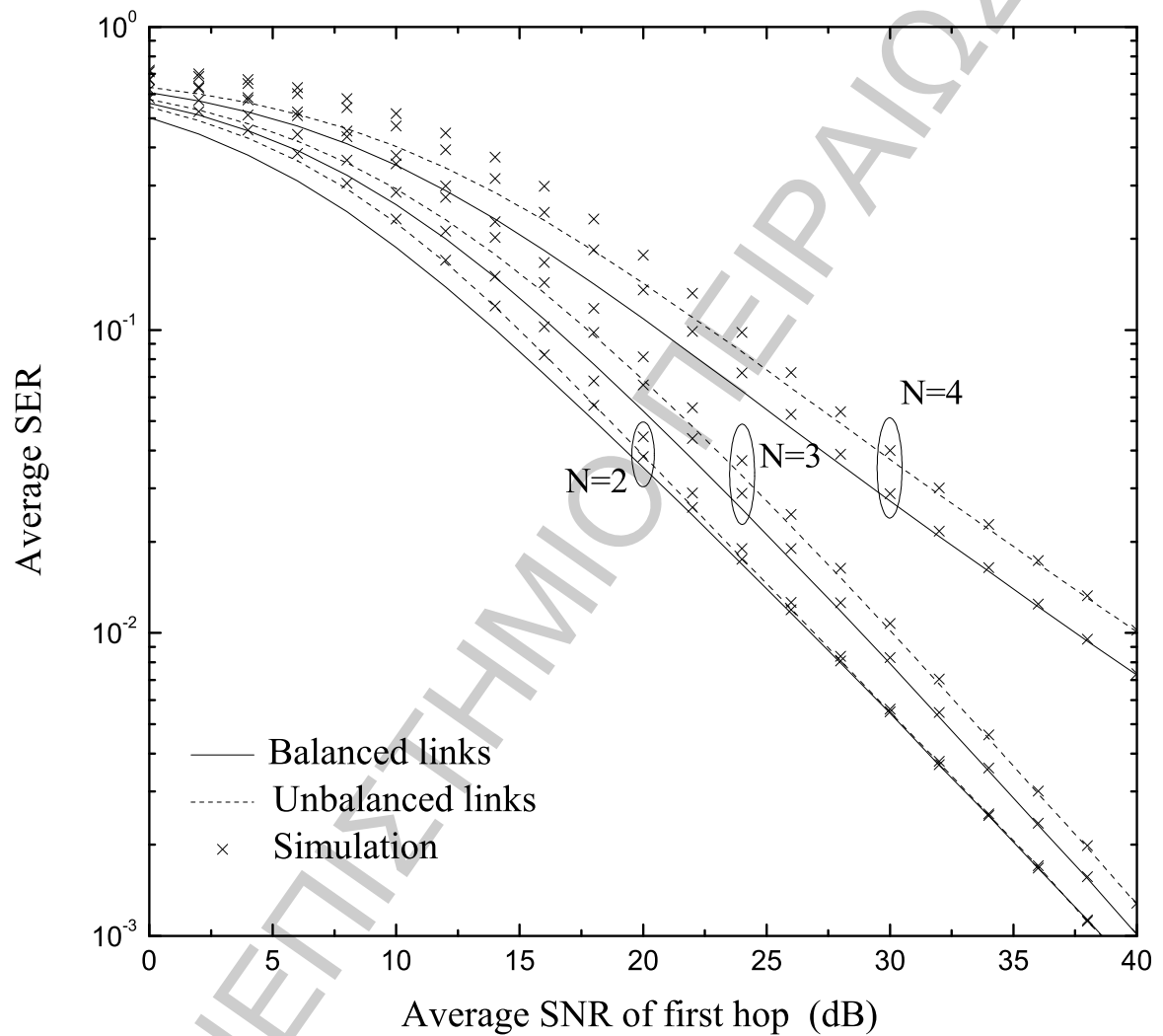


Figure 5.5: Average SER vs average SNR of first hop for QPSK with $N=2,3,4$ in different fading conditions.

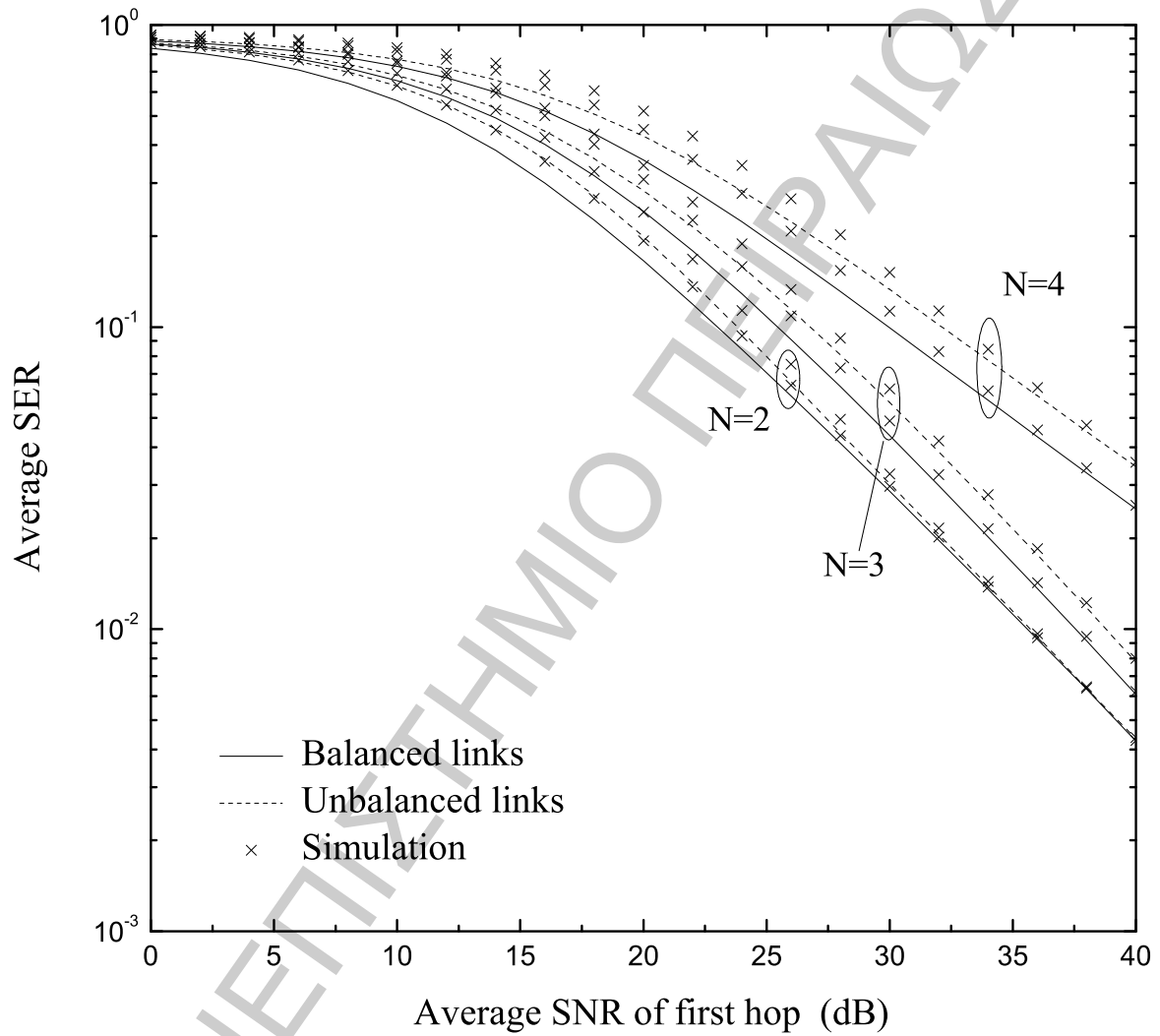


Figure 5.6: Average SER vs average SNR of first hop for 16-QAM with $N=2,3,4$ in different fading conditions.

Chapter 6

On the Performance of Multihop Relay Systems in Nakagami Fading Channel

WE DERIVE closed-form lower bounds on the performance of multihop communication W systems with non-regenerative relays operating in a Nakagami- m fading channel. The relay gains are assumed to be chosen to maximize the end-to-end signal-to-noise ratio (SNR), which is bounded by the geometric mean of the positive random variables. Closed-form expressions are then derived for the statistics of the geometric mean of the optimum end-to-end SNR. These, in turn, are used to derive tight bounds for the outage as well as average error performances of the system. An upper bound is also derived for the mean ergodic capacity of the end-to-end SNR.

6.1 Introduction

Multihop relaying in which the transmitted signal propagates through cascaded nodes, with each node amplifying and forwarding information from only the previous node to the next, has been shown to improve the performance and extend the coverage of many communication systems [24, 25]. The performances of such systems have been studied for a variety of fading environments, including the Rayleigh, Nakagami and Rice fading channels, among others [35, 36, 63]. For non-regenerative relay systems with an amplify-

and-forward transmission scheme in a fading environment, the end-to-end SNR at the receiving end depends on the amplification gain employed at the relays. In particular, it is known that the choice of the relay gain that maximizes the end-to-end SNR is to invert the combined instantaneous received power (i.e., sum of desired signal and noise powers) at the node [35]. However, the performances of multihop systems that use this optimum choice of the relay gains and operate in a cascaded channel environment are difficult to analyze. Consequently, exact performance results available in the literature are limited to only two-hop systems [35], [64]. For multihop relay systems, in order to obtain analytically tractable results, the analysis usually focuses on approximations or limiting cases. For example, when the channel gains are chosen to ignore the presence of noise, the relay gains simply invert the instantaneous signal power in the previous hop regardless of the noise of that hop [32], [33]. Also, in a noise-limited system, the effect of the instantaneous signal power at the relays is ignored and the relay gains are blindly chosen to be inversely proportional to the noise power at the previous relay [63], [33]. To the best of our knowledge, apart for the two-hop case, the performance of multihop relay system that considers the effects of both the useful instantaneous signal and noise powers on the relay gain selection is not available in the literature. The main aim of this chapter is to close this gap.

In this chapter, we consider a multihop relay system in which each relay gain is chosen to maximize the end-to-end SNR and operates in a Nakagami- m fading channel. We use the fact that the harmonic mean of positive variables is upper bounded by their geometric mean to express bounds for the end-to-end SNR.

6.2 End-To-End SNR

We consider the multihop relay system in which the communication between the source and the destination is achieved with the help of a series of non-regenerative relays. The links between the source and the destination are assumed to undergo independent but not necessarily identical Nakagami- m fading. In a multihop communications with N -hops, it

can be shown that the end-to-end SNR at the destination is given by [35],

$$\gamma_{\text{end}} = \frac{\prod_{i=1}^N \alpha_i^2 g_{i-1}^2}{\sum_{i=1}^N N_{0_i} \left(\prod_{j=i+1}^N \alpha_j^2 g_{j-1}^2 \right)} \quad (6.1)$$

where α_i denotes the fading envelope of the i -th channel, $i = 1, \dots, N$, g_i is the gain at the i -th node (with $g_0 = 1$) and N_{0_i} is the one-sided power spectral density of the noise. In general, the choice of the node gain g_i , for $i = 1, \dots, N$, determines the end-to-end SNR.

In CSI-based relays, the amplification gains at each relay are chosen, with the knowledge of the channel state information, to invert the fading state of the preceding link. It limits the instantaneous output power of the relay when the channel gain in the preceding hop is low. The corresponding relay gain is chosen as

$$g_i^2 = \frac{1}{\alpha_i^2 + N_{0_i}}. \quad (6.2)$$

Substituting (6.2) in (6.1), the exact end-to-end SNR is given by [35, eq. (16)]

$$\gamma_{\text{end}} = \left[\sum_{n=1}^N \frac{1}{\gamma_n} \prod_{i=1}^{n-1} \left(1 + \frac{1}{\gamma_i} \right) \right]^{-1} \quad (6.3)$$

where $\gamma_i = E(\alpha_i^2) / N_{0_i}$ is the SNR on the i -th link. By expanding the terms in (6.3), we have

$$\gamma_{\text{end}} = \left[\sum_{n=1}^N \frac{(\gamma_1 + 1)(\gamma_2 + 1) \cdots (\gamma_{n-1} + 1)}{\gamma_1 \gamma_2 \cdots \gamma_n} \right]^{-1}. \quad (6.4)$$

A careful examination of (6.4) shows that there are $(2^N - 1)$ terms in the summation. Therefore, the end-to-end SNR may be recognized as the harmonic mean [35], [63],

$$\gamma_{\text{end}} = \frac{1}{M} \left(\frac{1}{M} \sum_{n=1}^M \frac{1}{x_n} \right)^{-1} \quad (6.5)$$

of terms x_n , each of which is the product of the combinations of $\gamma_1, \gamma_2, \dots, \gamma_n$, where $M = 2^N - 1$. It is well known that for the sequence x_1, x_2, \dots, x_M , the harmonic mean

is upper bounded by the geometric mean as [63]

$$\left(\frac{1}{M} \sum_{i=1}^M \frac{1}{x_i} \right)^{-1} \leq \left(\prod_{i=1}^M x_i \right)^{1/M}. \quad (6.6)$$

It follows from (6.6) that the end-to-end SNR is upper-bounded by

$$\gamma_{\text{end}} \leq \gamma_{\alpha} = \frac{1}{(2^N - 1)} \left(\prod_{i=1}^N \gamma_i \right)^{2^{N-1}/(2^N - 1)}, \quad (6.7)$$

where we have taken the geometric mean of all $(2^N - 1)$ terms in the summation in which each γ_i ($i = 1, 2, \dots, N$) appears exactly 2^{N-1} times. The upper bound for the end-to-end SNR in (6.7) has not been considered in the literature, except from the special case when $N = 2$, which is treated in [36].

6.3 Performance in Nakagami Fading Channel

6.3.1 PDF of End-to-End SNR Bound

The pdf of the SNR on the i -th hop in a multi-hop link operating in a Nakagami- m fading environment is given by

$$f_{\gamma_i}(\gamma) \frac{(m_i/\bar{\gamma}_i)^{m_i}}{\Gamma(m_i)} \gamma^{m_i-1} \exp\left(-m_i \frac{\gamma}{\bar{\gamma}_i}\right) \quad (6.8)$$

where $m_i \geq 1/2$ is a parameter that describe the fading severity of the i -th hop. It can be shown that the pdf of the rational product of powers, $Y = \prod_{i=1}^N \gamma_i^{\ell_i/n}$, may be expressed in terms of the Meijer G-function as [33, eq. (4)]

$$\begin{aligned} f_Y(y) &= \frac{n}{y} \frac{\prod_{i=1}^N \ell_i^{m_i-1/2}}{(\sqrt{2\pi})^{r-N} \prod_{i=1}^N \Gamma(m_i)} \\ &\times G_{0,r}^{r,0} \left[y^n \prod_{i=1}^N \left(\frac{m_i}{\bar{\gamma}_i \ell_i} \right)^{\ell_i} \mid \begin{matrix} - \\ \phi_1, \phi_2, \dots, \phi_N \end{matrix} \right] \end{aligned} \quad (6.9)$$

where $\phi_i = \Delta(\ell_i, m_i)$ and $r = \sum_{i=1}^N \ell_i$, with ℓ_1, \dots, ℓ_N being positive integers. The corresponding cdf is given by [33, eq. (6)]

$$F_Y(y) = \frac{\prod_{i=1}^N \ell_i^{m_i-1/2}}{(\sqrt{2\pi})^{r-N} \prod_{i=1}^N \Gamma(m_i)} \times G_{1,r+1}^{r,1} \left[y^n \prod_{i=1}^N \left(\frac{m_i}{\bar{\gamma}_i \ell_i} \right)^{\ell_i} \middle| \begin{matrix} 1 \\ \phi_1, \phi_2, \dots, \phi_N, 0 \end{matrix} \right]. \quad (6.10)$$

Consequently, using a simple transformation of random variables, the pdf of γ_α is obtained by substituting $\ell_i = L = 2^{N-1}$ and $n = M$ in (6.9) to give

$$f_{\gamma_\alpha}(\gamma) = M \mathbf{P} \gamma^{-1} \mathbf{G}_{0,R}^{R,0} \left[\mathbf{R} \gamma^{\mathbf{M}} \middle| \begin{matrix} - \\ \beta_1, \beta_2, \dots, \beta_N \end{matrix} \right] \quad (6.11)$$

where, $R = N2^{N-1}$, $M = 2^N - 1$, $m_T = \sum_{i=1}^N m_i$, $\beta_i = \Delta(L, m_i)$, $\mathbf{P} = \frac{\mathbf{L}^{m_T - N/2}}{(\sqrt{2\pi})^{R-N} \prod_{i=1}^N \Gamma(\mathbf{m}_i)}$ and $\mathbf{R} = \frac{\mathbf{M}^{\mathbf{M}}}{\mathbf{L}^{\mathbf{R}}} \prod_{i=1}^N (\mathbf{m}_i / \bar{\gamma}_i)^{\mathbf{L}}$. In Fig. 6.1, several curves of the PDF of γ_α are depicted as a function of γ , assuming identical fading conditions and $N = 2, 3$.

6.3.2 Outage Probability

The outage probability, defined as the probability that the received end-to-end SNR falls below a threshold, γ_{th} , can be obtained directly as $P_{\text{out}}(\gamma_{\text{th}}) = F_{\gamma_{\text{end}}}(\gamma_{\text{th}})$. Based on the bound γ_α for the end-to-end SNR, the outage probability is obtained from (6.10) as

$$F_{\gamma_\alpha}(\gamma_{\text{th}}) = F_Y(M\gamma_{\text{th}}) = \mathbf{P} \mathbf{G}_{1,R+1}^{R,1} \left[\mathbf{R} \gamma_{\text{th}}^{\mathbf{M}} \middle| \begin{matrix} 1 \\ \beta_1, \beta_2, \dots, \beta_N, 0 \end{matrix} \right]. \quad (6.12)$$

6.3.3 Moments of End-to-End SNR Bound

The v -th moment of the end-to-end SNR bound is given by $E(\gamma_\alpha^v) = \int_0^\infty \gamma^v f_{\gamma_\alpha}(\gamma) d\gamma$. Replacing the pdf of γ_α given by (6.11), making the change of variables $y = \gamma^M$ and using [22, eq. (07.34.21.0009.01)] we obtain

$$\begin{aligned} E(\gamma_\alpha^v) &= \mathbf{P} \int_0^\infty y^{v/M-1} \mathbf{G}_{0,R}^{R,0} \left[\mathbf{R} y \middle| \begin{matrix} - \\ \beta_1, \beta_2, \dots, \beta_N \end{matrix} \right] dy \\ &= \mathbf{P} \prod_{i=1}^N \prod_{h=1}^{\mathbf{L}} \Gamma \left(\frac{\mathbf{m}_i + \mathbf{h} - 1}{\mathbf{L}} + \frac{\mathbf{v}}{\mathbf{M}} \right) \mathbf{R}^{-v/M}. \end{aligned} \quad (6.13)$$

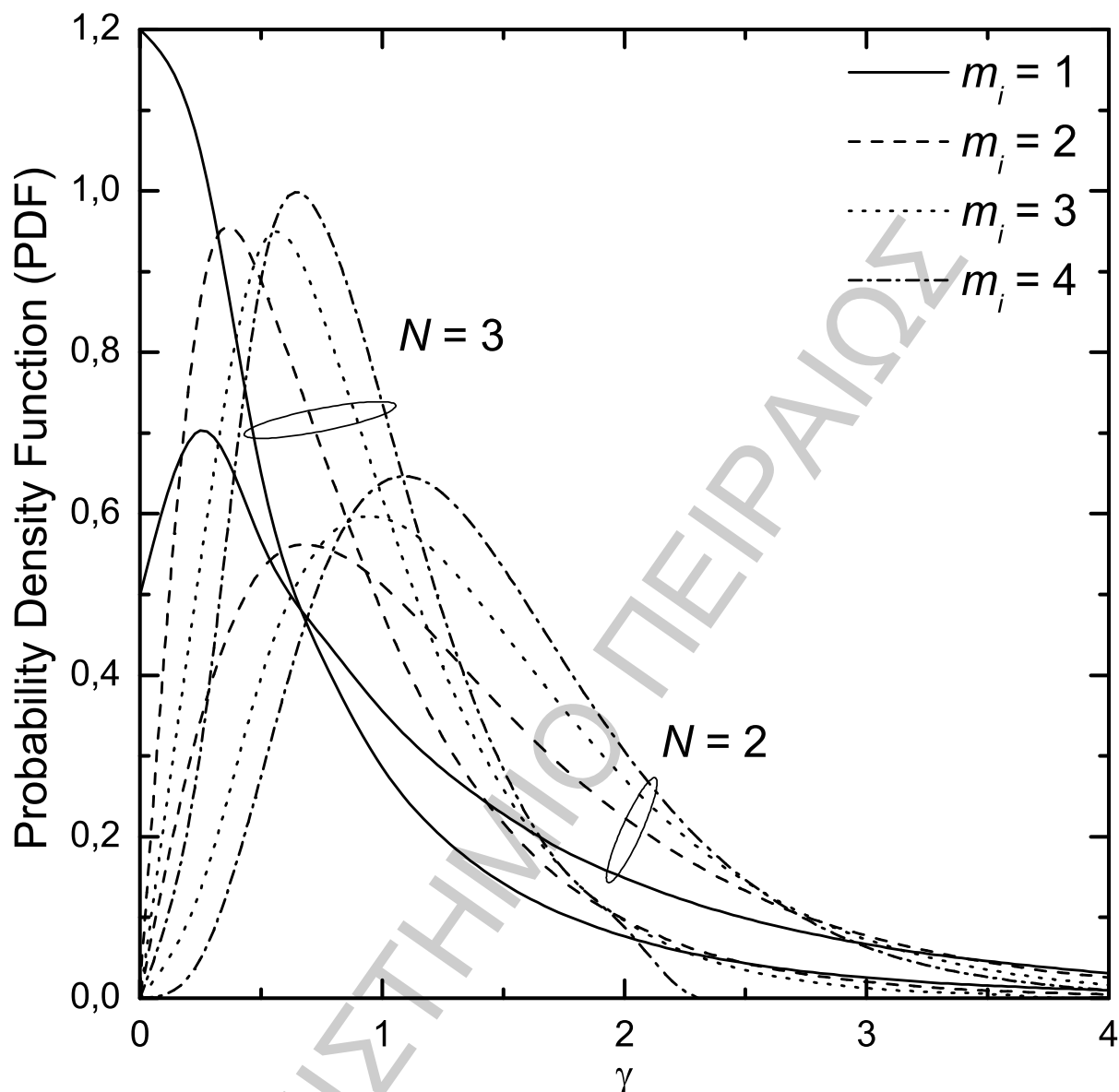


Figure 6.1: The PDF of γ_α for identical fading conditions and $N = 2, 3$.

6.3.4 Average Symbol Error Probability

The average symbol error probability (ASEP) for a variety of digital modulation schemes is given by

$$\bar{P}_s(M) = \frac{1}{\pi} \int_{\theta_A}^{\theta_B} \mathbf{M}_{\gamma_\alpha} \left(\frac{\mathbf{g}_M}{\sin^2 \theta} \right) d\theta \quad (6.14)$$

where the moment generating function of γ_α is obtained using [33, eq. (3)], as

$$\mathbf{M}_{\gamma_\alpha}(\mathbf{t}) = \frac{\sqrt{\mathbf{M}\mathbf{P}}}{(\sqrt{2\pi})^{M-1}} G_{R,M}^{M,R} \left[\left(\frac{-t}{M} \right)^M \prod_{i=1}^N \left(\frac{m_i}{L\bar{\gamma}_i} \right)^{-L} \middle| \begin{array}{c} \Delta(L,1-m_1), \dots, \Delta(L,1-m_N) \\ \Delta(M,0) \end{array} \right] \quad (6.15)$$

Using (6.15), the result in (6.14) can be evaluated numerically. Furthermore, for non-coherent demodulation schemes with conditional SER expressed as $P_{e,non}(\gamma) = C \exp(-D\gamma)$, where C and D are constants depending on the modulation scheme, the average SER can be given directly by the MGF of γ_α , as $\bar{P}_{e,non} = C\mathbf{M}_{\gamma_\alpha}(\mathbf{D})$.

6.3.5 Average Bit Error Probability

The conditional bit error probability (BEP) of many coherent modulation schemes in AWGN can be written as a linear combination of terms $P_e(\gamma) = A \operatorname{erfc}(\sqrt{B\gamma})$, where $\operatorname{erfc}(\cdot)$ is the complementary error function and A, B are constants that depend on the specific modulation [53]. It then follows that for the multihop relay system the average BER can be given as a linear combination of terms $\bar{P}_e = \int_0^\infty P_e(\gamma) f_{\gamma_\alpha}(\gamma) d\gamma$, where $f_{\gamma_\alpha}(\gamma)$ is the pdf of end-to-end SNR bound γ_α . Using the relation, $\operatorname{erfc}(\sqrt{B\gamma}) = (\sqrt{\pi})^{-1} G_{1,2}^{2,0} \left[B\gamma \middle| \begin{array}{c} 1 \\ 1, 1/2 \end{array} \right]$, we have

$$\bar{P}_e = A \frac{\mathbf{P}}{2\sqrt{\pi}} \int_0^\infty \gamma^{-1} G_{1,2}^{2,0} \left[B\gamma \middle| \begin{array}{c} 1 \\ 1, 1/2 \end{array} \right] \times G_{0,R}^{R,0} \left[\mathbf{R}\gamma^{\mathbf{M}} \middle| \begin{array}{c} - \\ \beta_1, \beta_2, \dots, \beta_N \end{array} \right] d\gamma. \quad (6.16)$$

which can be obtained in closed form, as

$$\bar{P}_e = \frac{A\mathbf{P}}{2\sqrt{\pi} (\sqrt{2\pi})^{M-1}} \times G_{2M, R+M}^{R, 2M} \left[\mathbf{R} \left(\frac{\mathbf{M}}{\mathbf{B}} \right)^{\mathbf{M}} \middle| \begin{array}{c} \Delta(M,1), \Delta(M,1/2) \\ \beta_1, \beta_2, \dots, \beta_N, \Delta(M,0) \end{array} \right]. \quad (6.17)$$

6.3.6 Ergodic Capacity

The ergodic capacity may be bounded as

$$\mathbf{E}_{\mathbf{AF}} = \int_0^\infty \log_2(\mathbf{1} + \gamma) \mathbf{f}_{\gamma_\alpha}(\gamma) \mathbf{d}\gamma \quad (6.18)$$

Substituting the following [4]

$$\ln(1 + \gamma) = G_{2,2}^{1,2} \left[\gamma \left| \begin{matrix} 1,1 \\ 1,0 \end{matrix} \right. \right] \quad (6.19)$$

and (6.11) in (6.18), with the help of [22, eq. (07.34.21.0013.01)], we obtain

$$\begin{aligned} \mathbf{E}_{\mathbf{AF}} &= \mathbf{P} \int_0^\infty \gamma^{-1} G_{2,2}^{1,2} \left[\gamma \left| \begin{matrix} 1,1 \\ 1,0 \end{matrix} \right. \right] G_{0,R}^{R,0} \left[\mathbf{R} \gamma^{\mathbf{M}} \left| \begin{matrix} - \\ \beta_1, \beta_2, \dots, \beta_N \end{matrix} \right. \right] \mathbf{d}\gamma \\ &= \frac{\mathbf{P}}{(2\pi)^{M-1} \ln(2)} G_{2M, R+2M}^{R+2M, M} \left[\mathbf{R} \left| \begin{matrix} \Delta(M,0), \Delta(M,1) \\ \beta_1, \beta_2, \dots, \beta_N, \Delta(M,0), \Delta(M,0) \end{matrix} \right. \right]. \end{aligned} \quad (6.20)$$

6.4 Numerical Results

In this section we present some numerical evaluated results for the multihop relay transmission scheme with non-regenerative relays operating over Nakagami- m fading channels. These results include lower bounds for the outage probability (P_{out}) and the average bit error probability (ABEP).

In Fig. 6.2, using (6.12), the P_{out} is plotted as a function of the average input SNR $\bar{\gamma}$, assuming identical fading parameters $m = m_i$ and $N = 3$. It is depicted that P_{out} improves by increasing $\bar{\gamma}$ and/or increasing m . In Fig. 6.3, using (6.15) the average BEP of binary differential phase shift keying (BDPSK) is plotted as a function of the $\bar{\gamma}$. Furthermore, it is assumed $N = 2, 3$ and several, identical values for m_i . It is depicted that the average BEP decreases with N increasing and/or m_i also increasing.

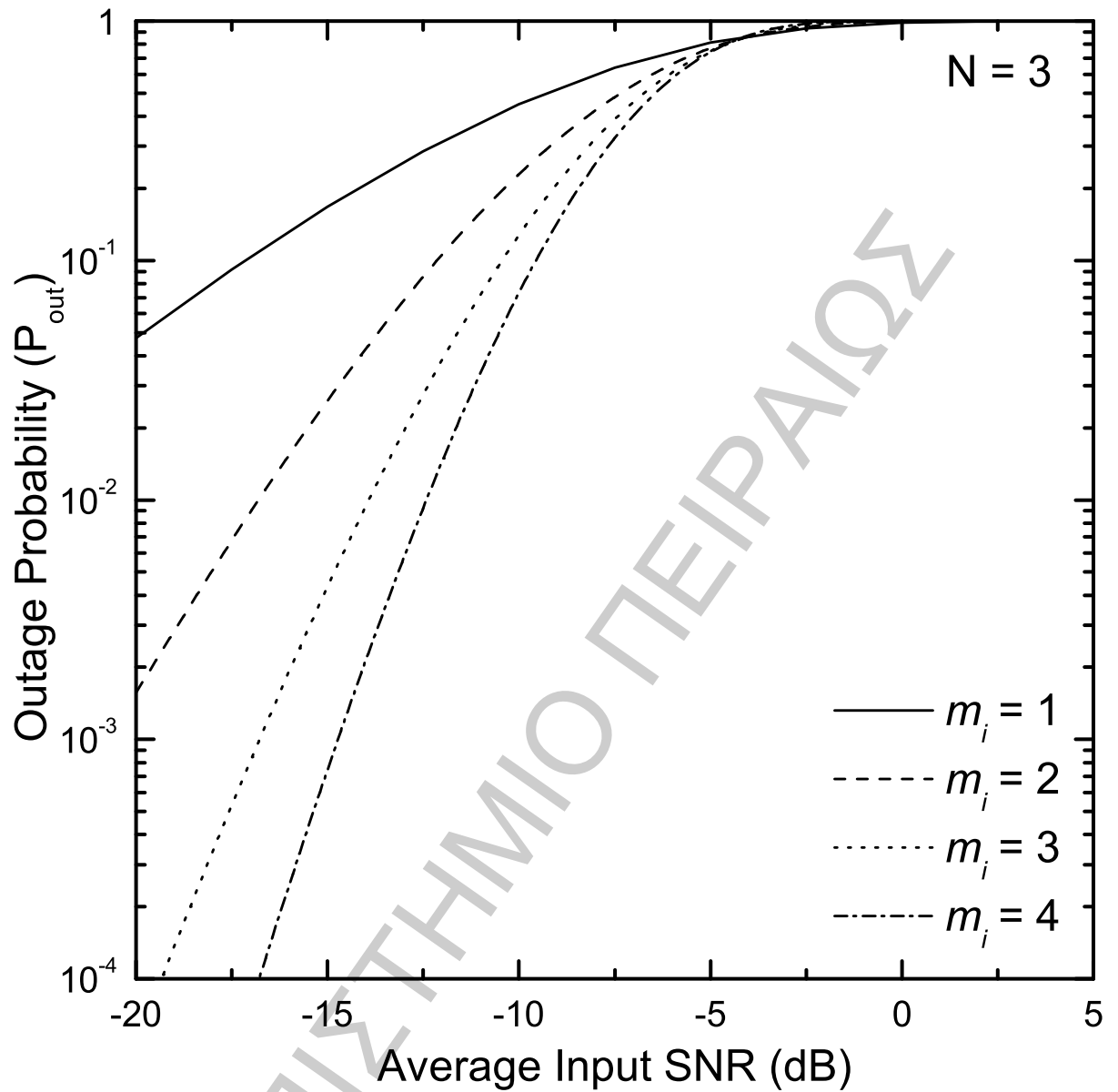


Figure 6.2: Outage Probability versus the average input SNR for several values of m and $N=3$.

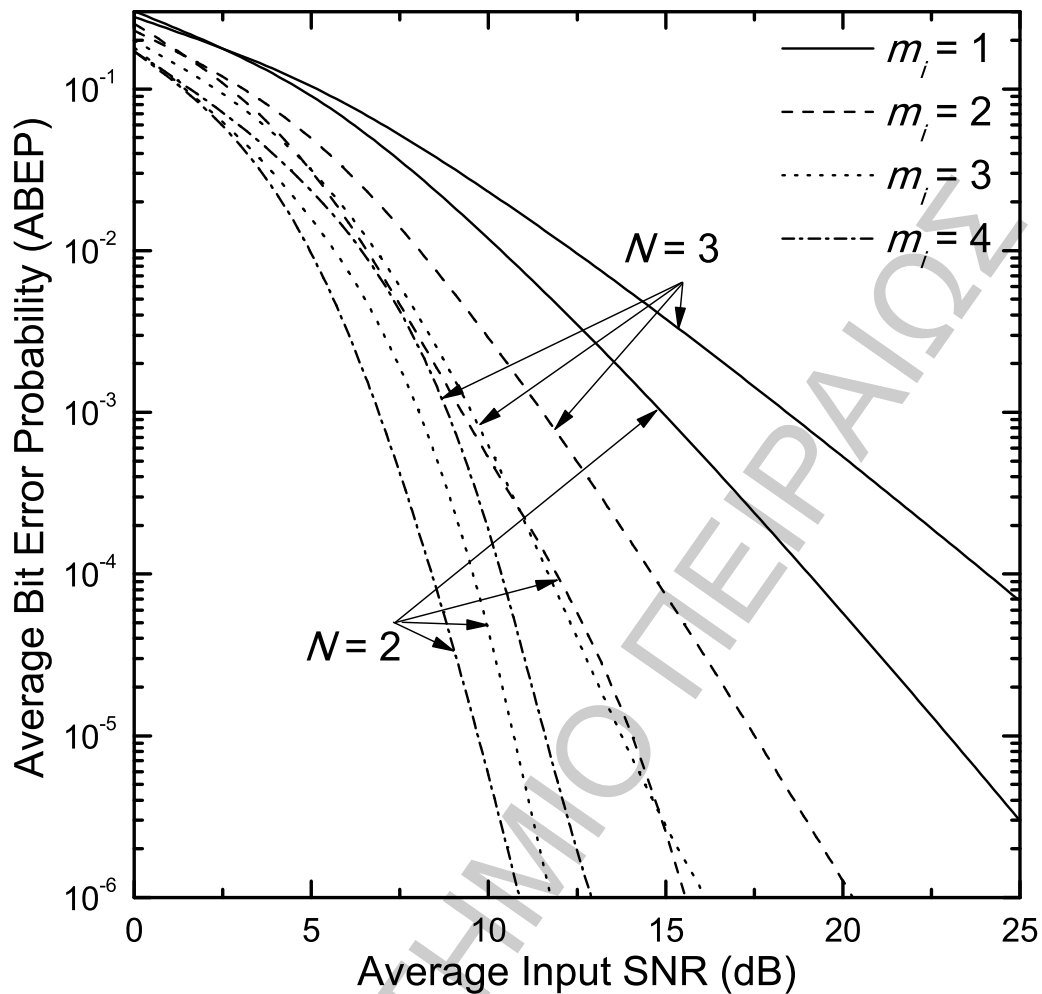


Figure 6.3: Average BER for BDPSK vs $\bar{\gamma}$ for $N = 2, 3$ and several values of m_i .

6.5 Conclusions

In this section, we provided a closed-form expression for the upper bound of the end-to-end SNR of a multi-hop relay system operating over a Nakagami- m fading environment. The effect of both the desired signal as well as the relay noise powers are considered in setting the relay gains with the aim to maximize the end-to-end SNR. The results using the analytical expressions offer a tight bound to the corresponding exact results obtained by simulation.

Chapter 7

Exact Outage Probability of Dual-Hop Relay Systems in a Rayleigh Fading Channel with Multiple Interferers

In this chapter, we study the effect of co-channel interference on the outage probability \bar{I} of dual-hop wireless communication systems with amplify-and-forward (AF) relays operating in a Rayleigh fading channel. A four-parameter model for the dual-hop AF relay system is introduced, in which two of the parameters specify the type of gain adopted at the relay node while the other two parameters account for the presence of channel noise and co-channel interference at the destination node. We then derive the exact outage probability in terms of the well-known incomplete Weber integral, which can be easily and accurately evaluated numerically. The analytical results are validated by computer simulation.

7.1 Introduction

The cooperative diversity realized through relaying can provide increased link quality and reliability, and mitigate channel impairments in next generation wireless systems [24], [25]. In an amplify-and-forward (AF) relay system, the signal received at the relay node is simply amplified and forwarded to the destination node. Until recently, the performance

study of a dual-hop relaying system has been limited to systems that are noise-limited and relied on the end-to-end signal-to-noise ratio (SNR), which depends on the choice of the amplification gain adopted at the relay node. The optimal choice of the relay gain that maximizes the end-to-end SNR inverts a linear combination of the instantaneous channel gain and noise power at that relay node; this is categorized as the optimum channel-state information (CSI) assisted relay scheme [26], [65]. Other categories of AF relays include the channel assisted (or suboptimum CSI assisted) relays which ignore the presence of channel noise in the relay gain [65], [31] and the fixed gain relays (which include blind and semi-blind relays) [66], [63]. In [65], a two-parameter model is proposed that encompasses all the categories of AF relays in noise-limited systems by an appropriate choice of two parameters.

However, since many practical wireless systems suffer from both interference and noise, attention has also turned recently to the analysis of dual-hop relay transmission in the presence of channel noise as well as multiple co-channel interferers; in many practical cases, the latter being more detrimental to system performance than thermal noise [67, 68, 69]. For example, in [67], dual-hop relaying is used to improve the throughput of an interference-limited time-division multiple-access (TDMA) scheme in which many relays share a single time-slot. In [68], asymptotic performance analysis of a CSI assisted dual-hop relay system is carried out to show that the presence of interference limits the system diversity gain. In [69], the outage probability of a fixed gain AF relay operating in a Rayleigh fading channel with interference-limited destination node (effect of noise ignored) was considered. Moreover, the authors in [70] derived the outage probability as well as the average bit error rate (BER) for a two-hop CSI assisted AF relay system operating in a Rayleigh fading channel with co-channel interference at the relay node only. Again, the effect of noise was ignored in their analysis. Ikki and Aissa [71] considered the presence of interference and noise at both the relay and destination nodes in deriving the outage probability and BER in a Rayleigh fading channel. However, for mathematical tractability, the end-to-end SNR was upper-bounded by selecting the weaker of the two

links between the source and the destination. Chen et al. [72] also considered the presence of noise and interference at both the relay and destination nodes but for the scenario in which the desired signal is assumed to have Rician fading due to the presence of line-of-sight propagation and the interfering signals from neighboring cells are assumed to experience Rayleigh fading. However, an exact performance analysis was not treated and only a bound on the outage probability was presented.

In this chapter, we consider a dual-hop relaying scheme in which the destination suffers from the presence of interference and noise and derive the exact outage probability. This work extends the analysis of [69] to include the effect of channel noise at the destination. In addition, we also extend the two-parameter model in [65] to include two additional parameters that account for the presence of interference and noise at the destination node. The exact expression for the outage probability is presented in terms of the incomplete Weber integral, which can be easily evaluated by several computer programs such as Matlab, Mathematica, or Maple. The analytical results are then validated by Monte Carlo simulation.

7.2 System Model

We consider a wireless communication system in which a source sends a message $x_s(t)$ to a destination via a non-regenerative relay. The signal received at the relay is given by

$$y_R(t) = \sqrt{P_s}\alpha_1 x_s(t) + n_1(t) \quad (7.1)$$

where P_s is the transmit power, α_1 is the instantaneous fading amplitude of the channel between the source and the relay, and $n_1(t)$ is the additive white Gaussian noise (AWGN) with average power σ_1^2 at the input of the relay. An AF relay multiplies the signal $y_R(t)$ by a gain G , and then re-transmits it to the destination, where the received signal is

given by

$$\begin{aligned}
 y_D(t) &= \alpha_2 G y_R(t) + \sum_{i=1}^M \sqrt{P_i} \beta_i x_i(t) + n_2(t) \\
 &= \alpha_2 G \left\{ \sqrt{P_s} \alpha_1 x_s(t) + n_1(t) \right\} \\
 &\quad + \sum_{i=1}^M \sqrt{P_i} \beta_i x_i(t) + n_2(t).
 \end{aligned} \tag{7.2}$$

In (7.2), α_2 denotes the fading envelope on the link between the relay and the destination, M is the number of interfering signals present at the destination, each with power P_i and fading amplitude $\beta_i (i = 1, 2, \dots, M)$, and σ_2^2 is the noise power at the destination node. In general, the choice of the node gain, G , determines the end-to-end signal-to-interference-plus-noise ratio (SINR). The best choice of the relay gain that maximizes the end-to-end SINR requires the knowledge of the CSI, which includes the signal fading level as well as the noise power on the source-relay link. In such CSI-based relays, the amplification gain at the relay is chosen to invert the fading state of the preceding link. Following the two-parameter model proposed in [65], the corresponding relay gain is chosen as

$$G^2 = \frac{P_R}{a P_s \alpha_1^2 + b \sigma_1^2}, \tag{7.3}$$

where P_R is the output power of the relay and the parameters $a \in \{0, 1\}$ and $b \in \{0, 1\}$ are chosen in a similar manner as in [65], to encompass the different categories of relays that have been studied for the noise-limited environment. The resulting SINR at the destination node may be expressed as

$$\gamma_{eq} = \frac{P_s \alpha_1^2 \alpha_2^2 G^2}{\alpha_2^2 \sigma_1^2 G^2 + c \sum_{i=1}^M P_i \beta_i^2 + d \sigma_2^2} \tag{7.4}$$

where the additional parameters $c \in \{0, 1\}$ and $d \in \{0, 1\}$ are introduced to account for the presence of co-channel interference and channel noise at the destination, respectively.

Substituting (7.3) in (7.4), the end-to-end SINR becomes

$$\gamma_{eq} = \frac{\gamma_1 \gamma_2}{\gamma_2 + (a\gamma_1 + b)(cZ + d)} \quad (7.5)$$

where $\gamma_1 = P_s \alpha_1^2 / \sigma_1^2$ is the instantaneous SNR on the source-relay link, $\gamma_2 = P_R \alpha_2^2 / \sigma_2^2$ is the instantaneous SNR on the relay-destination link, and $Z = \sum_{i=1}^M \zeta_i$, is the total interference at the destination, with $\zeta_i = P_i \frac{\beta_i^2}{\sigma_2^2}$ being the instantaneous interference-to-noise ratio (INR) of the i -th destination interferer. We consider a Rayleigh fading environment, i.e., the probability density function (pdf) of γ_i , $i = 1, 2$ and ζ_i , $i = 1, 2, \dots, M$, is given by

$$f_{\gamma_i}(\gamma) = \frac{1}{\lambda_i} e^{-\gamma/\lambda_i} u(\gamma) \quad (7.6)$$

$$f_{\zeta_i}(\zeta) = \frac{1}{\mu_i} e^{-\zeta/\mu_i} u(\zeta) \quad (7.7)$$

respectively, with $\lambda_i = \mathbb{E}(\gamma_i)$, $i = 1, 2$, and $\mu_i = \mathbb{E}(\zeta_i)$, $i = 1, 2, \dots, M$, where $\mathbb{E}(\cdot)$ denotes expectation. Note that as stated earlier in (7.3)-(7.5), the parameters a, b, c, d are appropriately chosen constants, introduced so that the result in (7.5) can conveniently generalize the special cases already reported in the literature.

Some of these special cases of (7.5) are considered next.

(i) In a noise-limited environment where there is no interfering signal ($c = 0, d = 1$), (7.5) reduces to [65, eq. (1)]. Similar to [65], standard configurations, namely, CSI optimum gain, CSI sub-optimum gain, and fixed gain relay configurations are represented, respectively, with $(a, b) \in \{(1, 1), (1, 0), (0, C)\}$, where C is a constant [65]-[63].

(ii) In an interference-limited environment with co-channel interference dominating the destination node and fixed gain relay ($c = 1, a = d = 0$), the effect of noise may be ignored. The resulting end-to-end signal-to-interference ratio (SIR) is given by

$$\gamma_{eq} = \frac{\gamma_1 \gamma_2}{\gamma_2 + bZ}, \quad (7.8)$$

with b being a constant. Note that this case is treated in [69] where the parameter b is chosen as $b = 1 + P_s \mathbb{E}(\alpha_1) / \sigma_1^2$. In the following section, we derive the outage probability

for the generalized end-to-end SINR given in (7.5).

7.3 Outage Probability

In a wireless communication system with co-channel interference and thermal noise, the outage probability is the probability that the instantaneous SINR exceeds a preset threshold γ_{th} , and is given by

$$\begin{aligned} P_{out} &= \Pr(\gamma_{eq} \leq \gamma_{th}) \\ &= \Pr\left(\gamma_2 \leq \frac{\gamma_{th}(a\gamma_1 + b)(cZ + d)}{(\gamma_1 - \gamma_{th})}\right) \end{aligned} \quad (7.9)$$

Conditioning on the random variables γ_1 and Z , the outage probability becomes

$$\begin{aligned} P_{out} &= \mathbb{E}_Z \left[\int_0^{\gamma_{th}} \Pr\left(\gamma_2 > \frac{\gamma_{th}(a\gamma_1 + b)(cZ + d)}{(\gamma_1 - \gamma_{th})}\right) f_{\gamma_1}(\gamma_1) d\gamma_1 \right. \\ &\quad \left. + \int_{\gamma_{th}}^{\infty} F_{\gamma_2}\left(\frac{\gamma_{th}(a\gamma_1 + b)(cZ + d)}{(\gamma_1 - \gamma_{th})}\right) f_{\gamma_1}(\gamma_1) d\gamma_1 \right] \end{aligned} \quad (7.10)$$

where $F_{\gamma_2}(\cdot)$ is the cumulative density function (cdf) of the random variable γ_2 and the expectation $\mathbb{E}_Z(\cdot)$ is taken over the random variable Z . Using the fact that the cdf of γ_2 is $F_{\gamma_2}(\gamma) = 1 - e^{-\gamma/\lambda_2}$, the integral in (7.10) becomes

$$\begin{aligned} I &= \int_0^{\gamma_{th}} f_{\gamma_1}(\gamma_1) d\gamma_1 + \int_{\gamma_{th}}^{\infty} f_{\gamma_1}(\gamma_1) d\gamma_1 \\ &\quad - \int_{\gamma_{th}}^{\infty} \exp\left(-\frac{\gamma_{th}(a\gamma_1 + b)(cZ + d)}{(\gamma_1 - \gamma_{th})\lambda_2}\right) \exp\left(-\frac{\gamma_1}{\lambda_1}\right) d\gamma_1 \\ &= 1 - \\ &\quad \cdot \int_{\gamma_{th}}^{\infty} \exp\left(-\frac{\gamma_{th}(a\gamma_1 + b)(cZ + d)}{(\gamma_1 - \gamma_{th})\lambda_2}\right) \exp\left(-\frac{\gamma_1}{\lambda_1}\right) d\gamma_1. \end{aligned} \quad (7.11)$$

Upon making the change of variable $x = \gamma_1 - \gamma_{th}$ in (7.11) and simplifying, we have

$$I = 1 - \exp\left(-\frac{\gamma_{th}}{\lambda_1} - \frac{\gamma_{th}(cz + d)a}{\lambda_2}\right) \cdot \int_0^\infty \exp\left(-\frac{x}{\lambda_1} - \frac{\gamma_{th}(cz + d)(a\gamma_{th} + b)}{\lambda_2 x}\right) dx. \quad (7.12)$$

The integral in (7.12) may be evaluated via [4, eq. (3.471.9)]; upon substituting (7.12) back in (7.10), the outage probability becomes

$$P_{out} = \mathbb{E}_Z \left[1 - 2 \exp\left(-\frac{\gamma_{th}}{\lambda_1} - \frac{\gamma_{th}(cZ + d)a}{\lambda_2}\right) \cdot \sqrt{\varphi(Z)} K_1\left(2\sqrt{\varphi(Z)}\right) \right] \quad (7.13)$$

where $\varphi(Z) = \frac{\gamma_{th}(cZ + d)(a\gamma_{th} + b)}{\lambda_1 \lambda_2}$ and $K_1(\cdot)$ is the modified Bessel function of the second kind and first order [20]. Note that in the case of a noise-limited system (no interference), we have $(c = 0, d = 1)$ and (7.13) becomes

$$P_{out} = 1 - 2 \exp\left(-\gamma_{th}(\lambda_1^{-1} + a\lambda_2^{-1})\right) \cdot \sqrt{\frac{\gamma_{th}(a\gamma_{th} + b)}{\lambda_1 \lambda_2}} K_1\left(2\sqrt{\frac{\gamma_{th}(a\gamma_{th} + b)}{\lambda_1 \lambda_2}}\right) \quad (7.14)$$

as expected [73, eq. (14)]. In the remainder of this section, we focus our attention on the presence of interference at the destination node (i.e., $c \neq 0$).

7.3.1 Distinct interferers

In the presence of M independent interferers with distinct average INRs, i.e., $\mu_1 \neq \mu_2 \neq \dots \neq \mu_M$, the pdf of $Z = \sum_{i=1}^M \zeta_i$ is given by

$$f_Z(z) = \sum_{i=1}^M \frac{\pi_i}{\mu_i} \exp\left(-\frac{z}{\mu_i}\right) \quad (7.15)$$

where $\pi_i = \prod_{k=1, k \neq i}^M \frac{\mu_i}{\mu_i - \mu_k}$. Taking the expectation in (7.13) over the pdf in (7.15), the outage probability in the presence of distinct power interferers at the destination may be

written as

$$P_{out} = 1 - 2 \exp \left(-\frac{\gamma_{th}}{\lambda_1} - \frac{ad\gamma_{th}}{\lambda_2} \right) \left(\sqrt{\frac{\gamma_{th}(a\gamma_{th} + b)}{\lambda_1\lambda_2}} \right) \cdot \sum_{i=1}^M \frac{\pi_i}{\mu_i} \int_0^{\infty} (cz + d)^{1/2} e^{-z(\mu_i^{-1} + \gamma_{th}ac\lambda_2^{-1})} \cdot K_1 \left(2\sqrt{\varphi(z)} \right) dz. \quad (7.16)$$

Making the change of variables $t = 2\sqrt{\frac{\gamma_{th}(cz+d)(a\gamma_{th}+b)}{\lambda_1\lambda_2}}$, the integral in (7.16) becomes

$$I = \frac{2}{A^3c} \exp \left(\frac{d}{c} (\mu_i^{-1} + \gamma_{th}ac\lambda_2^{-1}) \right) \int_A^{\infty} t^2 e^{-B_i t^2} K_1(t) dt \quad (7.17)$$

where $A = 2\sqrt{\frac{\gamma_{th}(a\gamma_{th}+b)d}{\lambda_1\lambda_2}}$, $B_i = \frac{\lambda_1\lambda_2(\mu_i^{-1} + ac\gamma_{th}\lambda_2^{-1})}{4\gamma_{th}(a\gamma_{th}+b)c}$, and $c \neq 0$. Finally, simplifying (7.17) and substituting in (7.16), the outage probability may be expressed as

$$P_{out} = 1 - \frac{1}{2c} \left(\frac{\lambda_1\lambda_2}{\gamma_{th}(a\gamma_{th} + b)} \right) \cdot \sum_{i=1}^M \frac{\pi_i}{\mu_i} \exp \left(\frac{d}{c\mu_i} - \frac{\gamma_{th}}{\lambda_1} \right) \cdot \left[\frac{1}{8B_i^2} \Psi \left(2; 2; \frac{1}{4B_i} \right) - K_{e_{2,1}^2}(B_i, A) \right] \quad (7.18)$$

where $\Psi(u; v; x) = \frac{1}{\Gamma(u)} \int_0^{\infty} e^{-xt} t^{u-1} (1+t)^{v-u-1} dt$ is the confluent hypergeometric function of the second kind [20] and

$$K_{e_{u,v}^2}(p, x) = \int_0^x t^u e^{-pt^2} K_v(t) dt \quad (7.19)$$

is the incomplete Weber integral, which has applications in several engineering fields [74, 75, 76]. Note that in the special case of interference-limited destination (no noise) and a fixed gain policy adopted at the relay (i.e., $c = 1, a = d = 0$), (7.18) reduces to [69, eq. (11)], as expected. Note that there are several numerical integration techniques that can be used to evaluate the incomplete Weber integral given in (7.19). For the special case of interest, i.e., when $u > 0$ and $v = 1$, it can be shown that $K_{e_{u,1}^2}(p, x)$ may be

written as

$$\begin{aligned}
 K_{e_{u,1}^2}(p, x) &= \frac{x^u}{u} \int_0^\infty e^{-\tau} {}_1F_1\left(\frac{u}{2}; 1 + \frac{u}{2}; -x^2\left(p + \frac{1}{4\tau}\right)\right) d\tau \\
 &\cong \frac{x^u}{u} \sum_{i=1}^N w_{i1} F_1\left(\frac{u}{2}; 1 + \frac{u}{2}; -x^2\left(p + \frac{1}{4y_i}\right)\right), \quad (7.20)
 \end{aligned}$$

where ${}_1F_1(\cdot)$ is the confluent hypergeometric function [4]; weights w_i and roots y_i are given in [20, eq. (25.4.45)] for different values of N . The result in (7.20) provides a very efficient technique for the numerical evaluation of the incomplete Weber integral and it is used to compute the numerical results in this chapter. The numerical integration based on (7.20) was done for $N = 8$ and a perfect match between the numerical integration and the exact results was observed. In fact, very close approximations were observed for values of N as low as $N = 2$. The proof of (7.20) is as follows: making the substitution substituting $s = t/x$ in (7.19) and using [4, eq. (8.432.6)], we have

$$\begin{aligned}
 K_{e_{u,v}^2}(p, x) &= \frac{x^{u+v+1}}{2^{v+1}} \\
 &\cdot \int_0^1 s^{u+v} e^{-p(xs)^2} \int_0^\infty z^{-v-1} e^{-z - \frac{(xs)^2}{4z}} dz ds. \quad (7.21)
 \end{aligned}$$

Interchanging the order of integration in (7.21) and introducing $\omega = s^2$, we have

$$\begin{aligned}
 K_{e_{u,v}^2}(p, x) &= \frac{x^{u+v+1}}{2^{v+2}} \int_0^\infty e^{-z} z^{-v-1} \\
 &\cdot \int_0^1 \omega^{(u+v-1)/2} e^{-\omega x^2\left(p + \frac{z}{4}\right)} d\omega dz \\
 &= \frac{x^{u+v+1}}{2^{v+2}} \\
 &L\left[z^{-v-1} \int_0^1 \omega^{(u+v-1)/2} e^{-\omega x^2\left(p + \frac{z}{4}\right)} d\omega; s = 1\right] \quad (7.22)
 \end{aligned}$$

where $L[f(z); s]$ is the Laplace transform of $f(z)$ [4, eq. (17.11)]. Using the identity of the Laplace transform in [4, eq. (17.12.2)], we have

$$\begin{aligned}
K_{e_{u,v}^2}(p, x) &= \frac{x^{u+v+1}}{2^{v+2}} \\
&\left\{ sL \left[\int_0^\tau z^{-v-1} \int_0^1 \omega^{(u+v-1)/2} e^{-\omega x^2 (p + \frac{1}{4z})} d\omega dz; s \right] \right\}_{s=1} \\
&= \frac{x^{u+v+1}}{2^{v+2}} \\
&\left\{ sL \left[\int_0^1 \omega^{(u+v-1)/2} e^{-\omega x^2 p} \int_0^\tau z^{-v-1} e^{-\frac{\omega x^2}{4z}} dz d\omega; s \right] \right\}_{s=1}
\end{aligned} \tag{7.23}$$

When $u > 0$ and $v = 1$, (7.23) becomes [4, eq. (3.371.3)]

$$\begin{aligned}
K_{e_{u,v}^2}(p, x) &= \frac{x^u}{2} \\
&\left\{ sL \left[\int_0^1 \omega^{\frac{u}{2}-1} \exp \left(-\omega x^2 \left(p + \frac{1}{4\tau} \right) \right) d\omega \right] \right\}_{s=1}
\end{aligned} \tag{7.24}$$

Finally, the integral in (7.24) may be evaluated via [20, eq. (13.2.1)] to yield the result in (7.20).

7.3.2 Identical interferers

When the M interferers at the destination are independent and identically distributed, i.e., $\mu_1 = \mu_2 = \dots = \mu_M = \mu$, the pdf of $Z = \sum_{i=1}^M \zeta_i$ is given by

$$f_Z(z) = \frac{z^{M-1}}{\mu^M (M-1)!} \exp \left(-\frac{z}{\mu} \right) \tag{7.25}$$

Taking the expectation in (7.13) over the pdf in (7.25), we obtain the outage probability in the presence of identical interferers at the destination node as

$$\begin{aligned}
P_{out} &= 1 - \frac{4 \exp(-\gamma_{th} \lambda_1^{-1} - ad \gamma_{th} \lambda_2^{-1})}{A \mu^M (M-1)!} \\
&\int_0^\infty z^{M-1} (cz + d)^{1/2} e^{-z(\mu^{-1} + \gamma_{th} ac \lambda_2^{-1})} K_1 \left(2\sqrt{\varphi(z)} \right) dz
\end{aligned} \tag{7.26}$$

Upon making a change of variable as before, performing the resulting binomial expansion, and simplifying the integral $\int_A^\infty t^{2(k+1)} e^{-Bt^2} K_1(t) dt$, (7.26) may be simplified as

$$P_{out} = 1 - \frac{\exp(-\gamma_{th}\lambda_1^{-1} + d/(c\mu))}{2(c\mu)^M (M-1)!} \left(\frac{\lambda_1\lambda_2}{\gamma_{th}(a\gamma_{th} + b)} \right) \sum_{k=0}^{M-1} \binom{M-1}{k} (-d)^{M-k-1} \left(\frac{\lambda_1\lambda_2}{4\gamma_{th}(a\gamma_{th} + b)c} \right)^k \cdot \left[\frac{k!(k+1)!}{8B^{k+2}} \Psi\left(k+2; 2; \frac{1}{4B}\right) - K_{e_{2(k+1),1}^2}(B, A) \right] \quad (7.27)$$

where $B = \frac{\lambda_1\lambda_2(\mu^{-1} + ac\gamma_{th}\lambda_2^{-1})}{4\gamma_{th}(a\gamma_{th} + b)c}$. Note that when $c = 1$ and $a = d = 0$, i.e., fixed gain relays in an interference-limited system, (7.27) agrees with [69, eq. (11)].

7.4 Numerical Results

In this section we present some numerical results to illustrate the analytical expressions of the outage probability derived in this chapter. Fig. 7.1 shows the outage probability with $\gamma_{th} = 3$ dB of a dual-hop AF relay system with CSI optimum gain in the presence of multiple interferers with distinct aver-age INRs at the destination node. For illustration purposes we assume equal transmit powers at the source and relay nodes and average INRs of the interfering signals for $M=1, \dots, 5$ given by $\mu = 3.1$ dB, $\{\mu\}_{i=1}^M = [3.1, 3.5]$ dB, $\{\mu\}_{i=1}^M = [3.1, 3.5, 4]$ dB, $\{\mu\}_{i=1}^M = [3.1, 3.5, 4, 4.5]$ dB, $\{\mu\}_{i=1}^M = [3.1, 3.5, 4, 4.5, 5]$ dB, respectively. We observe that as the number of interfering signals increases the outage probability increases, with the most dramatic performance deterioration occurring with the introduction of the first interferer. Moreover, perfect agreement between the analytical expression in (7.18) and simulation results is observed.

Fig. 7.2 compares the outage probability of dual-hop relay systems with CSI-assisted relays (optimum and suboptimum gains) and fixed-gain relays with the parameters $a = 0$, $b = \lambda_1/(\exp(1/\lambda_1) E(1/\lambda_1))$ [66], where $E_1(\cdot)$ is the error integral [4]) when there is no interferer ($M = 0$) and when there are five equal-power interferers ($M = 5$) with average

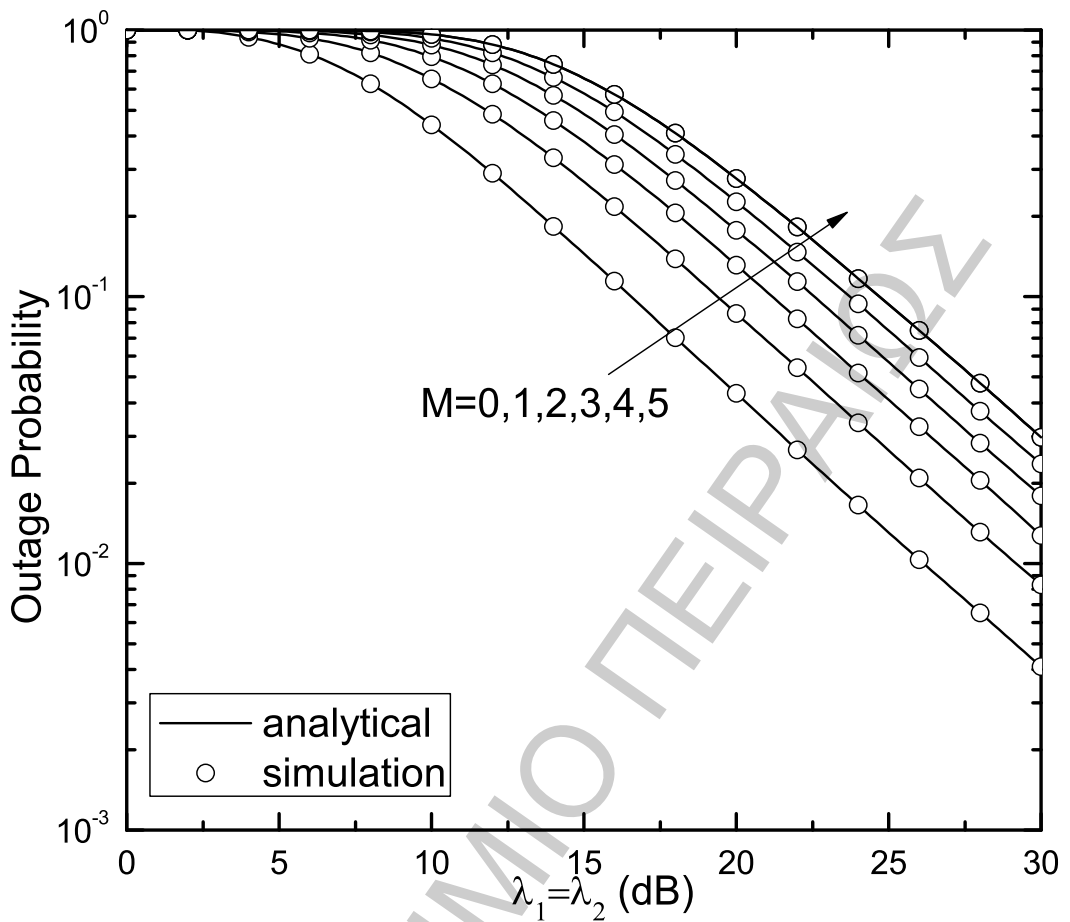


Figure 7.1: Outage probability for a dual-hop relay system with optimum CSI gain in the presence of distinct-power interferers.

INR $\{\mu\}_{i=1}^M = 5$ dB. We also assume that the average SNRs on the source-relay and relay-destination links are equal, whereas the threshold is set at $\gamma_{th} = 0$ and 5 dB. The results show that for medium to large average SNR per link, the systems with CSI optimum and suboptimum gains outperform those with fixed gain. However, the fixed-gain relays slightly outperform systems with variable-gain relays at low average SNRs. This is due to the fact that the variable gain relay has a gain floor when $\lambda_1 = \mathbb{E}(\gamma_1)$ is very small [66].

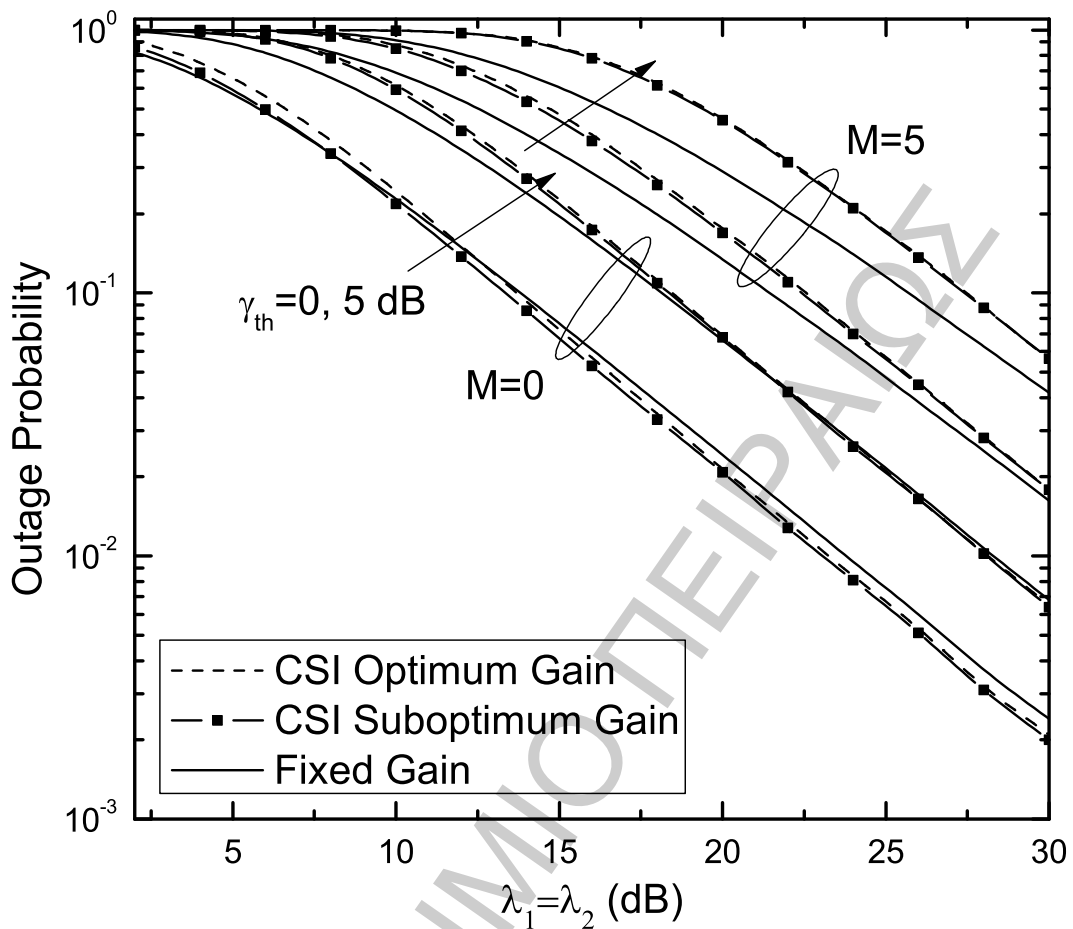


Figure 7.2: Outage probability for different categories of dual-hop AF relay systems with $M = 0$ (no interferer) and $M = 5$ equal-power interferers.

7.5 Conclusion

In this chapter, we derived the exact outage probability for a dual-hop AF relay system operating over a Rayleigh fading channel in the presence of co-channel interference at the destination. Specifically, we derived an exact expression for the outage probability in terms of the incomplete Weber integral, which can be easily and accurately evaluated. The derived results are sufficiently general to include several special cases already treated in the literature. The analytical results were validated by computer simulation.

Bibliography

- [1] V. Erceg, L. J. Greenstein, S. Y. Tjandra, S. R. Parkoff, A. Gupta, B. Kulic, A. A. Julius, and R. Bianchi, “An empirically based path loss model for wireless channels in suburban environments,” *IEEE J. Select. Areas Commun.*, pp. 1205–1211, Jul. 1999.
- [2] S. Ghassemzadeh, L. Greenstein, A. Kavcic, T. Sveinsson, and V. Tarokh, “Indoor path loss model for residential and commercial buildings,” in *IEEE Veh. Technol. Conf.*, 2003, pp. 3115–3119.
- [3] A. Papoulis, *Probability, Random Variables, and Stochastic Processes*, 2nd ed. McGraw-Hill, 1984.
- [4] I. S. Gradshteyn and I. M. Ryzhik, *Table of Integrals, Series, and Products*, 6th ed. New York: Academic Press, 2000.
- [5] H. B. James and P. I. Wells, “Some tropospheric scatter propagation measurements near the radio-horizon,” in *IRE*, 1955, pp. 1336–1340.
- [6] G. R. Sugar, “Some fading characteristics of regular VHF ionospheric propagation,” in *IRE*, 1955, pp. 1432–1436.
- [7] T. L. Staley, R. C. North, W. H. Ku, and J. R. Zeidler, “Performance of coherent MPSK on frequency selective slowly fading channels,” in *IEEE Veh. Technol. Conf. (VTC'96)*, 1996, pp. 784–788.

- [8] M. Nakagami, "The m -distribution-A general formula of intensity distribution of rapid fading," in *Statistical Methods in Radio Wave Propagation*, Oxford, U.K. Pergamon Press, 1960, pp. 3–36.
- [9] A. U. Sheikh, M. Handforth, and M. Abdi, "Indoor mobile radio channel at 946 MHz: Measurements and modeling," in *IEEE Veh. Technol. Conf. (VTC'93)*, 1993, pp. 73–76.
- [10] H. Suzuki, "A statistical model for urban multipath propagation," *IEEE Trans. Commun.*, vol. COM-25, pp. 45–53, May 1977.
- [11] J. Lieblein, "On moments of order statistics form the Weibull distribution," *Annals Math. Stat.*, vol. 26, pp. 330–333, Jun. 1955.
- [12] H. Hashemi, "The indoor radio propagation channel," *Proc. IEEE*, vol. 81, no. 7, pp. 943–967, Jul. 1993.
- [13] H. Bertoni, "Coverage prediction for mobile radio systems operating in the 800/900 MHz frequency range-received signal fading distributions," *IEEE Trans. Veh. Technol.*, vol. 37, no. 1, pp. 57–60, Feb. 1988.
- [14] N. C. Sagias and G. K. Karagiannidis, "Gaussian class multivariate Weibull distributions: Theory and applications in fading channels," *IEEE Trans. Inform. Theory*, vol. 51, no. 10, pp. 3608–3619, Oct. 2005.
- [15] E. W. Stacy, "A generalization of the Gamma distribution," *Annals Mathem Stat*, vol. 33, no. 3, pp. 1187–1192, 1962.
- [16] A. J. Coulson, A. G. Williamson, and R. G. Vaughan, "Improved fading distribution for mobile radio," *IEE Proc.-Commun.*, vol. 145, no. 3, pp. 197–202, Jun. 1998.
- [17] T. Piboongunon, V. A. Aalo, C. D. Iskander, and G. P. Efthymoglou, "Bivariate generalized gamma distribution with arbitrary fading parameters," *Electron. Lett.*, vol. 41, no. 12, pp. 709–710, Jun. 2005.

- [18] N. C. Sagias and P. T. Mathiopoulos, "Switch diversity receivers over generalized Gamma fading channels," *IEEE Commun. Lett.*, vol. 9, no. 10, pp. 871–873, Oct. 2005.
- [19] M. D. Yacoub, "The $\kappa - \mu$ distribution and the $\eta - \mu$ distribution," *IEEE Antennas Propagat. Mag.*, vol. 49, pp. 68–81, Feb. 2007.
- [20] M. Abramowitz and I. A. Stegun, *Handbook of Mathematical Functions, with Formulas, Graphs, and Mathematical Tables*, 9th ed. New York: Dover, 1972.
- [21] P. M. Shankar, "Error rates in generalized shadowed fading channels," *Wireless Pers. Commun.*, vol. 28, pp. 233–238, 2004.
- [22] "The Wolfram functions site." [Online]. Available: <http://functions.wolfram.com>
- [23] P. M. Shankar, "Performance analysis of diversity combining algorithms in shadowed fading channels," *Wirel. Pers. Commun.*, vol. 1.
- [24] J. Boyer, D. D. Falconer, and H. Yanikomeroglu, "Multihop diversity in wireless relaying channel," *IEEE Trans. Commun.*, vol. 52, no. 10, pp. 1820–1830, Oct. 2004.
- [25] I. H. Lee and D. Kim, "Coverage extension and power allocation in dual-hop space-time transmission with multiple antennas in each node," *IEEE Trans. Veh. Technol.*, vol. 56, no. 6, pp. 3524–3532, Nov. 2007.
- [26] J. N. Laneman and G. W. Wornell, "Energy-efficient antenna sharing and relaying for wireless networks," in *Proc. IEEE WCNC., Chicago, USA.*, vol. 1, pp. 7–12, 2000.
- [27] J. N. Laneman, D. N. C. Tse, and G. W. Wornell, "Cooperative diversity in wireless networks: Efficient protocols and outage behavior," *IEEE Trans. Inf. Theory*, vol. 50, no. 12, pp. 3062–3080, Dec. 2004.

- [28] X. Bao and J. Li, "Efficient message relaying for wireless user cooperation: Decode-amplify-forward (DAF) and hybrid DAF and coded-cooperation," *IEEE Trans. Wireless Commun.*, vol. 6, no. 11, pp. 3975–3984, 2007.
- [29] S. Tian, Y. Li, and B. Vucetic, "Piecewise-and-forward relaying in wireless relay networks," *IEEE Signal Proc. Lett.*, vol. 18, no. 5, pp. 323–326, May 2011.
- [30] K. S. Gomadam and S. A. Jafar, "Optimal relay functionality for SNR maximization in memory relay networks," *IEEE J. Sel. Areas Commun.*, vol. 25, no. 2, pp. 390–401, 2007.
- [31] M. O. Hasna and M. S. Alouini, "End-to-end performance of transmission systems with relays over Rayleigh-fading channels," *IEEE Trans. Wireless Commun.*, vol. 2, no. 6, pp. 1126–1131, Nov. 2003.
- [32] —, "Outage probability of multihop transmission over Nakagami fading channels," *IEEE Commun. Lett.*, vol. 7, no. 5, pp. 216–218, May 2003.
- [33] G. K. Karagiannidis, T. A. Tsiftsis, and R. K. Mallik, "Bounds on multihop relayed communications in Nakagami- m fading," *IEEE Trans. Commun.*, vol. 54, no. 1, pp. 18–22, Jan. 2006.
- [34] J. B. Si, Z. Li, and Z. Liu, "Outage probability of opportunistic relaying in Rayleigh fading channels with multiple interferers," *IEEE Signal Proc. Lett.*, vol. 17, no. 5, pp. 445–448, May 2010.
- [35] M. O. Hasna and M. S. Alouini, "Harmonic mean and end-to-end performance of transmission systems with relays," *IEEE Trans. Commun.*, vol. 52, no. 1, pp. 130–135, Jan. 2004.
- [36] T. A. Tsiftsis, G. K. Karagiannidis, S. A. Kotsopoulos, and F. N. Pavlidou, "BER analysis of collaborative dual-hop wireless transmissions," *Electron. Lett.*, vol. 40, no. 11, pp. 679–681, May 2004.

- [37] S. S. Ikki and M. H. Ahmed, "Performance analysis of cooperative diversity wireless networks over Nakagami- m fading channel," *IEEE Commun. Lett.*, vol. 11, no. 4, pp. 334–336, Apr. 2007.
- [38] —, "Performance analysis of dual hop relaying over non-identical Weibull fading channels," *Proc. IEEE VTC-Spring '09, Barcelona, Spain*, 2009.
- [39] —, "Performance analysis of dual-hop relaying communications over generalized Gamma fading channels," in *IEEE GLOBECOM*, Washington, USA, Nov 2007.
- [40] H. A. Suraweera and G. K. Karagiannidis, "Closed-form error analysis of the non-identical Nakagami- m relay channel," *IEEE Commun. Lett.*, vol. 12, no. 4, pp. 259–261, 2008.
- [41] A. Abdi and M. Kaveh, " K distribution: an appropriate substitute for Rayleigh-lognormal distribution in fading-shadowing wireless channels," *Electron. Lett.*, vol. 34, pp. 851–852, 1998.
- [42] P. Bithas, N. Sagias, P. Mathiopoulos, G. Karagiannidis, and A. A. Rontogiannis, "On the performance analysis of digital communications over generalized- K fading channels," *IEEE Commun. Lett.*, vol. 10, no. 5, pp. 353–355, May 2006.
- [43] P. S. Bithas, P. Mathiopoulos, and S. A. Kotsopoulos, "Diversity reception over generalized- K (KG) fading channels," *IEEE Trans. Wireless Commun.*, vol. 6, no. 12, pp. 4238–4243, 2007.
- [44] C. K. Datsikas, K. P. Peppas, F. Lazarakis, and G. S. Tombras, "Error rate performance analysis of dual hop relaying transmissions over generalized- K fading channels," *Electron. Commun. (AEU)*, doi:10.1016/j.aeue.2009.09.005.
- [45] G. P. Efthymoglou, "On the performance analysis of digital modulations in generalized- K fading channels," *Wireless Personal Commun.*, 2007.

- [46] A. Bletsas, A. Khisti, D. P. Reed, and A. Lippman, "A simple cooperative diversity method based on network path selection," *IEEE Trans. Commun.*, vol. 24, no. 3, pp. 659–672, Mar. 2006.
- [47] S. S. Ikki and M. H. Ahmed, "Performance of multi-hop relaying systems over Weibull fading channels," *Springer: New Technologies, Mobility and Security*, pp. 31–38, 2007.
- [48] —, "Performance of multiple-relay cooperative diversity systems with best relay selection over Rayleigh fading channel," *EURASIP Journal on Advances in Signal Processing*, 2008.
- [49] Y. Zhao, R. Adve, and T. J. Lim, "Symbol error rate of selection amplify-and-forward relay systems," *IEEE Commun. Lett.*, vol. 10, no. 11, pp. 757–759, Nov. 2006.
- [50] D. S. Michalopoulos and G. K. Karagiannidis, "Performance analysis of single relay selection in Rayleigh fading," *IEEE Trans. Wireless Commun.*, vol. 7, no. 10, pp. 3718–3724, Oct. 2008.
- [51] E. Beres and R. S. Adve, "Selection cooperation in multi-source cooperative networks," *IEEE Trans. Wireless Commun.*, vol. 7, no. 1, pp. 118–127, Jan. 2008.
- [52] L. Wu, J. Lin, K. Niu, and Z. He, "Performance of dual-hop transmissions with fixed gain relays over generalized- K fading channels," in *Proc. IEEE ICC '09*, 14-18 June 2009.
- [53] M. K. Simon and M.-S. Alouini, *Digital Communication over Fading Channels: A Unified Approach to Performance Analysis*. John Wiley, 2004.
- [54] Y. Chen and C. Tellambura, "Distribution function of selection combiner output in equally correlated Rayleigh, Rician, and Nakagami- m fading channels," *IEEE Trans. Commun.*, vol. 52, no. 11, pp. 1948–1956, Nov. 2004.

- [55] J. Lu, K. B. Letaief, J.-I. Chuang, and M. L. Liou, “ M -PSK and M -QAM BER computation using signal space concepts,” *IEEE Trans. Commun.*, vol. 47, no. 2, pp. 181–184, Feb. 1999.
- [56] M. Z. Win, G. Chrisikos, and J. H. Winters, “MRC performance of M -ary modulation in arbitrarily correlated Nakagami fading channels,” *IEEE Commun. Lett.*, vol. 4, no. 10, pp. 301–303, Oct. 2000.
- [57] W. C. Y. Lee, “Estimate of channel capacity in Rayleigh fading environment,” *IEEE Trans. Veh. Technol.*, vol. 39, no. 3, pp. 187–189, Aug. 1990.
- [58] K. P. Peppas, A. Mansour, and G. S. Tombras, “Dual-hop transmissions with fixed-gain relays over generalized Gamma fading channels,” *J. Telecom.*, vol. 1, no. 1, pp. 87–92, 2010.
- [59] F. Yilmaz and O. Kucur, “Exact performance of wireless multihop transmission for M -ary coherent modulations over generalized gamma fading channels,” *Proc. PIMRC’08, Cannes, France*, 2008.
- [60] G. K. Karagiannidis and et al., “Multihop communications with fixed-gain relays over generalized fading channels,” *Proc. IEEE GLOBECOM’04, Dallas, Texas, USA*, 2004.
- [61] G. P. Efthymoglou, N. Bissias, and V. A. Aalo, “On the error rate analysis of dual-hop amplify-and-forward relaying in generalized- K fading channels,” *J. of Elect. And Comp. Eng., Hindawi*, doi:10.1155/2010/584594.
- [62] A. H. Wojnar, “Unknown bounds on performance in Nakagami channels,” *IEEE Trans. Commun.*, vol. 34, no. 1, pp. 22–24, 1986.
- [63] G. K. Karagiannidis, “Performance bounds of multihop wireless communications with blind relays over generalized fading channels,” *IEEE Trans. Wireless Commun.*, vol. 5, no. 3, pp. 498–503, Mar. 2006.

- [64] T. A. Tsiftsis, G. K. Karagiannidis, and S. A. Kotsopoulos, "Dual-hop wireless communications with combined gain relays," *IET on Commun.*, vol. 152, no. 5, pp. 528–532, Oct. 2005.
- [65] D. Senaratne and C. Tellambura, "Unified exact performance analysis of two-hop amplify-and-forward relaying in Nakagami fading," *IEEE Trans. Veh. Technol.*, vol. 59, no. 3, pp. 1529–1534, Mar. 2010.
- [66] M. O. Hasna and M.-S. Alouini, "A performance study of dual-hop transmissions with fixed gain relays," *IEEE Trans. Wireless Commun.*, vol. 3, no. 6, pp. 1963–1968, Nov. 2004.
- [67] A. Agustin and J. Vidal, "Amplify-and-forward cooperation under interference-limited spatial reuse of the relay slot," *IEEE Trans. Wireless Commun.*, vol. 7, no. 5, pp. 1952–1962, May 2008.
- [68] I. Krikidis, J. S. Thompson, S. Mclaughlin, and N. Goertz, "Max-min relay selection for legacy amplify-and-forward systems with interference," *IEEE Trans. Wireless Commun.*, vol. 8, no. 6, pp. 3016–3027, Jun. 2009.
- [69] C. Zhong, S. Jin, and K. K. Wong, "Dual-hop systems with noisy relay and interference-limited destination," *IEEE Trans. Commun.*, vol. 58, no. 3, pp. 764–768, Mar. 2010.
- [70] H. A. Suraweera, H. K. Garg, and A. Nallanathan, "Performance analysis of two hop amplify-and-forward systems with interference at the relay," *IEEE Commun. Lett.*, vol. 14, no. 8, pp. 692–694, Aug. 2010.
- [71] S. S. Ikki and S. Aissa, "Performance analysis of dual-hop relaying systems in the presence of co-channel interference," in *IEEE GLOBECOM 2010*, Dec. 2010.
- [72] S. Chen, X. Zhang, F. Liu, and D. Yang, "Outage performance of dual-hop relay network with co-channel interference," in *IEEE VTC, Spring 2010*, 2010.

-
- [73] V. Emamian, P. Anhel, and M. Kaveh, "Multi-user spatial diversity in shadow-fading environment," in *IEEE VTC'02*, Sep. 2002, pp. 573–576.
- [74] A. R. Miller and I. S. Moskowitz, "Incomplete Weber integrals of cylindrical functions," *J. Franklin Inst.*, vol. 328, no. 4, pp. 445–457, 1991.
- [75] M. M. Agrest and M. S. Maksimov, *The Theory of Incomplete Cylinder Functions and Their Applications*. New York: Springer, 1971.
- [76] A. R. Miller, "Reduction of generalized incomplete gamma function, related Kampe De Feriet functions, and incomplete weber integrals," *Rocky Mountain Journal of Mathematics*, vol. 39, no. 2, pp. 703–714, 2000.